

Lehrstuhl für Organische Chemie und Biochemie  
der Technischen Universität München

**Role of the Tyrosine in the Highly Conserved *NPxxY*  
Sequence of the Human B<sub>2</sub> Bradykinin Receptor**

Irina Kalatskaya

Vollständiger Abdruck der von der Fakultät für Chemie der Technischen Universität München zur Erlangung des akademischen Grades eines

**Doktors der Naturwissenschaften**

genehmigten Dissertation.

Vorsitzende: Univ.-Prof. Dr. S. Weinkauf  
Prüfer der Dissertation: 1. Univ.-Prof. Dr. M. Jochum, Ludwig-Maximilians-Universität München  
2. Univ.-Prof. Dr. Dr. A. Bacher

Die Dissertation wurde am 23.05.2005 bei der Technischen Universität München eingereicht und durch die Fakultät für Chemie am 20.06.2005 angenommen.

Die vorliegende Arbeit wurde in der Zeit von September 2001 – April 2005  
in der Abteilung für Klinische Chemie und Klinische Biochemie  
in der Chirurgischen Klinik und Poliklinik der LMU München angefertigt  
(Leiterin der Abteilung: Prof. Dr. rer. nat. Marianne Jochum)

DEDICATED TO THE ONES  
I LOVE

## ACKNOWLEDGEMENTS

First of all, I want to warmly thank my supervisor Dr. Alexander Faussner for his leadership, his valuable help not only in scientific problems, but as well in daily questions, discussion of my results providing criticism, advice and encouragement in just the right proportions, and for giving me individual liberty. Moreover, I would like to acknowledge the skillful technical assistance of Cornelia Seidl and Steffen Schüssler of the working group of Dr. Faussner.

I am also deeply grateful to Prof. Dr. Marianne Jochum for accepting me in the Abteilung für Klinische Chemie und Klinische Biochemie, for her generous support during my stay, and for critical review of my work.

Particularly, I am thanking Prof. Dr. Bacher from the Chemistry Department of the Technical University Munich for taking over the mentorship.

I also express my thanks to Prof. Dr. Werner Müller-Esterl from the Medical School of the University of Frankfurt (Frankfurt/Main) for his cooperation and Dr. Andree Blaukat from the Institute for Pharmacology (Heidelberg) for teaching me the receptor phosphorylation assay and two-dimensional phosphopeptide mapping.

For organizing the “Journal club” for PhD-students, his constant generous scientific support and interesting discussions I also wish to express my thanks to Dr. Peter Neth.

Furthermore, I want to warmly thank Prof. Dr. Hans Fritz, Prof. Dr. Christian Sommerhoff, Prof. Dr. Edwin Fink, Dr. Shirly Gil Parrado, Dr. Dorit Nägler, Dr. Dusica Gabrijelcic-Geiger, Dr. Amaury Fernández, Alexandra Bauer, Oliver Popp, Virginia Egea, Annette Lechner, Lourdes Ruiz-Heinrich, Marianne Arnhold, Stefan Simon, Thomas Pitsch, and all other members of the Abteilung for help concerning all matters associated with being a PhD-student during the time I spent in the lab in Munich.

I also want to thank all my friends, especially Victoryia Sidarovich, Andrei Tamin, Roman Anisimov and Olga Ninichuk. They made my stay away from home bearable.

My full-hearted gratitude belongs to Dr. Anna G. Lapko for her sustained support of this endeavour from the outset and her decisive contribution to my qualification as a biochemist.

Last not least, I am especially indebted to all my family members for their patience, encouragement and love. They cheered me from afar.

## **Publications Related to the Dissertation Work**

- A) Faussner A, Bauer A, **Kalatskaya I**, Schüssler S, Seidl C, Proud D, Jochum M: The role of helix 8 and of the cytosolic C-termini in the internalization and signal transduction of B<sub>1</sub> and B<sub>2</sub> Bradykinin receptors. *FEBS J.* 272:129-140, 2005.
- B) **Kalatskaya I**, Schüssler S, Blaukat A, Müller-Esterl W, Jochum M, Proud D, Faussner A: Mutation of tyrosine in the conserved NPxxY-sequence leads to constitutive phosphorylation and internalization, but not signaling of the human B<sub>2</sub> bradykinin receptor. *J Biol. Chem.* 279:31268-31276, 2004.
- C) Faussner A, Bauer A, **Kalatskaya I**, Jochum M, Fritz H: Expression levels strongly affect ligand-induced sequestration of B<sub>2</sub> bradykinin receptors in transfected cells. *Am. J Physiol.* Jun 284(6):H1892-1898, 2003.
- D) Blaukat A, Micke P, **Kalatskaya I**, Faussner A, Müller-Esterl W: Down-regulation of bradykinin B<sub>2</sub> receptor in human fibroblasts during prolonged agonist exposure. *Am. J Physiol.* Jun; 284(6):H1909-1916, 2003.

## **Intended Publications Based on the Dissertation Work**

1. **Kalatskaya I**, Schüssler S, Müller-Esterl W, Jochum M, Proud D, Faussner A: Highly conserved Y<sup>7.53</sup> interacts with F<sup>7.60</sup> in the human B<sub>2</sub> bradykinin receptor. (manuscript in preparation)
2. **Kalatskaya I**, Schüssler S, Seidl C, Jochum M, Faussner A: C-terminal fusion of eGFP to B<sub>2</sub> bradykinin receptor does not affect internalization nor signaling, but blocks down-regulation. (manuscript in preparation)

## **Presentations of this Project**

### Oral presentations

1. Invitation to a Seminar by Dr. Nikolaus Heveker (interview for a Post-Doc position)

March 2005, Research Centre, Hospital Sainte-Justine, Montreal, Canada

**Kalatskaya I**: Function of the tyrosine in the highly conserved *NPxxY* motif of the B<sub>2</sub> bradykinin receptor.

2. International Multidisciplinary Symposium: "PEPTIDE RECEPTORS"

August 2004, Montreal, Canada

**Kalatskaya I**, Schüssler S, Blaukat A, Müller-Esterl W, Jochum M, Proud D, Faussner A: Mutation of tyrosine in the conserved *NPxxY*-sequence leads to constitutive phosphorylation and internalization, but not signaling of the human B<sub>2</sub> bradykinin receptor.

3. Invitation to a Seminar by Prof. Dr. Werner Müller-Esterl

August 2003, Institute of Biochemistry II, Johann Wolfgang Goethe University, Frankfurt am Main, Germany

**Kalatskaya I**: Function of the tyrosine in the highly conserved *NPxxY* motif of the B<sub>2</sub> bradykinin receptor.

4. 20<sup>th</sup> Winterschool "Proteases and their Inhibitors"

March 2003, Tiers, Italy

**Kalatskaya I**, Bauer A, Schüssler S, Seidl C, Jochum M, Faussner A: Function of the tyrosine in the highly conserved *NPxxY*-motif of the B<sub>2</sub> bradykinin receptor.

### Posters

1. 8<sup>th</sup> Joint Meeting "SIGNAL TRANSDUCTION: Receptors, Mediators and Genes"

November 2004, Weimar, Germany

**Kalatskaya I**, Schüssler S, Blaukat A, Müller-Esterl W, Jochum M, Proud D, Faussner A: Highly conserved *Y7.53* interacts with *F7.60* in the human B<sub>2</sub> bradykinin receptor (Poster and one-minute presentation).

2. The PhD Course "MEMBRANE PROTEINS: Biophysics and Biochemistry"

April 2004, Aalborg, Denmark

**Kalatskaya I**, Schüssler S, Blaukat A, Müller-Esterl W, Jochum M, Proud D, Faussner A: Mutation of tyrosine in the conserved *NPxxY*-sequence leads to constitutive phosphorylation and internalization, but not signalling of the human B<sub>2</sub> bradykinin receptor.

**ABBREVIATIONS**

aa	amino acids
ADR	adrenergic receptor
ACE	angiotensin-converting enzyme
ATP	adenosine-5'-triphosphate
BK	bradykinin
[ <sup>3</sup> H]BK	tritium-labeled bradykinin
BGH	bovine growth hormone
bp	base pair
BSA	bovine serum albumin
CHAPS	3-[(3-cholamidopropyl)dimethylammonio]-l-propanesulfonic acid
CHO cell	Chinese hamster ovary cell
Ci	Curie, 1 Ci = $2.22 \times 10^{12}$ disintegrations/min
CMV	cytomegalovirus
COS cell	green monkey kidney cell
DAG	diacylglycerol
DMEM	Dulbecco's modified Eagle's medium
DMSO	dimethyl sulfoxide
DTT	1,4-dithiothreitol
EDTA	ethylenediaminetetraacetic acid
eGFP	enhanced green fluorescent protein
eYFP	enhanced yellow fluorescent protein
ERK1/2	extracellular signal-regulated kinase 1/2
FCS	fetal calf serum
FRT	Flp recombinase target
g	gravity acceleration
GPCR	G protein-coupled receptor
GRK	G protein-coupled receptor kinase
GTP	guanosine-5'-triphosphate
h	hour
HA	hemagglutinin
HEPES	2-[4-(2-hydroxyethyl)-1-piperazinyl]ethanesulfonic acid
HEK cell	human embryonic kidney cell
HOE 140	D-Arg[Hyp <sup>3</sup> , Thi <sup>5</sup> , D-Tic <sup>7</sup> , Oic <sup>8</sup> ]BK
HRP	horse radish peroxidase
Ins 1,4,5-P <sub>3</sub>	<i>myo</i> -inositol 1,4,5-triphosphate
IP	inositol phosphate
ISO	isoproterenol
KD	kallidin
KLK	kallikrein
LDL	low density lipoprotein

min	minute
nd	not determined
NMR	nuclear magnetic resonance
NPC17731	D-Arginyl-L-arginyl-L-prolyl-(4R)-4-hydroxy-L-prolylglycyl-L-phenylalanyl L-seryl-(4S)-4-propoxy-D-prolyl-(2S,3aS,7aS)-octahydro-1H-indole-2- carbonyl- L-Arg
PAGE	polyacrylamide gel electrophoresis
PBS	phosphate buffered saline
PCR	polymerase chain reaction
PKA	protein kinase A
PKC	protein kinase C
PLC- $\beta$	phospholipase C- $\beta$
Rho	rhodopsin
RIPA	radio-immunoprecipitation assay
RT	room temperature
s	second
SDS	sodium dodecyl sulfate
TBS	Tris-buffered saline buffer
TBST	Tris-buffered saline buffer with 0.1% Tween 20
TLC	thin layer chromatography
TMD	transmembrane domain
Tris	tris(hydroxymethyl)-aminomethane
wt	wild type
v/v	volume/volume
w/v	weight/volume

### One-letter-code for amino acid residues

Alanine	A	Glutamate	E	Proline	P
Arginine	R	Histidine	H	Serine	S
Asparagine	N	Isoleucine	I	Threonine	T
Aspartate	D	Leucine	L	Tryptophan	W
Cysteine	C	Lysine	K	Tyrosine	Y
Glycine	G	Methionine	M	Valine	V
Glutamine	Q	Phenylalanine	F		



## CONTENTS

<b>A</b>	<b>SUMMARY</b>	<b>1</b>
<b>B</b>	<b>INTRODUCTION</b>	<b>6</b>
B.1	The kallikrein-kinin system (KKS)	7
B.1.1	Historic background	7
B.1.2	Kinins	7
B.1.3	Kinin receptors	8
B.1.3.1	General introduction	8
B.1.3.2	The signalling pathways of the kinin receptors	10
B.1.3.3	Regulation of the kinin receptors	11
B.2	Superfamily of G protein-coupled receptors (GPCRs)	13
B.2.1	Structure and classification of GPCRs	13
B.2.2	The highly conserved tyrosine of <i>NPxxY</i> : facts and assumptions	15
B.2.3	Rhodopsin: function of the helix VIII and <i>NPxxY</i> motif	15
B.2.4	$\beta_2$ -Adrenergic receptor: general characteristics and function of the highly conserved tyrosine of <i>NPxxY</i> motif	16
B.2.5	Short characteristics of the G proteins	19
B.3	Aim of the thesis	20
<b>C</b>	<b>MATERIALS AND METHODS</b>	<b>21</b>
C.1	Materials	21
C.1.1	Equipment	21
C.1.2	Chemicals and materials	22
C.1.3	Strains and cell lines	24
C.1.4	Expression vectors	25
C.1.5	Oligonucleotides used as primers for PCR amplification	26
C.1.6	Computer programs	26
C.1.7	Solutions	27
C.2	Methods	28
C.2.1	Molecular biological methods	28
C.2.1.1	Polymerase chain reaction (PCR)	28
C.2.1.2	DNA cleavage with restriction endonucleases	34
C.2.1.3	Agarose gel electrophoresis	34
C.2.1.4	Extraction of DNA fragments from agarose gels	34
C.2.1.5	Ligation of DNA fragments	35
C.2.1.6	Culture of <i>E. coli</i> strains	35
C.2.1.7	Transformation of <i>E. coli</i> strains	35
C.2.1.8	Plasmid preparation from <i>E. coli</i>	36
C.2.1.9	Confirmation of correct DNA sequence	37
C.2.1.10	Determination of DNA concentration	37

C.2.2	Cell culture methods	37
C.2.2.1	Culture of mammalian cells	37
C.2.2.2	Cell freezing and thawing	38
C.2.2.3	<i>Flp-In</i> expression system	38
C.2.2.4	Transformation of <i>HEK293</i> cells	40
C.2.3	[ <sup>3</sup> H]Bradykinin binding studies	41
C.2.4	Receptor sequestration and ligand internalization assays	42
C.2.4.1	Internalization of [ <sup>3</sup> H]Bradykinin	42
C.2.4.2	Receptor sequestration assay	42
C.2.4.3	Measurement of changes in surface receptor number by ELISA	42
C.2.5	Measurement of total inositol phosphate (IP) release	43
C.2.6	Protein biochemical methods	44
C.2.6.1	Crude membrane preparation	44
C.2.6.2	Co-immunoprecipitation assay	44
C.2.6.3	Electrophoresis of proteins on SDS-PAGE	45
C.2.6.4	Transfer of proteins from gel to nitrocellulose membrane	45
C.2.6.5	Immunoprinting of blotted proteins	46
C.2.7	Receptor phosphorylation and phosphopeptide mapping	47
C.2.7.1	Phosphorylation assay	47
C.2.7.2	Two-dimensional phosphopeptide mapping assay	48
C.2.8	Confocal microscopy	49
C.2.9	[ <sup>35</sup> S]GTP $\gamma$ S binding assay	49
C.2.10	Determination of the protein concentration	49
<b>D</b>	<b>RESULTS</b>	<b>50</b>
D.1	Development of methods	50
D.1.1	Ligand internalization and receptor sequestration assays	50
D.1.1.1	Ligand internalization assay: optimization	50
D.1.1.2	Receptor sequestration assay: optimization	52
D.1.2	Elaboration of the B <sub>2</sub> R immunoprecipitation and immunoprinting assay	53
D.1.2.1	Selection of the appropriate antibodies for receptor immunoprecipitation	54
D.1.2.2	Selection of the appropriate antibodies for receptor immunoprinting	55
D.1.3	Solubilization of the receptor in its active conformation	56
D.1.4	Elaboration of a co-immunoprecipitation assay	57
D.1.5	Co-immunoprecipitation of G <sub>q/11</sub> protein	58
D.2	Investigation of the role of highly conserved Y <sup>7.53</sup>	59
D.2.1	Generation of high- and low-expressing B <sub>2</sub> R wt, Y7.53F and Y7.53A mutants	59
D.2.2	Investigation of the receptor binding properties	59
D.2.3	[ <sup>3</sup> H]Bradykinin internalization	60
D.2.4	Investigation of the Y7.53A mutant sequestration	61
D.2.5	Measurement of the PLC activation	61
D.2.6	Western blotting analysis of the expression level	62
D.2.7	Receptor localization studies using eYFP-constructs	63
D.2.8	Receptor phosphorylation	65

D.2.8.1	Agonist-induced receptor phosphorylation assay	65
D.2.8.2	Two-dimensional phosphopeptide mapping	66
D.2.9	Uptake of rhodamine-labelled antibodies	68
D.2.10	Co-immunoprecipitation of G <sub>q/11</sub> protein	70
D.2.11	[ <sup>35</sup> S]GTPγS binding assay	71
D.3	Role of Y <sup>7.53</sup> in the β <sub>2</sub> -adrenergic receptor	72
D.3.1	Receptor sequestration	72
D.3.2	Ligand-induced phosphorylation	73
D.3.3	Interaction of β <sub>2</sub> -ADR-Y7.53A with G <sub>s</sub> proteins	73
D.3.4	Interaction of β <sub>2</sub> -ADR-Y7.53A with GRKs	75
D.4	Role of the interaction between Y <sup>7.53</sup> and F <sup>7.60</sup> in the human B <sub>2</sub> R	76
D.4.1	Generation of F7.60A, Y7.53F/Y7.60A and Y7.53A/F7.60A mutants	76
D.4.2	Investigation of the binding properties of the constructed mutants	77
D.4.3	[ <sup>3</sup> H]Bradykinin internalization	77
D.4.4	Measurement of the activation of PLC	78
D.4.5	Ligand-induced phosphorylation and phosphopeptide mapping	79
D.4.6	Interaction of Y7.53F/F7.60A mutant with the G <sub>q/11</sub> protein	81
D.4.7	Interaction of Y7.53A/F7.60A mutant with the G <sub>q/11</sub> protein	82
D.4.8	Interaction of Y7.53A/F7.60A mutant with GRKs	83
<b>E</b>	<b>DISCUSSION</b>	<b>84</b>
E.1	Mutation of tyrosine in the conserved NPxxY sequence leads to constitutive phosphorylation and internalization, but not signalling of the human B <sub>2</sub> R	84
E.2	Phenotypes of Y7.53F and F7.60A mutants resembled that of the wild-type	87
E.3	Y7.53F/F7.60A construct did not resemble the phenotype of Y7.53A mutant	90
E.4	Y7.53A/F7.60A exhibited a less conservative phenotype than Y7.53F/F7.60A	90
E.5	Y <sup>7.53</sup> and its microenvironment are important for keeping B <sub>2</sub> R in its inactive state	92
E.6	Mutation of Y <sup>7.53</sup> to alanine in the human β <sub>2</sub> -adrenergic receptor leads to irreversible interaction with GRKs	93
E.7	The various phenotypes of “tyrosine mutants” could be explained on the basis of their different affinities for cognate G proteins and/or GRKs	94
<b>F</b>	<b>OUTLOOK</b>	<b>98</b>
<b>G</b>	<b>REFERENCES</b>	<b>99</b>
<b>H</b>	<b>CURRICULUM VITAE</b>	<b>107</b>

**A SUMMARY**

Although the G protein-coupled receptors (GPCRs) share a similar seven-transmembrane domain structure, only a limited number of amino acid residues is conserved in their protein sequences. One of the most highly conserved sequences is the *NPxxY* motif located at the cytosolic end of helix VII of those GPCRs that belong to the family of the rhodopsin/ $\beta$ -adrenergic-like receptors (Family A). The crystal structure of bovine rhodopsin indicates a hydrophobic interaction between Y<sup>7.53</sup> of the *NPxxY* motif and F<sup>7.60</sup> in the helix VIII; moreover, the hydroxyl group of Y<sup>7.53</sup> is located close to N<sup>2.40</sup> at the cytosolic end of helix II suggesting an interhelical hydrogen bond between helix VII and helix II (Palczewski *et al.*, 2000). Because conservation of a sequence implies an important structural and/or functional role, this motif has been examined by mutagenesis studies in several GPCRs. Interestingly, these mutations affected receptor affinity, signalling, sequestration, and internalization of GPCRs to quite different extents, depending on the receptor under investigation. So far, no general theory could be elaborated that would explain all the observed results.

The main purpose of the presented thesis was the investigation of the function of the highly conserved tyrosine (Y<sup>7.53</sup>) in the *NPxxY* motif of the human B<sub>2</sub> bradykinin receptor (B<sub>2</sub>R) and its potential interaction partners. Similar to bovine rhodopsin, the B<sub>2</sub>R also a tyrosine amino acid residue (Y) at position 7.53, a phenylalanine (F) at position 7.60, but a glutamate (E) at position 2.40. The latter, however, is also able to form a hydrogen bond with the hydroxyl group of Y<sup>7.53</sup>. To study of E<sup>2.40</sup> ↔ Y<sup>7.53</sup> ↔ F<sup>7.60</sup> loci we generated a series of receptor mutants and investigated them with regards to signalling, ligand-inducible phosphorylation, receptor internalization/sequestration and localization as well as interaction with the G<sub>q/11</sub> protein and G protein-coupled receptor kinases. All experiments were done relatively to the wild-type (wt) receptor.

Mutation of F<sup>7.60</sup> in helix VIII of the B<sub>2</sub>R to alanine resulted in a mutant, termed F7.60A. This mutation did not much affect the affinity to its main ligand bradykinin (BK), ligand-inducible phosphorylation, internalization or signalling. In addition, mutant Y7.53F displayed also the properties of the B<sub>2</sub>R wt. As both point mutants Y7.53F and F7.60A resembled the wild-type phenotype, we assume that the interaction Y<sup>7.53</sup> ↔ F<sup>7.60</sup> could still compensate the absence of an interaction between Y<sup>7.53</sup> ↔ E<sup>2.40</sup> and vice versa.

Furthermore, exchange of Y<sup>7.53</sup> to alanine resulted in a mutant, termed Y7.53A, in which both interactions (Y<sup>7.53</sup> ↔ F<sup>7.60</sup> and Y<sup>7.53</sup> ↔ E<sup>2.40</sup>) were lost. This mutant internalized the ligand [<sup>3</sup>H]BK almost as rapidly as the B<sub>2</sub>R wt. However, receptor sequestration of the mutant after stimulation with BK was clearly reduced relatively the B<sub>2</sub>R wt. Confocal fluorescence microscopy revealed that, in contrast to the B<sub>2</sub>R, the Y7.53A was predominantly located intracellularly even in the absence of BK. Two-dimensional phosphopeptide analysis showed that the mutant Y7.53A

constitutively exhibits a phosphorylation pattern similar to that of the BK-stimulated B<sub>2</sub>R wt. Ligand-independent Y7.53A internalization was demonstrated by the uptake of rhodamine-labelled antibodies directed to a tag sequence at the N-terminus of the mutated receptor. Co-immunoprecipitation revealed that Y7.53A is pre-coupled to G<sub>q/11</sub> without activating the G protein because the basal accumulation rate of inositol phosphate (IP) was unchanged as compared with B<sub>2</sub>R wt.

We conclude, therefore, that the Y7.53A mutation of B<sub>2</sub>R induces a semi-active receptor conformation which is prone to ligand-independent phosphorylation and, as a consequence, also to internalization. The mutated receptor binds to, but does not activate, its cognate heterotrimeric G protein G<sub>q/11</sub>, thereby limiting the extent of ligand-independent receptor internalization through steric hindrance.

Whereas mutation of Y<sup>7.53</sup> to phenylalanine (F) or F<sup>7.60</sup> to alanine (A) did not much affect ligand-inducible phosphorylation and ligand internalization, the double mutant Y7.53F/F7.60A exhibited a dramatically reduced capability to internalization, most likely caused by the observed resistance to ligand-induced phosphorylation. Co-immunoprecipitation showed that G<sub>q/11</sub> protein was partially pre-coupled to the mutant receptor that probably led to inaccessibility of the mutated receptor for G protein-coupled receptor kinases (GRKs) and, consequently, failure of phosphorylation. However, signal transduction via the G protein G<sub>q/11</sub> was unaffected.

The less conservative double mutant Y7.53A/F7.60A was also resistant to phosphorylation and lost its internalization capacity. Moreover, it also showed a strongly reduced IP signal. This double mutant inclined to interaction with GRKs in a ligand-independent manner. But, in contrast to mutant Y7.53A, GRKs phosphorylate the double mutant neither prior nor after stimulation with BK obviously staying bound to the receptor. This may cause the abolished signalling, as the cognate G protein – for sterical reasons – does not have access to the receptor.

To summarize, these data demonstrate that the highly conserved Y<sup>7.53</sup> of the *NPxxY* motif and its potential partners F<sup>7.60</sup> and E<sup>2.40</sup> play an important role in the interaction of the B<sub>2</sub>R with the G protein G<sub>q/11</sub> and the GRKs. The binding to/activation of the specific G proteins or recognition by specific kinases requires presentation of a particular spatial distribution of the intracellular docking sites that are normally closed in the inactive state. Thus, our results suggest that the mutation of the Y<sup>7.53</sup>↔F<sup>7.60</sup> locus interferes with a mechanism responsible for stabilizing the receptor in an inactive conformation. Thereby the receptor conformation may be altered and, consequently, the phenotype of the resulting mutants. Finally, it may be concluded that normal receptor activation most likely leads to the disruption of the Y<sup>7.53</sup>↔F<sup>7.60</sup> interaction, too.

This information will contribute to a better understanding of the activation mechanism of the B<sub>2</sub>R; in addition, these data will be very helpful in the creation of the high therapeutic potential B<sub>2</sub> receptor agonists and antagonists.

**A ZUSAMMENFASSUNG**

Obwohl die G-Protein-gekoppelten Rezeptoren (GPCRs) eine gemeinsame Sieben-Transmembran-Domänenstruktur aufweisen, ist nur eine begrenzte Anzahl an Aminosäureresten in ihren Proteinsequenzen konserviert. Eine der am höchsten konservierten Sequenzen ist das *NPxxY*-Motiv, das sich am zytosolischen Ende der Helix VII befindet, vor allem bei den GPCRs, die zur Familie der Rhodopsin/beta-Adrenorezeptor-ähnlichen Rezeptoren (Familie A) gehören. Die Kristallstruktur des bovinen Rhodopsins legt eine hydrophobe Interaktion zwischen Y<sup>7.53</sup> des *NPxxY*-Motivs und F<sup>7.60</sup> in der Helix VIII nahe; außerdem befindet sich die Hydroxyl-gruppe von Y<sup>7.53</sup> in der Nähe von N<sup>2.40</sup> am zytosolischen Ende der Helix II, was auf eine interhelikale Wasserstoffbrücke zwischen Helix VII und Helix II hindeutet (Palczewski *et al.*, 2000). Da die Konservierung einer Sequenz eine wichtige strukturelle und/oder funktionelle Rolle nahelegt, wurde dieses Motiv in Mutagenesestudien schon bei mehreren GPCRs untersucht. Diese Mutationen beeinflussten die Rezeptoraffinität, die Signaltransduktion und die Internalisierung der entsprechenden GPCRs, aber in ziemlich unterschiedlichem Ausmaß in Abhängigkeit von den untersuchten Rezeptoren. Bis jetzt konnte noch keine allgemeine Hypothese ausgearbeitet werden, die alle beobachteten Ergebnisse erklären würde.

Die wichtigste Zielsetzung der vorgestellten Doktorarbeit war die Aufklärung der Funktion des hochkonservierten Tyrosins (Y<sup>7.53</sup>) im *NPxxY*-Motiv des humanen B<sub>2</sub> Bradykinin-Rezeptors (B<sub>2</sub>R) und seiner möglichen Interaktionspartner. Ähnlich wie bovines Rhodopsin, hat auch der humane B<sub>2</sub> Bradykinin-Rezeptor einen Tyrosinrest (Y) in Position 7.53, ein Phenylalanin (F) in Position 7.60, allerdings ein Glutamat (E) in Position 2.40. Letzteres kann aber ebenfalls eine Wasserstoffbrückenbindung mit der Hydroxylgruppe von Y<sup>7.53</sup> bilden.

Um die Interaktion der E<sup>2.40</sup> ↔ Y<sup>7.53</sup> ↔ F<sup>7.60</sup> Loci aufzuklären, haben wir eine Reihe von Rezeptormutanten generiert und sie hinsichtlich der Signaltransduktion, der Liganden-induzierbaren Phosphorylierung, der Rezeptorinternalisierung/Sequestrierung sowie bezüglich der Interaktion mit G<sub>q/11</sub>-Protein und G-Protein-gekoppelte Rezeptorkinasen (GRKs) untersucht. Alle Experimente wurden im Vergleich zu Wildtyp(wt)-Rezeptor durchgeführt.

Die Mutation von F<sup>7.60</sup> in Helix VIII des B<sub>2</sub>R zu Alanin (=F7.60A) hatte keinen großen Einfluss auf die Affinität zu seinem Hauptliganden Bradykinin (BK), auf die Liganden-induzierbare Phosphorylierung, auf die Liganden-Internalisierung und auch nicht auf die Signaltransduktion. Auch die Mutante Y7.53F zeigte vergleichbare Eigenschaften wie der B<sub>2</sub>R wt. Da beide Punkt-Mutanten Y7.53F und F7.60A den Phänotyp des Wildtyps aufweisen,

nehmen wir an, daß die noch vorhandene Interaktion  $Y^{7.53} \leftrightarrow F^{7.60}$  die Abwesenheit einer Interaktion zwischen  $Y^{7.53} \leftrightarrow E^{2.40}$  kompensieren kann und vice versa.

Der Austausch von  $Y^{7.53}$  gegen Alanin (Y7.53A) ergab eine Mutante, in der beide Interaktionen ( $Y^{7.53} \leftrightarrow F^{7.60}$  und  $Y^{7.53} \leftrightarrow E^{2.40}$ ) verloren gingen. Diese Mutante internalisierte den Liganden [ $^3$ H]BK fast genauso schnell wie B<sub>2</sub>R wt. Die Rezeptorsequestrierung dieser Mutante nach Stimulation mit BK war jedoch deutlich reduziert im Vergleich zu B<sub>2</sub>R wt. Konfokale Fluoreszenz-Mikroskopie zeigte, daß im Gegensatz zu B<sub>2</sub>R die Mutante Y7.53A vorzugsweise intrazellulär lokalisiert war, sogar in Abwesenheit von BK. Die zweidimensionale Phosphopeptid-Analyse zeigte, daß die Mutante Y7.53A konstitutiv dasselbe Phosphorylierungsmuster aufwies wie der BK-stimulierte B<sub>2</sub>R wt. Eine Liganden-unabhängige Internalisierung von Y7.53A wurde durch die Aufnahme von Rhodamin-markiertem Antikörper – gerichtet gegen eine Peptidsequenz am N-terminus des mutierten Rezeptors gerichtet waren. Co-Immunopräzipitationsuntersuchungen belegten, daß Y7.53A an G<sub>q/11</sub> vorgekoppelt ist, ohne das G-Protein jedoch zu aktivieren, da die basale Akkumulationsrate für Inositolphosphate (IP) unverändert blieb im Vergleich zum B<sub>2</sub>R wt.

Wir folgern daher, daß die Y7.53A-Mutation beim B<sub>2</sub>R eine semi-aktive Rezeptorkonformation erzeugt, die Liganden-unabhängig phosphoryliert wird und daher auch internalisiert. Der mutierte Rezeptor bindet an sein entsprechendes heterotrimeres G-Protein G<sub>q/11</sub>, wodurch das Ausmass der Liganden-unabhängigen Internalisierung auf Grund einer sterischer Blockade verringert wird.

Während die Mutation von  $Y^{7.53}$  zu Phenylalanin (F) oder von  $F^{7.60}$  zu Alanin (A) die Agonisten-induzierbare Phosphorylierung und Liganden-Internalisierung nicht wesentlich beeinflusste, zeigte die Doppelmutante Y7.53F/F.7.60A eine dramatisch reduzierte Fähigkeit zur Internalisierung, die sehr wahrscheinlich durch ihre fehlende Liganden-induzierte Phosphorylierbarkeit bedingt ist. Auch hier belegte Co-Immunopräzipitationsexperimente, daß das G-Protein G<sub>q/11</sub> bereits an den mutierten Rezeptor gebunden war, was wahrscheinlich zu einer Unzugänglichkeit des mutierten Rezeptors für GRKs führte, und als Folge davon in einer schlechten Phosphorylierbarkeit resultierte. Die Signaltransduktion über das G-Protein G<sub>q/11</sub> hingegen blieb unbeeinflusst.

Die weniger konservative Doppelmutante Y7.53A/F.7.60A zeigte ebenfalls eine schlechte Phosphorylierbarkeit und hatte zudem die Fähigkeit zur Internalisierung verloren. Darüber hinaus war auch das IP-Signal deutlich reduziert. Diese Doppelmutante neigte dazu, mit GRKs auch ohne Stimulation durch einen Agonisten zu interagieren. Aber im Gegensatz zur Mutante

Y7.53A phosphorylierten die GRKs die Doppelmutante weder vor noch nach der Stimulation mit Bradykinin, sondern blieben offensichtlich inaktiv an die Mutante gebunden. Dies führte wahrscheinlich zur Blockade der Signaltransduktion, da das entsprechende G-Protein aus sterischen Gründen keinen Zugang zum Rezeptor erhielt.

Zusammengefaßt zeigen die Daten, daß das hoch konservierte Y<sup>7.53</sup> im NPxxY-Motiv und seine potentiellen Partner F<sup>7.60</sup> und E<sup>2.40</sup> eine wichtige Rolle bei der Interaktion des B<sub>2</sub>R mit dem G-Protein G<sub>q/11</sub> und den GRKs spielen. Die Bindung an die entsprechenden spezifischen G-Proteine und ihre Aktivierung oder die Erkennung durch spezifische Rezeptor-Kinasen erfordert die Präsentation einer besonderen räumlichen Verteilung intrazellulärer Andockstellen, die normalerweise im inaktiven Zustand verborgen sind. Unsere Resultate lassen folglich vermuten, daß die Mutation des Y<sup>7.53</sup>↔F<sup>7.60</sup>-Locus mit einem Mechanismus interferiert, der für die Stabilisierung des Rezeptors im inaktiven Zustand verantwortlich ist. Mutationen in diesen Bereich führen offensichtlich zu einer Änderung der Rezeptorkonformation und demzufolge auch zu veränderten Phänotypen der resultierenden Mutanten. Es liegt nahe anzunehmen, daß eine normale Rezeptoraktivierung ebenfalls über eine Änderung der Interaktion Y<sup>7.53</sup>↔F<sup>7.60</sup> läuft.

Diese Information wird zu einem besseren Verständnis des B<sub>2</sub>R-Aktivierungsmechanismus beitragen. Zusätzlich sollten diese Daten sehr nützlich bei der Herstellung von hochwirksamen B<sub>2</sub>R Agonisten und Antagonisten sein.



**B INTRODUCTION**

Membrane proteins constitute around 30% of all proteins and about 70% of all pharmaceutically relevant proteins, yet they are difficult to characterize due to their biophysical properties. They require an amphiphilic environment to remain soluble, aggregate easily and are generally expressed at low levels. Only a small number of membrane protein structures have been solved by biophysical methods such as X-ray crystallography and NMR. Although G protein-coupled receptors (GPCRs) belonging to the membrane proteins make up to ca. 1 % of all genes present in a mammalian genome (Wess, 1998) and represent approximately 40% of all targets for therapeutic drugs currently available, presently only the crystal structure of bovine rhodopsin has been resolved (Palczewski *et al.*, 2000). Therefore, classical pharmacological assays, mutagenesis studies and biochemical methods are the main tools in the study of GPCR function and regulation.

Out of GPCRs, the human B<sub>2</sub> bradykinin receptor (B<sub>2</sub>R) is an important pharmacological target as several B<sub>2</sub>R antagonists are currently in clinical studies for the treatment of diseases such as hereditary angiooedema or refractory ascites in liver cirrhosis (Marceau & Regoli, 2004). In addition, one of the main drugs given in the treatment of heart failure, the ACE inhibitors (inhibitors of the angiotensin-converting enzyme), exert their beneficial effect through the prevention of angiotensin II release but may also act in part through the reduction of bradykinin degradation via ACE.

B<sub>2</sub>R and its main agonist, bradykinin, are essential parts of the kallikrein-kinin system (KKS). Thus, a brief overview of this system will be given in the first part of the introduction. Moreover, as the highly conserved tyrosine in the *NPxxY* motif seems to play an essential functional role not only in the B<sub>2</sub>R but also in several other GPCRs, the second part of the introduction will deal with some important members of the GPCR superfamily, indicating their characteristic protein structure and modes of action with respect to this motif.

## **B.1 The kallikrein-kinin system (KKS)**

### **B.1.1 Historic background**

In 1909 two French surgeons measured a transient fall in blood pressure in a patient after an intravenous injection of fractions extracted from human urine (Abelous & Bardier, 1909). In 1925, the German surgeon Emil-Karl Frey similarly observed a considerable reduction in blood pressure when he injected the urine of humans into dogs. Together with the biochemist Heinrich Kraut, he attributed this effect to a substance with potential biological functions (Frey & Kraut, 1926; Frey, 1926). "It is a substance that probably originates from several organs, is eliminated by the kidneys and has a pronounced cardioactive and vasoactive effect; a substance that is assigned the role of a hormone in the organism". This substance was later termed kallikrein (KLK) (Kraut *et al.*, 1930). Ten years later, the biochemist Eugen Werle found that KLK is a proteolytic enzyme, which liberates the biologically highly active basic polypeptide kallidin (KD) from a plasma protein termed kallidinogen or kininogen (Werle *et al.*, 1937). Werle also observed the degradation/inactivation of kinins, identified these inactivators as peptidases, and termed them "kininases" (Werle & Grund, 1939).

In 1949, it was discovered that trypsin, when incubated with blood, releases an agent that contracts the guinea-pig ileum (Rocha e Silva *et al.*, 1949). Since the response of this tissue developed slowly, the authors called the agent "bradykinin" (brady = slow). Later, bradykinin (BK) was purified and determined as a nonapeptide (Andrade & Rocha e Silva, 1956). The exact sequence of BK was published by Swiss chemists and the nonapeptide could therefore be chemically synthesized (Boissonnas *et al.*, 1960).

### **B.1.2 Kinins**

Nowadays, the peptides usually referred to as kinins comprise BK and Lys-BK, the latter also known as kallidin (KD), and their carboxypeptidase cleavage products, des-Arg<sup>9</sup>-BK and des-Arg<sup>10</sup>-Kallidin.

BK is a positively charged nonapeptide (Arg-Pro-Pro-Gly-Phe-Ser-Pro-Phe-Arg) that basically can be found in all secretions of the body, i.e. urine, saliva, and sweat, but also in feces and in several tissues, such as the heart, vasculature, blood, kidneys, liver, skin, small intestine, colon, pancreas, salivary glands, reproductive organs, lungs, and adrenal glands (Campbell *et al.*, 1993; Hibino *et al.*, 1994; Madeddu *et al.*, 2001; Meneton *et al.*, 2001; Patel *et al.*, 1999; Schremmer-Danninger *et al.*, 1999). KD has been found in the heart, urine, and circulation (Campbell *et al.*, 1999; Duncan *et al.*, 2000).

These nona- and decapeptides, respectively, are released from their precursors, the high (HMW) and low (LMW) molecular weight kininogens, through the action of the kallikreins (KLK). BK is produced by plasma KLK, whereas KD is generated by tissue KLK. BK can also be derived from KD by several aminopeptidases through cleavage of the amino-terminal lysine. Carboxyl-terminal trimming of BK and KD by carboxypeptidases yields the truncated versions des-Arg<sup>9</sup>-BK and des-Arg<sup>10</sup>-KD (Figure 1).

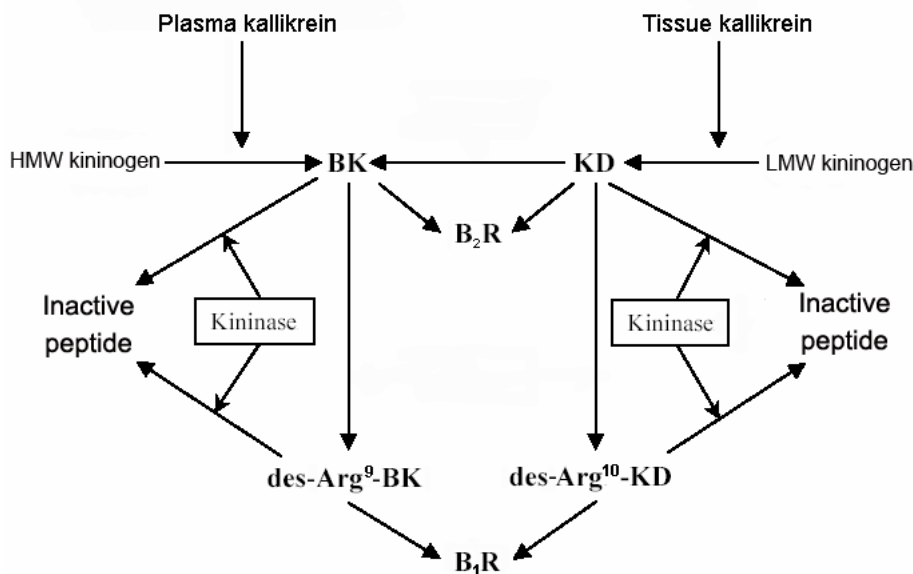


**Figure 1. Schematic representation of the kallikrein-kinin system.**

B<sub>1</sub>R and B<sub>2</sub>R – B<sub>1</sub> and B<sub>2</sub> bradykinin receptors;

KD – kallidin;

BK – bradykinin;

HMW and LMW – high and low molecular weight kininogens.

### B.1.3 Kinin receptors

#### B.1.3.1 General introduction

Kinins induce their effects via two main types of receptors designated B<sub>1</sub> and B<sub>2</sub>, both of which belong to the superfamily of the GPCRs. These two receptors show a 36 % identity, mostly located in the transmembrane regions. The human, dog, mouse, and rat B<sub>2</sub> and B<sub>1</sub> receptors have been cloned, sequenced, expressed and characterized pharmacologically (Hess *et al.*, 1992; Hess *et al.*, 2001; McEachern *et al.*, 1991). BK and KD are selective high affinity ligands of the B<sub>2</sub> receptor, whereas des-Arg<sup>9</sup>-BK and des-Arg<sup>10</sup>-KD are selective ligands of the B<sub>1</sub> receptor (Table 1). The B<sub>2</sub> receptor is generally present in a wide variety of tissues; the B<sub>1</sub> receptor, in contrast, is expressed *de novo* under certain pathological conditions, i.e. inflammation, sepsis, etc. A short comparison of the main characteristics of the bradykinin receptors is presented in the Table 1.

**Table 1. Comparison of the main characteristics of the bradykinin B<sub>1</sub> and B<sub>2</sub> receptors.**

Currently accepted name	B <sub>1</sub> R	B <sub>2</sub> R
<i>Structural information</i>	353 aa (human)	391 aa (human)
<i>Selective agonists</i>	des-Arg <sup>9</sup> -BK des-Arg <sup>10</sup> -KD	BK KD (Lys-BK)
<i>Selective antagonist</i>	des-Arg <sup>9</sup> -[Leu <sup>8</sup> ]-BK des-Arg <sup>9</sup> -HOE 140	NPC17731* HOE 140*
<i>Main signal transduction mechanism</i>	G <sub>q/11</sub> (increase IP <sub>3</sub> */DAG*)	G <sub>q/11</sub> (increase IP <sub>3</sub> */DAG*)
<i>Expression</i>	<i>de novo</i>	ubiquitous

\* Abbreviations: see page I.

Genomic sequencing of the human chromosomal regions encoding the B<sub>1</sub> and B<sub>2</sub> receptors revealed that the two genes are located in tandem orientation with the B<sub>2</sub> receptor gene being proximal to the B<sub>1</sub> receptor gene, separated by an intergenic region of only 12 kb (Cayla *et al.*, 2002). The close proximity of the two genes clearly suggests that they evolved from a common ancestor by a gene duplication event.

The B<sub>1</sub>R is one of the few receptors belonging to the family of rhodopsin/β<sub>2</sub>-adrenergic-like GPCRs which is not get internalized, i.e. sequestered to intracellular compartments upon agonist stimulation (Austin *et al.*, 1997). It does, however, respond with translocation to caveolae but these remain essentially on the cell surface (Sabourin *et al.*, 2002; Lamb *et al.*, 2002). No phosphorylation of B<sub>1</sub>R either under basal conditions or after stimulation has been detected (Blaukat *et al.*, 1997; Pizard *et al.*, 1999).

The B<sub>2</sub>R is encoded in humans by a single copy gene which is located on chromosome 14 (Powell *et al.*, 1993) and more precisely at 14q32 (Ma *et al.*, 1994; Kammerer *et al.*, 1995). The gene structure is arranged in three exons and two introns and codes for a single transcript of approximately 4 kb. The cDNA coding for the human B<sub>2</sub>R contains three in-frame methionine codons which could be used as an initiation site for translation (the first two in-frame AUG codons are located on exon-2 and the third on exon-3 together with the part coding for the seven transmembrane spanning sequence segments). Initially, the third in-frame AUG of the human B<sub>2</sub> receptor mRNA was assumed to be the preferred start codon (Hess *et al.*, 1992) giving rise to a 364 amino acid residues protein. Later it was demonstrated that the B<sub>2</sub>R mRNA is translated from the first in-frame initiator AUG codon, however, presence or absence of this extra segment of 27 amino acid residues does not significantly alter the binding characteristics of the receptor

(Abd-Alla *et al.*, 1996). Thus, the coding region of the human B<sub>2</sub>R is located in the second and third exons (Ma *et al.*, 1994). The full-length human B<sub>2</sub>R is composed of 391 amino acid residues with a calculated molecular weight of 41 kDa (Abd-Alla *et al.*, 1996).

In most primary and cultured cells the B<sub>2</sub>R is modified by complex glycosylation resulting in a broad 60–80 kDa band after electrophoretic separation (Blaukat *et al.*, 1996).

The intracellular C-terminal domain of the B<sub>2</sub>R has two potential palmitoylation sites that, at least in CHO, COS-7, and HEK293 cells can both be modified by esterification (Pizard *et al.*, 2001). The palmitoylation is thought to associate the receptor carboxyl tail with the plasma membrane, thus creating a fourth intracellular loop.

It has been reported that binding of BK to the B<sub>2</sub>R endogenously expressed in PC12 cells or transiently expressed in *HEK293* cells resulted in the formation of receptor dimers/oligomers and the amino-terminus of the receptor seemed to be involved in this dimerization (Abd-Alla *et al.*, 1999). The functional importance of receptor dimerization has not been clarified so far.

### **B.1.3.2 The signalling pathways of the kinin receptors**

In all cells analyzed till now, kinin receptors couple after stimulation to G $\alpha_{q/11}$  proteins leading to an activation of phospholipase C- $\beta$  (PLC- $\beta$ ) and subsequent generation of second messengers: inositol-1,4,5-trisphosphate (Ins 1,4,5-P<sub>3</sub>), diacylglycerol (DAG) and calcium. The increase in intracellular calcium can activate the NO/cGMP pathway that primarily mediates the strong hypotensive effect of kinins in the vasculature. Furthermore, DAG and calcium, alone or in combination, activate several isoforms of protein kinase C (PKC) that participate in a number of cellular signalling pathways, including those that control cell proliferation (Tippmer *et al.*, 1994; Nishizuka, 1992).

In addition to PLC- $\beta$ , kinin receptors can also activate phospholipase A<sub>2</sub> and D as well as sphingosine kinase resulting in increased cellular concentrations of lipidic second messengers: arachidonic acid (subsequently converted to prostaglandins), phosphatidic acid, and sphingosine 1-phosphate (Burch & Axelrod, 1987; Blaukat *et al.*, 2000; Blaukat *et al.*, 2001). Prostaglandins and sphingosine 1-phosphate may be released from the cells and act in an autocrine and paracrine manner via their specific GPCRs. Prostaglandins are assumed to be the key mediators of the bradykinin-induced edema formation, but it is yet completely unknown whether phosphatidic acid and sphingosine 1-phosphate also participate in physiological actions of kinins.

The B<sub>2</sub>R can also stimulate GDP/GTP exchange of G $\alpha_i$  and G $\alpha_s$  (Table 2) in many cell types. Activation of G $\alpha_s$  and G $\alpha_i$  modulates intracellular cAMP levels and thus protein kinase A (PKA)

activity (Graness *et al.*, 1997). The bradykinin-induced  $G\alpha_i$  stimulation observed in several cells has recently gained attention because of its involvement in the activation of the ERK/MAPK cascade and mitogenic signalling (Blaukat *et al.*, 2000; Liebmann, 2001). While the biochemical signalling pathways have been elaborated to some extent, the physiological significance of the  $B_2R$  mediated  $G\alpha_i$  and  $G\alpha_s$  activation remains to be determined.

In addition to the well-established association with heterotrimeric G proteins, direct and functional interactions of the  $B_2R$  with a number of signalling molecules including phospholipase C- $\gamma$ 1 (Venema *et al.*, 1998), endothelial nitric oxide synthase (Marrero *et al.*, 1999), angiotensin-converting enzyme (ACE), Janus kinases (Ju *et al.*, 2000), and signal transducers and activators of transcription (Marcic *et al.*, 2000) have been reported.

The  $B_2$  receptor gene knockout mouse showed to have increased blood pressure, heart weight/body weight ratio and exaggerated pressure response to angiotensin II infusion and chronic dietary salt loading (Maddedu *et al.*, 1997).

### B.1.3.3 Regulation of the kinin receptors

Given the remarkable physiological effects of kinins, it is obvious that the action of the kinins and their receptors must be carefully controlled.

The kinin signalling pathways are regulated at multiple levels:

1. As the kinins have a very short half-life [ $<15$  s in the plasma (Roberts & Gullick, 1990)], physiologically active concentrations of these peptides are presumably only locally generated. They are subjected to rapid degradation, for example, by ACE and neutral endopeptidase (Bhoola *et al.*, 1992).
2. Activated heterotrimeric G protein hydrolyse the bound GTP to GDP as a result of their intrinsic GTPase activity returning to their inactive GDP-bound ground state.
3. However, impairment of the ability of receptors to activate G proteins appears to be most important for regulation and seems to involve an agonist-induced receptor phosphorylation, desensitization, sequestration/internalization and down-regulation.

*Desensitization* is the phenomenon of attenuation or even loss of the functional response under repeated or continuous agonist stimulation (Böhm *et al.*, 1997). GPCR desensitization is primarily mediated by second-messenger responsive kinases, such as PKA and PKC, and by G protein-coupled receptor kinases (GRKs).

*Phosphorylation* by GRKs causes the recruitment of the cytosolic protein  $\beta$ -arrestin, which binds to the phosphorylated receptor, thereby uncouples it from the G-protein and promotes the receptor internalization.

The endogenously expressed B<sub>2</sub>R in human fibroblasts becomes rapidly phosphorylated in response to stimulation by its cognate ligand (Blaukat *et al.*, 1996). This has also been observed in other native cell lines such as human umbilical vein endothelial cells (Blaukat, personal communication) indicating that ligand-induced phosphorylation of the B<sub>2</sub>R is a general feature in the regulation of this receptor.

Two-dimensional phosphopeptide mapping of B<sub>2</sub>R revealed that the unstimulated B<sub>2</sub>R in *HEK293* cells as well as in human fibroblasts displays basal phosphorylation of S<sup>348</sup>, the physiological role of which remains to be elucidated. Activation of the receptor with BK resulted in the phosphorylation of three additional amino acid residues: pS<sup>339</sup>, pS<sup>346</sup>, and pT<sup>342</sup> (Blaukat *et al.*, 2001).

A correlation between agonist-induced phosphorylation of B<sub>2</sub>R tail and desensitization has been observed for endogenous and recombinant receptors (Blaukat *et al.*, 1996; Blaukat *et al.*, 2001). Using a mutagenesis approach, it could also be shown that B<sub>2</sub>R phosphorylation triggers its internalization into intracellular compartments, thus rendering B<sub>2</sub>R inaccessible for further ligand stimulation (Pizard *et al.*, 1999).

The *sequestration/internalization* of many GPCRs, in particular of the β<sub>2</sub>-adrenergic receptors, involves β-arrestin and dynamin-dependent formation of clathrin-coated vesicles (Laporte *et al.*, 2002) and/or caveolin-rich vesicles (Chini & Parenti, 2004). Early events following agonist stimulation in DDT1 MF-2 (hamster smooth muscle cells) or A431 cells (a human epithelial carcinoma cell line) include redistribution of B<sub>2</sub>R in caveolae and the formation of endocytic vesicles that are not clathrin-coated (de Weerd & Leeb-Lundberg, 1997; Haasemann *et al.*, 1998). In COS-7 cells internalization of B<sub>2</sub>R could be inhibited by co-expression of dominant-negative forms of arrestin or dynamin (Pizard *et al.*, 1999) but not in *HEK293* cells (Lamb *et al.*, 2001). So, the sequestration of B<sub>2</sub>R seems to depend on the cell types where the receptors are expressed and/or on the applied experimental conditions.

The fate of the internalized B<sub>2</sub>R – *down-regulation* or *recycling back* to the plasma membrane – is still unclear and currently a matter of intensive studies. For the reuse of the receptor it appears that internalization of the receptors is essential for the resensitization process, since inhibition of internalization delays the dephosphorylation (Blaukat & Müller-Esterl, 1997) and therefore renewed capacity to signal.

The fate of endogenously expressed B<sub>2</sub>R on human fibroblasts during prolonged agonist treatment was also studied. Stimulation of the B<sub>2</sub>R on human fibroblasts with bradykinin for up to 24 h resulted in a strong reduction of surface binding sites that was paralleled by a similar decrease of total B<sub>2</sub>R protein confirmed by Western blotting. However, B<sub>2</sub>R mRNA levels did

not change during 24 h of agonist treatment, in spite of the fact that the receptor *de novo* synthesis was attenuated by 35-50%. This demonstrates that the B<sub>2</sub>R expression during long-term agonist treatment is primarily regulated on the (post)translational level, i.e., by attenuation of *de novo* synthesis and by reduction of receptor stability (Publication D).

## **B.2 Superfamily of G protein-coupled receptors (GPCRs)**

### **B.2.1 Structure and classification of GPCRs**

Cell surface receptors belonging to the superfamily of GPCRs – also known as seven-transmembrane domain, heptahelical, or serpentine receptors – are involved in the regulation of diverse signalling processes. Among the different families of transmembrane receptors, GPCRs form the largest superfamily. Molecular cloning studies and genome data analyses have revealed ca. 1200-1300 members of the GPCR superfamily in mammalian genomes (Schöneberg *et al.*, 2002), most of them, however, being receptors for odorants.

The structure of GPCR is composed of a single polypeptide chain of variable length that traverses the lipid bilayer seven times, forming transmembrane helices and alternating extracellular and intracellular loops (Figure 2).

The members of this superfamily are involved in a wide variety of biological processes ranging from neurotransmission and hormonal control of virtually all physiological responses to perception of taste, smell, light, and pain (Claing *et al.*, 2002).

Different classification schemes can be used to subdivide the GPCR superfamily. Based on sequence similarity, mammalian GPCRs tend to fall into one of three families:

- rhodopsin/β-adrenergic-receptor-like family or class A.
- glucagons-receptor-like family or class B.
- metabotropic glutamate neurotransmitter receptor family or class C.



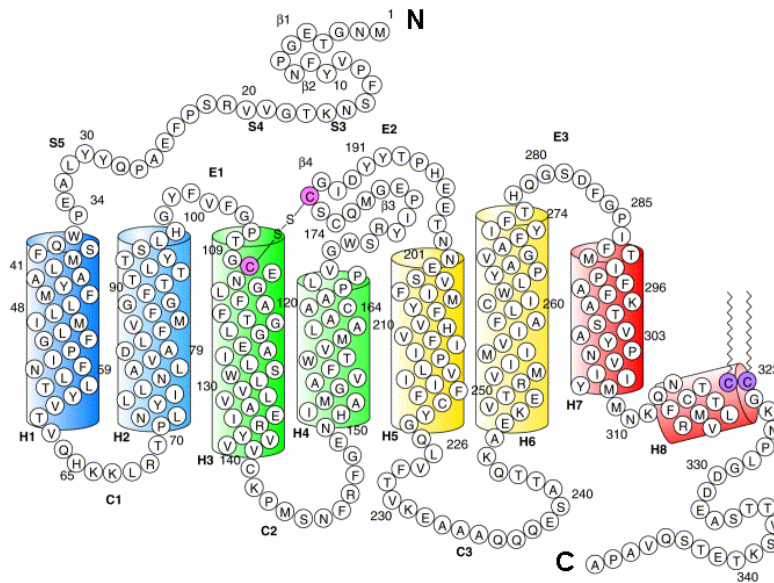


**Figure 2. The secondary structure of bovine rhodopsin.**

Amino acid residues are depicted in single letter code. The amino-terminal tail (N) and extracellular domains are depicted towards the top and the carboxy-terminal tail (C) with the cytoplasmic domains are shown towards the bottom. Transmembrane  $\alpha$ -helical segments (H<sub>I</sub>-H<sub>VII</sub>) and helix VIII (H<sub>VIII</sub>) are given as cylinders (from Sakmar, 2002).

The rhodopsin/ $\beta$ -adrenergic-like receptors (class A) form by far the largest family. Although the members of this family do not share a high overall sequence identity, they have a characteristic pattern of a few highly conserved residues and motifs (ca. 20 aa in all) in analogous positions (most of them located in the transmembrane domains). They are hallmarks of this class and are not present in the other GPCR classes B or C. One of the most highly conserved motifs, together with the *E/DRY* sequence at the cytosolic end of transmembrane domain III (TMD III), is the NPxxY sequence (where *x* usually represents a hydrophobic residue and *N* is rarely exchanged against *D*) located at the C-terminus of TMD VII.

High conservation of protein sequences often indicates an important functional or structural role. Conserved amino acid patterns can be responsible for protein stability (or protein folding) or they can interact to form the scaffold required for the conformational rearrangements that result in receptor activation (Wess *et al.*, 1993; Baldwin, 1994; van Rhee & Jacobson, 1996; Wess, 1997). As all GPCRs are thought to operate through coupling to a limited number of G proteins (often stimulating different types of G proteins depending on e.g. the cell type) one can assume that some of the conserved motifs are involved in a conserved molecular mechanism of G-protein recruitment and/or activation (promotion of the GDP/GTP exchange). And finally, desensitization plays a pivotal role in the regulation of receptor activity. Consequently,

conserved amino acid residues may take part in the interaction and/or activation of e.g. G protein-coupled receptor kinases (GRKs) and  $\beta$ -arrestins.

### **B.2.2 The highly conserved tyrosine of *NPxxY*: facts and assumptions**

The present research was focused on the investigation of the role of the highly conserved tyrosine in the *NPxxY* motif. Although it has been investigated intensively so far in many GPCRs, there is no single theory capable to explain all the received results. One of the first functions claimed for a *NPxxY* sequence in GPCRs was that of being an endocytotic motif. This hypothesis was based on the observation that a similar sequence, *NPxY*, plays a fundamental role in the internalization of the low density lipoprotein (LDL) receptor because replacement of the tyrosine by an alanine residue abrogated the internalization capacity of this receptor (Trowbridge *et al.*, 1993). Moreover, a naturally occurring mutation of this tyrosine to cysteine in the LDL receptor was found in some patients with familiar hypercholesterolemia (Brown & Goldstein, 1976).

In GPCRs, mutation of the tyrosine in the *NPxxY* motif affected receptor affinity (Prioleau *et al.*, 2002; Hukovic *et al.*, 1998; Wang *et al.*, 1997), signalling (Böhm *et al.*, 1997; Prioleau *et al.*, 2002; Fritze *et al.*, 2003; Rosendorff *et al.*, 2000), sequestration (Bouley *et al.*, 2003; Barak *et al.*, 1994), and internalization (Hunyady *et al.*, 1995) but to quite different extents, depending on the receptor under study. This may, in part, reflect the microenvironment surrounding this motif in the respective receptor sequence, the assays applied, or the cells used for expression.

### **B.2.3 Rhodopsin: function of the helix VIII and *NPxxY* motif**

Bovine rhodopsin is a prominent member of class A GPCRs. Although being a visual pigment, rhodopsin shares many similarities with other GPCRs, but it also displays many specialized features not found in other GPCRs. In particular, rhodopsin is an integral membrane protein located only in the outer segment of rod cells and is made up by the apoprotein opsin plus the chromophore retinal. The latter is not a ligand in the classical sense because it is linked covalently via a protonated Schiff base to a conserved lysine residue (K<sup>7.43</sup>) within its TMD<sub>VII</sub>. 11-*cis*-retinal acts as an inverse agonist, as the opsin in the absence of the retinal has low basal activity. The visual pigment is activated by light-induced *cis-trans* isomerization of the bound retinal.

Rhodopsin activates a specific G protein termed G<sub>t</sub> or transducin (Table 2). Light-dependent rhodopsin phosphorylation is catalyzed primarily by the specific rhodopsin kinase (GRK1) and a special visual arrestin binds to the phosphorylated rhodopsin to prevent it from activating G<sub>t</sub>.

Finally, rhodopsin does not become internalized in response to activation and therefore has to be reactivated while remaining in the plasma membrane.

Currently, a high-resolution crystal structure is available only for bovine rhodopsin (Palczewski *et al.*, 2000) (Figure 3, *right*). Because the crystal structure depicts the inactive rhodopsin structure that does not interact significantly with cytoplasmic proteins, it can provide only indirect information about the activated state.

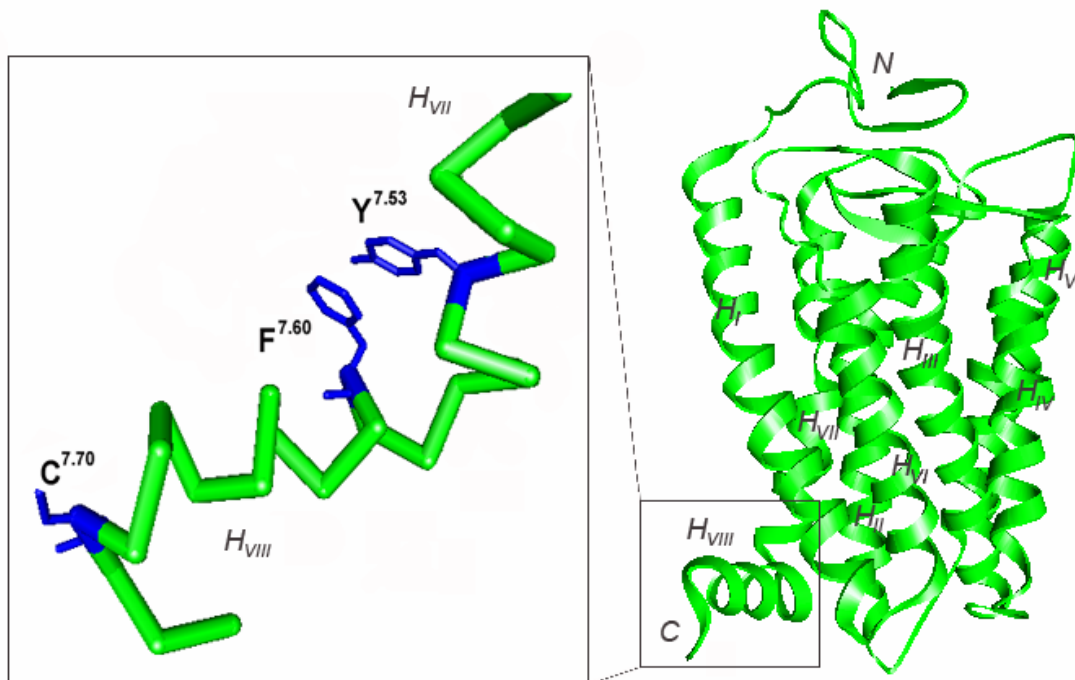


**Figure 3. Ribbon diagram of rhodopsin derived from the crystal structure.**

The amino-terminus (N) and extracellular surface are shown towards the top of the figure and the carboxyl-terminus (C) and intracellular surface towards the bottom. Seven transmembrane segments ( $H_I$ - $H_{VII}$ ), characteristic of GPCRs, are given.

A three-dimensional model of the  $NPxxY$  motif and neighboring helix  $H_{VIII}$  based on the crystal structure of rhodopsin showing proximity of the  $Y^{7.53}$  and  $F^{7.60}$  side chains is depicted in the *inset*.

One of the most striking features of this rhodopsin structure is the presence of the helix VIII ( $H_{VIII}$ ), which begins just beyond helix VII and appears to lie roughly parallel to the plane of the membrane.  $H_{VIII}$  extends from  $N^{7.57}$  to  $C^{7.71}$  where the palmitoyl groups linked to  $C^{7.70}$  and  $C^{7.71}$  by thioester bonds are anchored in the membrane bilayer (Teller *et al.*, 2001). The environment around  $H_{VIII}$  is partially hydrophobic which may lead to increased helical stability (Sakmar *et al.*, 2002).

$H_{VIII}$  might be best described as a cationic amphipathic  $\alpha$ -helix, with  $L^{7.58*}$  and  $R^{7.61}$  on one face of the helix and  $F^{7.60}$ ,  $M^{7.64}$ , and  $L^{7.69}$  buried in the hydrophobic core of the bilayer. High

conservation of F<sup>7.60</sup> and R<sup>7.61</sup> suggests that the amphipathic character of H<sub>VIII</sub> may be functionally important.

Moreover, the crystal structure of rhodopsin indicates a hydrophobic interaction between Y<sup>7.53</sup> and F<sup>7.60</sup> (Palczewski *et al.*, 2000) (Figure 3, *left*). Spin labels introduced at the positions of Y<sup>7.53</sup> and its companion phenylalanine in the H<sub>VIII</sub> showed strong immobilization, consistent with the tertiary interaction found in the crystal structure (Altenbach *et al.*, 1999). Activation induced a change in the mobility of H<sub>VIII</sub>, complementing an immunological study (Abdulaev & Ridge, 1998) that showed exposure of an epitope spanning the junction of TMD<sub>VII</sub> and H<sub>VIII</sub>.

The function of the Y<sup>7.53</sup> and F<sup>7.60</sup> amino acid residues was intensively investigated in the rhodopsin molecular by mutagenic approach (Fritze *et al.*, 2003). Replacement of Rho-Y<sup>7.53</sup> or Rho-F<sup>7.60</sup> with alanine facilitated formation of Meta II state (active form of rhodopsin) that was surprisingly accompanied by a reduction of the light-induced affinity of these pigments toward cognate G protein. Furthermore, the authors suggested that the interaction between Y<sup>7.53</sup> and F<sup>7.60</sup> residues is disrupted during the Meta I/Meta II transition, as a disulfide bond linking residues 7.53 and 7.60 prevented Meta II formation, whereas the reduced form of the mutant readily transformed to Meta II after illumination. This interaction could be one of the critical constrains holding rhodopsin in the inactive state.

High-resolution crystal structure of the bovine rhodopsin showed also that the hydroxyl group of Y<sup>7.53</sup> is close to N<sup>2.40</sup> (cytoplasmic border of H<sub>II</sub>), which is also highly conserved, suggesting the presence of additional interhelical hydrogen-bonding constraints between H<sub>VII</sub> and H<sub>II</sub> (Palczewski *et al.*, 2000).

There have been also reports that this region of rhodopsin interacts directly with G<sub>t</sub> protein. More precisely, the amino-terminal region of the fourth cytoplasmic loop of rhodopsin presumably interacts with the C-terminal peptide of the  $\alpha$ -subunit of G<sub>t</sub> (Ernst *et al.*, 2000; Marin *et al.*, 2000).

---

\* Here and later the numbering scheme of Ballesteros/Weinstein (1995) has been used. According to it, the most conserved residue in a transmembrane segment was named by the number of the helix followed by the number 50. Upstream residues are then named by counting down, downstream residues by counting up from 50. For example, the most conserved amino acid residue in the helix VII is proline from the NPxxY motif, therefore it was named as P<sup>7.50</sup>. In turn, the tyrosine from the same motif is named Y<sup>7.53</sup>. Helix VIII is not a transmembrane helix, therefore its amino acid residues are also counting down from P<sup>7.50</sup>.

The C-terminus distal to the palmitoylated C<sup>7.70</sup> and C<sup>7.71</sup> residues appears to be highly disordered and dynamic based upon the results of site-directed electron paramagnetic resonance spin labeling (Langen *et al.*, 1999).

#### **B.2.4 $\beta_2$ -Adrenergic receptor: general characteristics and function of the high conserved tyrosine of NPxxY motif**

The  $\beta_2$ -adrenergic receptor ( $\beta_2$ -ADR) was the first GPCR to be cloned (Dixon *et al.*, 1986; Kobilka *et al.*, 1987) and has served as a prototype for elucidating the molecular mechanisms involved in GPCR regulation. Along with the visual pigment rhodopsin, it has been one of the most extensively studied members of the class A.

The exposure of the  $\beta_2$ -ADR to catecholamines initiates its biological response via coupling to the stimulatory G protein ( $G_s$ ), which then mediates the stimulation of adenylyl cyclase (Gilman, 1987). However, this receptor-mediated adenylyl cyclase response to agonist is followed by a rapid desensitization. Several studies have demonstrated that the functional uncoupling of the  $\beta_2$ -ADR from  $G_s$  is the consequence of its phosphorylation by specific kinases that, in turn, serves to promote the binding of  $\beta$ -arrestin to the receptor and its sequestration to an intracellular compartment (von Zastrow *et al.*, 1993).

Mutation of tyrosine residue 7.53 in the NPxxY motif to an alanine ( $\beta_2$ -ADR-Y7.53A) resulted in the complete loss of ligand-induced phosphorylation as well as sequestration (Barak *et al.*, 1994). In addition, the ability to activate adenylyl cyclase was markedly reduced (Gabilondo *et al.*, 1996). Receptor phosphorylation could only be partially reconstituted, for example, through overexpression of GRK2 ( $\beta$ ARK1) (Ferguson *et al.*, 1995). Moreover, insertion of an additional amino acid residue in the NPxxY motif (NPLIY  $\rightarrow$  NPLIAY) of  $\beta_2$ -ADR – i.e. displacement of Y<sup>7.53</sup> – also resulted in abolishment of receptor sequestration, phosphorylation and signalling similar to  $\beta_2$ -ADR-Y7.53A mutant (Barak *et al.*, 1995). In that way, not only the amino acid but also its precise position appears to be important.

### B.2.5 Short characteristics of the G proteins

Heterotrimeric G proteins comprise three kinds of subunits ( $\alpha$ ,  $\beta$ , and  $\gamma$ ). The  $\alpha$ -subunits are the largest in apparent size ( $M_r = 39\ 000 - 52\ 000$ ), contain the binding site for guanine nucleotides, and are the most diverse as more than 20 different  $\alpha$ -subunits have been identified so far (Wess, 1998). On the basis of amino acid similarity, the G protein  $\alpha$ -subunits can be grouped into several major classes. Historically, G proteins are named according to classes of their  $\alpha$ -subunits, meaning, for instance, that  $G_q$  is a G protein including  $G\alpha_q$  (Table 2) without further specification of the  $\beta$  or  $\gamma$  subunits, as in most cases their subtypes is not known.

**Table 2. Major classes of mammalian trimeric G proteins and their effectors.**

Classes	Associated effector	2 <sup>nd</sup> Messenger	Receptor examples
* $G_{q/11}$	**PLC- $\beta$	Ins 1,4,5- $P_3$ $\uparrow$ , DAG $\uparrow$	$B_1R$ and $B_2R$
$G_s$	Adenylyl cyclase	cAMP $\uparrow$	$\beta_2$ -ADR
$G_i$	Adenylyl cyclase	cAMP $\downarrow$	$\beta_1$ -ADR, $B_2R$
$G_t$	cGMP phosphodiesterase	cGMP $\downarrow$	Rhodopsin

\* The  $G_{q/11}$  class includes  $G_q$ ,  $G_{11}$ ,  $G_{14}$ ,  $G_{15}$  proteins

\*\* Abbreviations: see page I.

The  $\beta\gamma$  complexes are extremely stable and are, therefore, usually regarded as one functional unit. The inactive form of the G protein consists of the GDP bound  $\alpha$ -subunits and  $\beta\gamma$ -complexes. Interaction of the ligand-activated receptor with the G protein triggers the change of GDP to GTP and results in the dissociation of the G protein from the receptor as well as of the  $\alpha$ -subunit from the  $\beta\gamma$ -complex. The  $\alpha$ -GTP and the free  $\beta\gamma$ -complex are then able to interact with distinct effector enzymes and ion channels leading to the desired physiological response. For example,  $B_2R$  realizes its major effect through the activation of a  $G_q$  protein that leads to the activation of phospholipase C- $\beta$  (PLC- $\beta$ ) and generation of inositol 1,4,5-triphosphate (Ins 1,4,5- $P_3$ ) and diacylglycerol (DAG). The  $\beta_2$ -adrenergic receptor is coupled to  $G_s$  protein that activates the membrane-bound enzyme adenylyl cyclase resulting in the synthesis of the second messenger cAMP (Table 2). Because of the intrinsic GTPase activity of the  $\alpha$ -subunit, the bound GTP is eventually hydrolysed to GDP, allowing the  $\alpha$ -subunit to re-unite with a free  $\beta\gamma$ -complex returning all subunits to the inactive state.

### B.3 Aim of the thesis

The principal goal of my thesis was the investigation of the *significance and function of the highly conserved tyrosine in the NPxxY motif of the human B<sub>2</sub> bradykinin receptor*. In particular, attempts have been made to elucidate the roles of this tyrosine residue in B<sub>2</sub>R signalling, phosphorylation and internalization/sequestration through mutagenesis studies. Moreover, using the same approach, we set out to identify the microenvironment surrounding this amino acid residue in the receptor, i.e. to localize possible interaction partners of this residue, in order to gain insight into the mechanisms of signal transduction and receptor desensitization as consequences of structural changes within a receptor molecule.

To reach our aim, we applied the following working program:

- Generation of expression plasmids harbouring genes to mutate the tyrosine of the *NPxxY* motif in the B<sub>2</sub>R.
- Expression of the receptor mutants in mammalian cells, if possible as stably expressing clones.
- Pharmacological and biochemical characterization of the expressed mutants, including receptor binding properties, internalization and signal transduction capacity, receptor localization, agonist-induced phosphorylation and interaction with adaptor proteins (cognate G proteins and GRKs).
- Development of a model that can explain the obtained results within the frame of the classical theory of GPCR activation/desensitization and possibly also the results observed with the  $\beta_2$ -ADR-Y7.53A mutant and other published “tyrosine mutants” of A-type GPCRs.

**C MATERIALS AND METHODS****C.1 Materials****C.1.1 Equipment**Balances:

Analytic Balance, A 120 S (0-12 g range)

Sartorius, Göttingen

Analytic Balance, 3716MP (0-250 g range)

Sartorius, Göttingen

β-Counter

Liquid Scintillation Analyzer, Mod. 2300TR

Packard, Meriden, CT

β-γ-Counter, LB122

Berthold Technology, Canada

Cell Incubators:Type B5060 EC-CO<sub>2</sub>

Heraeus Sepatech, München

Centrifuges:

Kontron, Centrikon H-401 with rotor A8.24

Kontron Instruments, Eching

Heraeus, Varifuge 3.2 RS

Heraeus Sepatech, München

Heraeus, Sepatech Biofuge A (rotor 1230)

Heraeus Sepatech, München

Heraeus, Sepatech Biofuge A (rotor 3042)

Heraeus Sepatech, München

Clean Bench:

BDK 7419, Mod. UVF 6.18S

BDK, Sonnenbühl-Genkingen

Herasafe type HS18/2

Heraeus Instruments, München

ELISA-Reader

DigiScan 400

ASYS Hitech GmbH, Austria

PCR Thermal Cycler:

Primus type 25

MWG-Biotech, Ebersberg

Power Supply:

Type EPS 301

Amersham-Pharmacia-Biotech

Mod. 2103

LKB, Biochrom

Protein Transfer Apparatus:XCell *SureLock*<sup>TM</sup> Mini-Cell

Invitrogen, Karlsruhe

Sonifier

Type B12

Branson Sonic Power Company, Danburg

Spectral Confocal Microscope

Zeiss LSM 410

Carl Zeiss, Thornwood, NY, USA

Fluorescence Microscopes

Olympus IX-70

Olympus Optical Co., LTD, Tokyo, Japan

Other Equipments

Filtration device

Hoeffler Instruments, San Francisco, CA

2D-Electrophoresis apparatus, HTLE-7000-02

CBS, Del Mare, USA

Dounce homogenizer, type 853202

B.Braun, Melsungen, Germany



### C.1.2 Chemicals and materials

#### Chemicals for the molecular biology techniques

Gel Extraction Kit	Qiagen (Hilden, Germany)
QIAprep Spin Miniprep (and Maxiprep) Kit	Qiagen (Hilden, Germany)
PCR primers	Invitrogen (Groningen, Netherlands)

#### Enzymes

Restrictase <i>Bam HI</i>	New England BioLabs (England)
Restrictase <i>Hind III</i>	Hybaid (Heidelberg, Germany)
Restrictase <i>Xho I</i>	New England BioLabs (England)
T <sub>4</sub> -DNA ligase (EC 6.5.1.1)	Roche (Mannheim, Germany)
<i>Taq</i> DNA polymerase	Qiagen (Hilden, Germany)
<i>Pfu</i> DNA polymerase	Stratagene (La Jolla, CA, USA)

#### Cell culture

DMEM-medium	PAA (Cölbe, Germany)
DMEM phosphate-free-medium	PAA (Cölbe, Germany)
Dulbecco's PBS (1×)	PAA (Cölbe, Germany)
Trypsine/EDTA (1×)	PAA (Cölbe, Germany)
Poly-D-lysine hydrobromide	Sigma (Taufkirchen, Germany)
FuGENE 6	Roche (Mannheim, Germany)
FCS	PAA (Cölbe, Germany)
Hygromycin B	PAA (Cölbe, Germany)

#### Enzyme inhibitors

Aprotinin	Sigma (Taufkirchen, Germany)
Bacitracin	Sigma (Taufkirchen, Germany)
Captopril	Sigma (Taufkirchen, Germany)
Leupeptin	Sigma (Taufkirchen, Germany)
Okadaic acid	Calbiochem (Bad Soden, Germany)
1.10-Phenantroline	MERCK (Darmstadt, Germany)
Pefabloc SC	MERCK (Darmstadt, Germany)
Pepstatin A	Sigma (Taufkirchen, Germany)
Sodium orthovanadate	Sigma (Taufkirchen, Germany)

#### Detergents

CHAPS	Sigma (Taufkirchen, Germany)
Deoxycholic acid	Sigma (Taufkirchen, Germany)
Nonidet P-40	Sigma (Taufkirchen, Germany)
SDS	Serva (Heidelberg, Germany)
Triton X-100	Sigma (Taufkirchen, Germany)
Tween 20	Sigma (Taufkirchen, Germany)

**Antibodies**

Anti-HA-antibody, rat monoclonal clone 3F10	Roche (Mannheim, Germany)
Rhodamine-labeled-anti-HA, mouse monoclonal	Roche (Mannheim, Germany)
HRP-labeled-anti-HA antibody, rat monoclonal	Roche (Mannheim, Germany)
Anti-HA matrix, immobilized, rat monoclonal	Roche (Mannheim, Germany)
Anti-B <sub>2</sub> bradykinin receptor antibody, mouse	BD Transduction Laboratories
Anti-G <sub>q</sub> - antibody, rabbit polyclonal	Santa Cruz (Heidelberg, Germany)
Anti-Gs-antibody, rabbit polyclonal	Santa Cruz (Heidelberg, Germany)
Anti-GRK 2/3, mouse monoclonal	Sigma (Taufkirchen, Germany)
HRP-labeled goat anti-rabbit antibody	DAKO (Glostrup, Denmark)
HRP-labeled rabbit anti-rat antibody	DAKO (Glostrup, Denmark)
HRP-labeled horse anti-mouse antibody	New England BioLabs, England

**Radioactive chemicals**

Myo-[2- <sup>3</sup> H]-inositol (21 Ci/mmol)	PerkinElmer Life Sciences (Boston, MA)
[2,3-Prolyl-3,4- <sup>3</sup> H]bradykinin (108 Ci/mmol)	PerkinElmer Life Sciences (Boston, MA)
[ <sup>3</sup> H]NPC17731	PerkinElmer Life Sciences (Boston, MA)
[ <sup>32</sup> P]Orthophosphate (500 mCi/ml)	ICN (Eschwege, Germany)
[ <sup>35</sup> S]GTP $\gamma$ S (1250 mCi/mmol)	PerkinElmer Life Sciences (Boston, MA)

**Miscellaneous**

AG 1-X8 anion exchange columns	BioRad (Munich, Germany)
Bradykinin	Bachem (Heidelberg, Germany)
Chemiluminescence's reagent plus	PerkinElmer Life Sciences (Boston, MA)
Cellulose TLC plates	MERCK (Darmstadt, Germany)
Glass fiber filters (Whatman GF/C)	Adi Hassel (Munich, Germany)
HyperFilm ECL	Amersham (Buckinghamshire, UK)
Liquid scintillation mixture	ZINSSER ANALYTIC (Frankfurt, Germany)
Medical X-ray film	Fuji (Tokyo, Japan)
Micro BSA protein assay reagent	Pierce (Rockford, IL)
Nitrocellulose membrane 0.45 $\mu$ m	BioRad (Munich, Germany)
Protein G agarose	Roche (Mannheim, Germany)
Protein markers	BioRad (Munich, Germany)
Sequencing grade trypsin	Promega (Mannheim, Germany)
TMB peroxidase EIA substrate kit	BioRad (Munich, Germany)

- JE049 was a generous gift from Jerini AG (Berlin, Germany).
- Anti-serum AS346/2 and monoclonal MBR1 antibody were kindly supplied by Prof. Dr. Werner Müller-Esterl (Frankfurt/Main, Germany).
- All other reagents were of analytical grade and are commercially available from MERCK, SIGMA or ROTH.

### C.1.3 Strains and cell lines

#### ***Bacterial strain***

*E. coli* Top 10 (Invitrogen)

Lab. strain # 1557

Genotype: F<sup>-</sup> mcrA  $\Delta$ (*mrr-hsdRMS-mcrBC*)  $\phi$ 80*lacZ* $\Delta$ M15  $\Delta$ *lac* X74 *deoR* A1 *araD*139  
 $\Delta$ (*ara-leu*)7697 *galU galK rpsL* (Str<sup>R</sup>) *endA1 nupG*

#### ***Mammalian cell line***

*Flp-In*<sup>TM</sup> *T-REx*<sup>TM</sup>-293 (Invitrogen)

Cell type: Human Embryonic Kidney (HEK) cells

Collected from: European Collection of Cell Culture

Cytogenetics: 2n=46

This cell line contains a single stably integrated FRT site at a transcriptionally active genomic locus.

### C.1.4 Expression vectors

#### pcDNA5/FRT vector

##### Comments for pcDNA/FRT

CMV promoter: bases 232-819

CMV forward priming site: bases 769-789

T7 promoter/priming site: bases 863-882

Multiple cloning site: bases 895-1010

BGH reverse priming site: bases 1022-1039

BGH polyadenylation signal: bases 1028-1252

FRT site: bases 1536-1583

Hygromycin resistance gene (no ATG): bases 1591-2611

SV40 early polyadenylation signal: bases 2743-2873

pUC origin: bases 3256-3929 (complementary strand)

Ampicillin resistance gene: bases 4074-4934

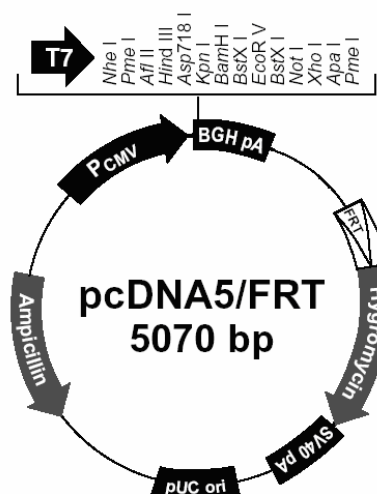


**Figure 4. Schematic representation of the pcDNA5/FRT (Invitrogen).**

The vector was designed for stable expression of the gene of interest in mammalian hosts. It has a multiple cloning site that contains cleavage sites for several common restriction endonucleases.

#### pOG44 vector

##### Comments for pOG44 vector:

CMV promoter: bases 234-821

Synthetic intron: bases 871-1175

FLP gene: bases 1202-2473

SV40 early polyadenylation signal: bases 2597-2732

pUC origin: bases 3327-3993

Ampicillin resistance gene: bases 4138-4998

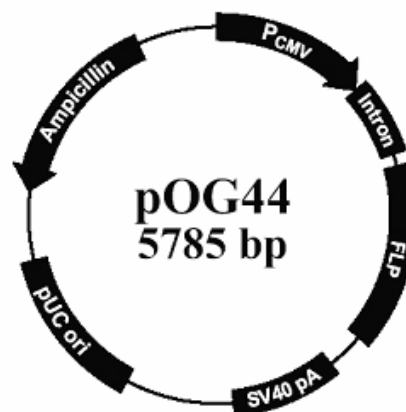


**Figure 5. Schematic representation of the vector pOG44 (Invitrogen).**

This vector expresses the Flp recombinase under the control of the CMV promoter. Flp recombinase is a member of the integrase family of recombinases, which mediates a site-specific recombination reaction between interacting DNA molecules via pairing of interacting FRT (*FLP* Recombinase Target) sites.

### C.1.5 Oligonucleotides used as primers for PCR amplification

#### General primers:

CMV SE	5'-GTACATGACCTTATGGGACTTTCC -3'
BGH AS	5'-GGCAACTAGAAGGCACAGTCGAGG -3'
<i>Bam</i> HI - B <sub>2</sub> R SE	5'- <u>GGATCC</u> *ATGCTCAATGTCACCTTGC-3'
<i>Xho</i> I - B <sub>2</sub> R AS	5'- <u>CTCGAG</u> *TTTGCTCACTGTCTGC-3'
<i>Bam</i> HI - ADR SE	5'- <u>GGATCC</u> *ATGGGGCAACCCGGGAACGGCAGC-3'
<i>Xho</i> I - ADR AS	5'- <u>CTCGAG</u> *TTACAGCAGTGAG TCATTTGTACTAC-3'
<i>Bam</i> HI - GFP SE	5'-GCT <u>GGATCC</u> *ATGGTGAGCAAGGGCGAGGAG-3'
<i>Xho</i> I - GFP AS	5'-ACAT <u>CTCGA</u> *GTTACTTGTACAGCTCGTCCATGCC-3'

#### Point mutated primers:

F7.60A SE	5'-CGTGATCGTGGGCAAG <u>CG</u> **CGCCCCGAAAGAAGTCTTGGGAGG-3'
Y7.53A SE	5'-CCTCAACCCACTGGTGG <u>CC</u> **GTGATCGTGGGCAAGC-3'
Y7.53F SE	5'-CCTCAACCCACTGGTGT <u>TC</u> **GTGATCGTGGGCAAGC-3'

#### Chimera primer:

B2eGFP SE	5'- GGACTGGGCAGGGAGCAGACAGATGGTGAGCAAGGGCGAGGAG-3'
-----------	----------------------------------------------------

\* Underlined sequence represents the restriction site for the indicated restrictase.

\*\* Underlined sequence represents the point mutation.

### C.1.6 Computer programs

- Adobe Acrobat Writer 5.0
- 3D-Mol Viewer 5.1 of Vector *NTI* Suite 7.1
- Internet Explorer
- Macromedia Flash MX
- Office XP, 2003
- Opera 7.23 for Windows
- Photoshop 7.0, CS
- Prism 3.03
- Reference Manager 10
- *SE* Central
- TotalLab v2.01
- Windows 2003 Professional

### C.1.7 Solutions

#### Solutions used in molecular and cell biological methods

TAE buffer	40 mM Tris, 20 mM acetate, 2 mM EDTA pH 8.3
Loading buffer	30% (w/v) glycerol, 0.25% (w/v) bromophenol blue, 0.25% (w/v) xylencyanol FF, 0.25% (w/v) orange G
SOC medium	20 g/l Bacto-tryptone, 5 g/l Bacto-yeast extract, 10 mM MgCl <sub>2</sub> , 20 mM glucose, 10 mM NaCl, 10 mM KCl pH 7.0
LB growth medium	10 g/l Bacto-tryptone, 5 g/l Bacto-yeast extract, 10 g/l NaCl

#### Solutions used in protein chemical methods

RIPA buffer	50 mM Tris-HCl, 150 mM NaCl, 1% Nonidet P-40, 0.5% sodium deoxycholate, 0.1% SDS, 2 mM EDTA, pH 7.5
Sample buffer	5% (w/v) SDS, 30% glycerol, 150 mM Tris-HCl, 1% (w/v) Coomassie Brilliant Blue G-250 pH 6.8
Running buffer	24 mM Tris-HCl, 192 mM glycine, 0.1% (w/v) SDS pH 8.25
Homogenization buffer	20 mM HEPES/Na HEPES, 10 mM EDTA pH 7.4
½ Towbin buffer	50 mM Tris-HCl, 40 mM glycine, 20% (w/w) methanol
Blocking buffer	0.25% gelatin in 50 mM Tris-HCl, 150 mM NaCl, 5 mM EDTA, 0.05% Triton X-100 pH 7.5
TBS buffer	50 mM Tris-base, 150 mM NaCl pH 7.5
Electrophoresis buffer for phosphopeptide mapping	formic acid/acetic acid/water 46:156:1790 (v/v/v) pH 1.9
Chromatography buffer	isobutyric acid/n-butanol/pyridine/acetic acid/water 1250:38:96:58:558 (v/v/v/v/v)

#### Solutions used in pharmacological methods

Incubation buffer	40 mM PIPES, 109 mM NaCl, 5 mM KCl, 0.1% glucose, 0.05% BSA, 2 mM CaCl <sub>2</sub> , 1 mM MgCl <sub>2</sub> , 2 mM bacitracin, 0.8 mM 1.10-phenanthroline, 100 μM captopril pH 7.0
Dissociation solution	0.2 M acetic acid, 0.5 M NaCl pH 2.7
Assay buffer	20 mM HEPES/Na-HEPES, 100 mM NaCl, 10 mM MgCl <sub>2</sub> , 1 μM GDP pH 7.4

## C.2 Methods

### C.2.1 Molecular biological methods

#### C.2.1.1 Polymerase chain reaction (PCR)

DNA fragments were amplified and mutagenized by PCR.

Primers were designed following standard rules. Firstly, the length of primer complementary to the template should be 18-25 nucleotides to minimize problems of nonspecific annealing. Secondly, the G+C content should be between 40 % and 60%. Thirdly, the melting temperature calculated by the formula:

$$T_m \text{ (in } ^\circ\text{C)} = 2(A+T) + 4(G+C),$$

where (A + T) is a sum of the A and T residues and (G + C) is a sum of the G and C residues in the oligonucleotide should not be less than 50°C. The designed primers were synthesized by Invitrogen or MWG and are listed in section C.1.5.

Two properties are required of thermostable DNA polymerase used for mutagenesis of denaturated plasmid template: an efficient proofreading activity and a lack of terminal transferase activity. Therefore, in all following reactions *Pfu* polymerase was used that completely satisfied the above-listed regulations.

The PCR was used for the following purposes:

1. Attachment of the restriction sites

To clone a DNA insert into a cloning vector, both were treated with two restriction enzymes that created compatible ends. Whereas cloning vector pcDNA5/FRT has multiple cloning sites including cleavage sites for *Bam* III and *Xho* I restriction endonucleases (Figure 4), cleavage sites for above cited restrictases by DNA insert were introduced using PCR. For that pairs of primers were designed with restriction sites for *Bam* III in the 5' region of the sense-primer and for *Xho* I in the 5' region of the anti-sense primer (section C.1.5). To improve restrictive reaction (some restriction enzymes fail to cleave recognition sequences located close to the end of linear double-stranded DNA fragments) 3-4 additional bp were introduced at the 5' end of each primer (Figure 6). After PCR, the amplified DNA fragment was digested with the appropriate restriction enzyme and ligated into the multiple cloning site of a linearized vector.

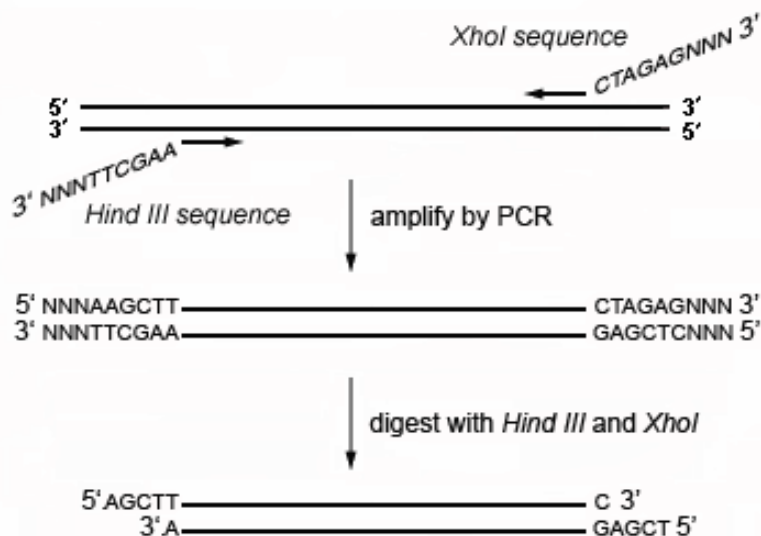


**Figure 6. Cloning of PCR product by addition of restriction sites.**

Specific PCR primers were designed to amplify a region of interest with the *Hind* III (at the beginning) and *Xho* I (at the end) recognition sequences for the restriction endonuclease included at the 5' end of the primer. To achieve high efficiency digestion, additional nucleotides were included on both sides of the restriction endonuclease sequence.

## 2. Site-directed mutagenesis

For the site-directed mutagenesis of the  $B_2R$  and  $\beta_2$ -ADR the so-called “megaprimer method” was applied. This method uses three oligonucleotide primers and two rounds of PCR. One of the oligonucleotides is mutagenic, containing the desired base substitution(s), and the other two are forward and reverse primers that lie upstream and downstream from the binding site for the mutagenic oligonucleotide. The flanking primers were complementary to sequences in the cloned gene or to adjacent vector sequences. The mutagenic primer was oriented towards the nearer of the two flanking primers so that the length of the megaprimer was kept to a minimum (Figure 7A).

The mutagenic oligonucleotide was designed to a length of 20-25 bases. The desired mutation, and therefore the mismatched region of the primer, was located in the middle of the primer with 8-12 correctly matched bp on each side of the mismatched region (for less than 3 mismatching bp).



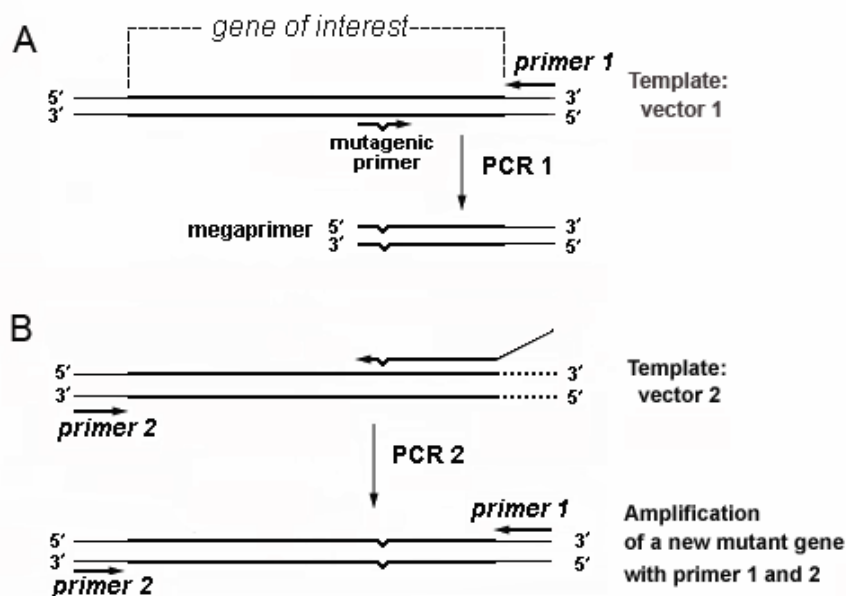


**Figure 7. The principle of the “megaprimer method”.**

A) PCR1 was performed with a mutagenic primer and an outside primer (primer 1) to generate and amplify a double-stranded megaprimer.

B) The “megaprimer” was purified and used with an additional outside primer (primer 2) in PCR 2 to obtain the desired full-length mutant. To increase the efficacy of PCR 2, the primer 1 was added to the reaction mixture and as a template was used wild-type DNA embedded into another vector not containing a site for primer 1.

The first PCR was performed according to Table 3 using the mutagenic internal primer designed as it was described before and the first flanking primer (Figure 7A).

**Table 3. Composition of the PCR 1 used in the megaprimer method.**

Components	Working concentration	Stock	Volume
Template 1	0.1 µg	-	-
PCR buffer	1×	10×	3 µl
<i>Pfu</i> polymerase	0.05 U/µl	2.5 U/µl	0.6 µl
Primer 1	0.2 µM	10 µM	0.6 µl
Mutagenic primer	0.2 µM	10 µM	0.6 µl
Solution Q	1×	5×	3 µl
dNTP	0.8 mM	10 mM	2.4 µl
H <sub>2</sub> O	-	-	to 30 µl

The first PCR was carried out according to the following cycle program:

<i>Denaturation</i>	92°C	3 min
<i>Cycle (25 ×)</i>		
<i>Denaturation</i>	92°C	30 sec
<i>Annealing</i>	50°C	30 sec
<i>Elongation</i>	72°C	60 sec/1000 bp
<i>Elongation</i>	72°C	10 min
<i>Storage</i>	4°C	∞

The product of this first PCR - the “megaprimer” - was purified as described in section C.2.1.4. In the first and second PCRs the used wild type templates were embedded into two different vectors. In this case the usage of the primer 1 in the PCR 2 led to preferable amplification of the newly synthesized mutated DNA as to amplification of the wild-type template (Figure 7B). The reaction mixture of the PCR 2 was also prepared according to Table 4.

**Table 4. Composition of the PCR 2 used in the megaprimer method.**

<b>Components</b>	<b>Volume</b>
Template 2	0.1 µg
PCR buffer	3 µl
<i>Pfu</i> polymerase	0.6 µl
Primer 1	0.6 µl
Primer 2	0.6 µl
Megaprimer	3 µl
Solution Q	3 µl
dNTP	2.4 µl
H <sub>2</sub> O	to 30 µl

A longer region of the template DNA was amplified using the following cycle program:

<i>Denaturation</i>	92°C	3 min
<i>Cycle (35 ×)</i>		
<i>Denaturation</i>	92°C	30 sec
<i>Annealing</i>	53°C	60 sec
<i>Elongation</i>	72°C	90 sec
<i>Elongation</i>	72°C	10 min
<i>Storage</i>	4°C	∞

The final PCR product containing the desired mutation was separated by gel electrophoresis (section C.2.1.3) and purified from agarose (section C.2.1.4).

### 3. Generation of the B<sub>2</sub>eYFP chimera

The coding region of the B<sub>2</sub>R gene and the eYFP gene were fused using the megaprimer method in a two-step reaction. The stop codon of the B<sub>2</sub>R was omitted, whereas the first methionine of the eYFP-construct was included. A 43-bp chimera-primer contained 22 bp encoding C-terminal amino acids of B<sub>2</sub>R followed by 21 bp encoding the proximal end of the eYFP gene (Figure 8A).

As described before, a megaprimer was prepared in the PCR 1 according to Table 2 using the pEYFPC-3 (CLONTECH) gene as a template and chimera primer (Figure 8B).

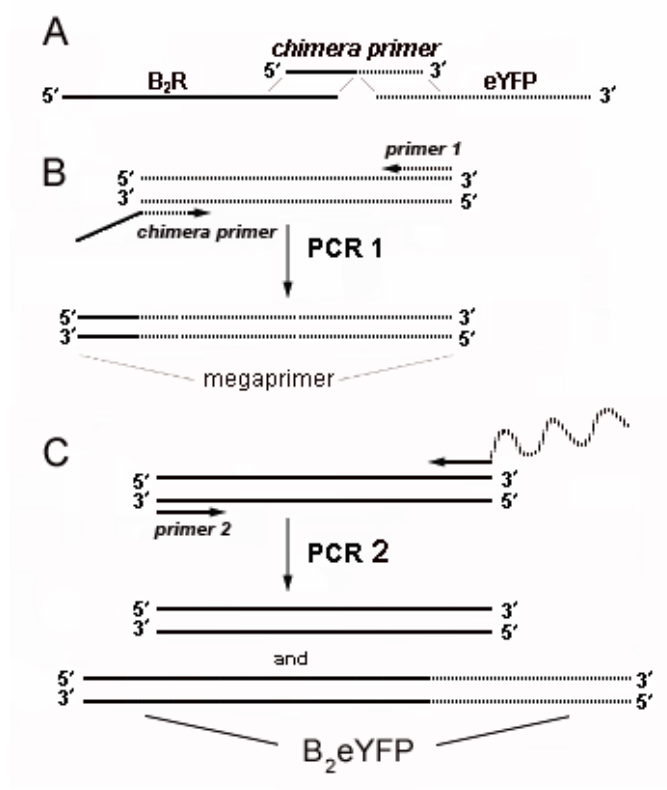


**Figure 8. Generation of the eYFP chimera.**

A) The chimera-primer contained C-terminal amino acids of B<sub>2</sub>R followed by the proximal end of the eYFP gene.

B) PCR 1 was performed with a mutagenic chimera primer and the reverse primer for eYFP (primer 1) to generate and amplify a double-stranded megaprimer.

C) The megaprimer was purified and used with the forward primer for B<sub>2</sub>R (primer 2) in PCR 2 to obtain the desired full-length chimera mutant.

The first PCR reaction was carried out using the following cycle program:

<i>Denaturation</i>	92°C	10 min
<i>Cycle (25 ×)</i>		
<i>Denaturation</i>	92°C	30 sec
<i>Annealing</i>	50°C	30 sec
<i>Elongation</i>	72°C	60 sec
<i>Elongation</i>	72°C	10 min
<i>Storage</i>	4°C	∞

The megaprimer was purified by agarose gel electrophoresis and extracted using a gel extraction kit.

A second PCR mixture (Table 5) contained B<sub>2</sub>R gene as the template, the megaprimer described above and the reverse primer for eYFP (Figure 8C).

**Table 5. Composition of the PCR 2 used for eYFP chimera generation.**

Components	Volume
B <sub>2</sub> R	0.3-0.4 µg
PCR buffer	3 µl
<i>Pfu</i> polymerase	0.6 µl
Reverse primer for eYFP	0.6 µl
Megaprimer	5 µl
Solution Q	3 µl
dNTP	2.4 µl
H <sub>2</sub> O	to 30 µl

The second PCR reaction was carried out using the following cycle program:

<i>Denaturation</i>	92°C	10 min
<i>Cycle (25 ×)</i>		
<i>Denaturation</i>	92°C	30 sec
<i>Annealing</i>	45°C	30 sec
<i>Elongation</i>	72°C	2 min
<i>Elongation</i>	72°C	10 min
<i>Storage</i>	4°C	∞

The final PCR product was a 1.8-kb fragment containing the B<sub>2</sub>R coding sequence fused to the eYFP gene. This B<sub>2</sub>eYFP fragment was extracted from agarose gel (section C.2.1.4).

### C.2.1.2 DNA cleavage with restriction endonucleases

Optimal buffer conditions were chosen for each restriction enzyme digest according to supplier's information. The reaction mixture was prepared on ice according to the protocol for DNA restriction mentioned below. DNA was usually digested at 37°C for about 1 h.

#### Protocol for DNA restriction

DNA	2 µg
Restrictase	2 µl (2 unit)
Buffer	2 µl
H <sub>2</sub> O	to 20 µl

### C.2.1.3 Agarose gel electrophoresis

For preparation of the gels, agarose was dissolved in TAE buffer in a microwave oven. The final concentration of agarose was 0.5-2 % depending on the size of the separated DNA fragments. Ethidium bromide was added to a final concentration of 1 µg/ml for later visualization of the DNA under UV light. The loading buffer was added to the samples (ratio 1:5) before loading the gel in order to control the separation during the run.

The running buffer was also TAE. Electrophoretic separation was achieved by constant currents at 5-7 V/cm for about 30 min. The gels were observed under UV light (312 nm) and the size of the fragments was determined by comparing their mobility with that of DNA standards. To avoid DNA degradation UV radiation was carried out as short as possible.

### C.2.1.4 Extraction of DNA fragments from agarose gels

After separation of the DNA fragments by agarose gel electrophoresis, the band corresponding to the fragment of interest was isolated using the QIAquick gel extraction kit following the protocol of the supplier:

- The band of interest was cut out with a scalpel.
- The agarose gel slice containing the DNA fragment was solubilized by addition of the buffer QX1 and by incubation shaking for 10 min at 50°C. The high concentration of a chaotropic salt in buffer QX1 disrupts hydrogen bonding between sugars in a agarose polymer and promotes the dissociation of DNA binding proteins from the DNA fragments.
- The DNA fragment was selectively bound to a silica-gel resin in the presence of a high concentration of chaotropic salts (buffer QX1).
- Salts were washed out by the PE buffer containing ethanol.
- Residual PE buffer was removed by an additional centrifugation step.

- DNA was typically eluted with 10  $\mu$ l of 10 mM Tris-HCl, pH 8.5 or water, as elution is most efficient under low salt concentration and basic conditions. As the pH is critical for binding and therefore for DNA recovery, the pH was controlled even when water was used.

#### **C.2.1.5 Ligation of DNA fragments**

The insert obtained after adding restriction sites (section C.2.1.1) and pcDNA5/FRT vector were restricted with *Bam* III and *Xho* I (section C.2.1.2). A 3-5 molar excess of DNA fragment (estimated by intensity of the bands on the agarose gel) was added to a linearized vector in a final volume of 10  $\mu$ l at RT. 1  $\mu$ l (1 U/ $\mu$ l) of T<sub>4</sub> ligase as well as 1  $\mu$ l of T<sub>4</sub> ligase buffer were then added on ice. The ligation mixture was incubated 1 h in a waterbath at 16°C.

#### **C.2.1.6 Culture of *E. coli* strains**

LB (*Luria Bertani*) growth medium was sterilized by autoclaving for 20 min at a pressure of  $1.2 \times 10^5$  Pa and a temperature of 121°C. The ampicillin was added to the media in the concentration 50 mg/ml when the temperature was below 50°C. 15 g/l agar was added for the preparation of LB plates before autoclaving.

For short term storage the strains were spread onto agar plates containing the appropriate antibiotics and then stored at 4°C (for not longer than 4 weeks).

#### **C.2.1.7 Transformation of *E. coli***

Transformation of *E. coli* strains was performed by heat shock reaction with slight modification of the supplier protocol.

2  $\mu$ l of the ligation reaction (section 2.1.5) or plasmid (< 0.1  $\mu$ g) was added to 15-25  $\mu$ l of competent cells (*E. coli* TOP 10) and mixed gently in a 1.5 ml reaction cup. After incubation on ice for 30 min, the cells were heat shocked for 30 sec in a waterbath at 42°C without shaking. The tubes were immediately transferred onto ice and incubated there for another 2 min. After addition of 100  $\mu$ l of SOC medium the tube was shaken at 37°C for 1 h and then again placed on ice. The whole volume of the transformation mixture was spread on a LB plate containing 50 mg/ml ampicillin and incubated overnight at 37°C.

To screen and select cell colonies that had the correct plasmid insert colony-PCR was used. This method is appropriate for determining whether or not a specific colony on a plate has the desired sequence.

The reaction mixture was prepared in an application tube on ice according to Table 6. A small part of colony was picked from the agarose plate with a plastic tip and resuspended in 15  $\mu\text{l}$  of reaction mixture. Usually 3-4 colonies were checked.

**Table 6. Composition of the colony-PCR reaction.**

Components	Working concentration	Stock	Volume
PCR buffer	1 $\times$	10 $\times$	1.5 $\mu\text{l}$
Taq polymerase	0.05 U/ $\mu\text{l}$	5 U/ $\mu\text{l}$	0.15 $\mu\text{l}$
Primer 1	0.5 $\mu\text{M}$	10 $\mu\text{M}$	0.75 $\mu\text{l}$
Primer 2	0.5 $\mu\text{M}$	10 $\mu\text{M}$	0.75 $\mu\text{l}$
Solution Q	1 $\times$	5 $\times$	3 $\mu\text{l}$
dNTP	0.8 mM	10 mM	1.2 $\mu\text{l}$
H <sub>2</sub> O	-	-	7.55 $\mu\text{l}$

The PCR was carried out according to the following cycle program:

<i>Denaturation</i>	92°C	3 min
<i>Cycle (25 <math>\times</math>)</i>		
<i>Denaturation</i>	92°C	30 sec
<i>Annealing</i>	50°C	30 sec
<i>Elongation</i>	72°C	60 sec/1000 bp
<i>Elongation</i>	72°C	10 min
<i>Storage</i>	4°C	$\infty$

Analysis of the PCR products was performed by agarose gel electrophoresis (section C.2.1.3).

### C.2.1.8 Plasmid preparation from *E.coli*

For most purposes like testing of recombinant DNA by restriction endonuclease digestion, for DNA sequencing or transfection with the *Flp-In* system plasmid DNA was prepared from 6 ml overnight cultures of recombinant *E.coli* using the QIAprep Spin Miniprep Kit. This kit is based on a modified alkaline lysis procedure protocol (Birnboim & Doly, 1979) of the cell pellet.

Bacteria were lysed under alkaline conditions in the presence of RNase A, and the lysate was subsequently neutralized. Afterwards, the chromosomal DNA was discarded by centrifugation, and the soluble plasmid DNA was selectively bound to a silica-gel membrane of QIAprep column which was washed twice in order to eliminate all the other contaminants (proteins, RNA, and low molecular weight impurities). Elution from the column was achieved by addition of water or 10 mM Tris-HCl, pH 8.5.

### C.2.1.9 Confirmation of correct DNA sequence

If a new plasmid was made only by cleavage and restriction, correctness of DNA ligation was checked by cleavage using the same restriction nucleases.

As the DNA-polymerases sometimes induce mistakes, after site-directed mutagenesis or generation chimera mutants DNA sequencing was performed by a commercial service (MediGenomix, Martinsried, Germany).

### C.2.1.10 Determination of DNA concentration

The concentration of DNA was determined spectroscopically by measuring the absorbance at 260 nm. For a 50 µg/ml solution of dsDNA the absorption coefficient was assumed to be 1 (1 cm pathlength) (Sambrook & Gething, 1989). 5 µl of DNA sample was dissolved in 495 µl of water or TAE buffer. The final concentration of DNA was calculated by the following formula:

$$C_{\text{DNA}} (\mu\text{g/ml}) = 50 \mu\text{g/ml} \times \text{dilution factor} (\times 50) \times \text{OD}_{260}.$$

The purity of the preparation was estimated by measuring the UV absorption spectrum at 260 and 280 nm. The absorbance ratio  $A_{260\text{nm}}/A_{280\text{nm}}$  (between 1.8 and 2.0) was calculated to detect the presence of proteins.

## C.2.2 Cell culture methods

### C.2.2.1 Culture of mammalian cells

*HEK293* cells were grown as adherent monolayers at 37°C, 5% CO<sub>2</sub>/air in DMEM supplemented with 10 % fetal calf serum (FCS) and 100 Unit·ml<sup>-1</sup>/100 µg·ml<sup>-1</sup> penicillin-streptomycin. Under optimal conditions, *HEK293* cells double every 18-24 h and were normally subcultured twice a week according to the following procedure: After removing the old medium, cells were washed twice with PBS. Subsequently, we added the appropriate volume of EDTA-trypsin solution to the culture flasks and the cells were incubated at RT for 5-10 min. Trypsinization was stopped by resuspending the cells in complete growth media and plating them on cell culture plates for experiments. For experiments that required rinsing of the cells, the plates were shortly prewashed with 0.01% poly-D-lysine hydrobromide ( $M_r > 300,000$ ) in PBS to improve the cell adherence to the flask surface.



### C.2.2.2 Cell freezing and thawing

Cells were spun down under sterile conditions for 2-5 min at 200 g. The cell pellet was maintained on ice and carefully resuspended in cold freezing medium (DMEM with 10 % FCS, penicillin-streptomycin and 7 % DMSO) by pipetting the suspension repeatedly up and down. 1.8 ml aliquots were quickly dispensed into freezing vials (4°C). The cells were slowly frozen at -20°C for 1 h and then at -70°C overnight. The next day, they were transferred to liquid nitrogen.

In order to thaw cells a freezing vial was removed from liquid nitrogen and put in a waterbath at 37°C. The cells were then dispensed in 5 ml of warm complete growth medium and spun down at 200 g for 10 min. Then the old medium was removed and the cells were resuspended in fresh medium. The medium was changed once more after 24 h.

### C.2.2.3 *Flp-In* expression system

As the main expression system we used the *Flp-In*<sup>TM</sup> system from Invitrogen which was selected because it allows integration and expression of our gene of interest in mammalian cells at the specific genomic location.

The *Flp-In*<sup>TM</sup> system contains three main components (Figure 9):

- The first major component of the *Flp-In*<sup>TM</sup> system is *Flp-In*<sup>TM</sup> cell line containing a single integrated FRT site. Flp-In<sup>TM</sup> T-REx<sup>TM</sup>-293 cell line was bought from Invitrogen.
- The second major component of the described system is the pcDNA5/FRT (Figure 4) expression vector into which the gene of interest was cloned. Expression of the gene of interest is controlled by the CMV promoter. The vector also contains the hygromycin resistance gene with a FRT site which is embedded in the 5' coding region and lacks a promoter and the ATG initiation codon.
- The third major component of the *Flp-In*<sup>TM</sup> system is the pOG44 (Figure 5) plasmid which expressed the Flp recombinase under control of the CMV promoter. Flp recombinase is a member of the integrase family of recombinases which mediates a site-specific recombination reaction between interacting DNA molecules via pairing the interacting FRT (FLP Recombinase Target) sites.

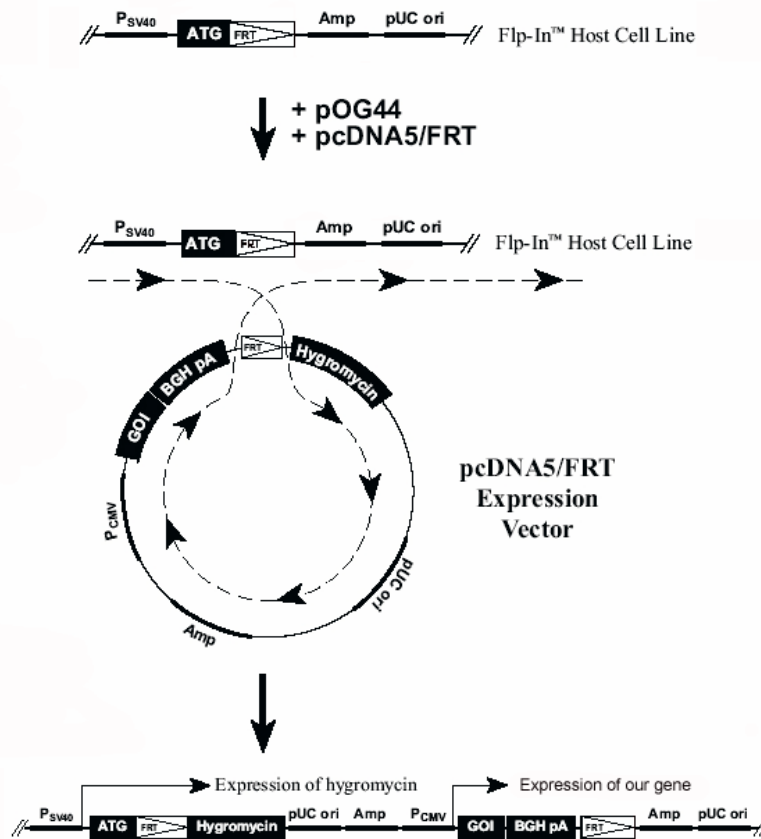


**Figure 9. Diagram of the *Flp-In*<sup>TM</sup> system.**

pUC ori: replication origin, Ampicillin: ampicillin resistance gene, SV40 pA: simian virus polyadenylation sites, P<sub>CMV</sub>: cytomegalovirus promoter. T7: T7 promoter and binding site. BGH pA and SV40 pA: bovine growth hormone and simian virus polyadenylation sites, respectively.

The pOG44 plasmid and the pcDNA5/FRT vector with the gene of interest were co-transfected into the *Flp-In*<sup>TM</sup> *T-REx*<sup>TM</sup>-293 cell line. Upon co-transfection, the Flp recombinase expressed from pOG44 mediated a homologous recombination between the FRT sites (integrated into the genome and on pcDNA5/FRT) such that the pcDNA5/FRT construct was inserted into the genome at the integrated FRT site. Insertion of pcDNA5/FRT into the genome at the FRT site brought the SV40 promoter and the ATG initiation codon (integrated in the *Flp-In*<sup>TM</sup> cell line) into proximity with the hygromycin resistance gene. Thus, stable *Flp-In*<sup>TM</sup> expression cell lines can be selected for hygromycin resistance (Figure 9).

The *Flp-In*<sup>TM</sup> system provides a number of advantages:

- It allows the generation of *isogenic* stable cell lines meaning that all clones of one construct have the same amount of receptors per cell. This facilitates the interpretation of the results and comparison of the different constructs. Traditional methods for creating

stable cell lines result in the integration of the gene of interest at random locations throughout the host genome leading to expression variability between clones, because protein expression levels are affected by the location of genomic integration.

- The system permits polyclonal selection of stable expression cell lines.
- The generation of the cell lines is quite rapid and efficient.

The wild type B<sub>2</sub>R gene and all other constructs started with the third encoded methionine (Hess *et al.*, 1992) which initially was assumed to be the start codon.

All receptor coding sequences were preceded at the N-terminus by a single hemagglutinin (HA)-tag (MGYPYDVPDYAGS), with the last two amino acids (Gly-Ser) of the tag being generated by the insertion of a *Bam*HI site and were cloned into the *Hind*III and the *Xho*I sites of the pcDNA5/FRT vector (Figure 4).

#### C.2.2.4 Transfection of *HEK293* cells

Due to a variety of experimental approaches, the following protocol was found to be optimal for our cells: 100 µl of serum-free medium, 1.6 µg of pOG44, 0.4 µg of plasmid of interest and 5 µl of FuGENE<sup>TM6</sup> Reagent were mixed in a well of 96-well plate. This mixture was incubated at 37°C for 15 min. Then the mixture was added dropwise directly to cells (with < 60% confluence) growing on 6- or 12-well plates in the complete DMEM medium supplemented with FCS.

Next day the cells were trypsinized and transferred to a 100-mm dish. After 2 days, hygromycin B was added to the medium in a concentration 250 µg/ml and selection was started. After another 3 days the medium was changed and cells were incubated without hygromycin.

Within approximately 12 days after transfection 6-20 clones were usually observed. The clones were then transferred to a 12-well plate by picking with a plastic tip. When enough cells were available the ligand binding was estimated in a binding assay at 4°C using 10 nM of radio-labelled bradykinin ([<sup>3</sup>H]BK) (section C.2.3). Clones exhibiting similar high binding activity were considered to represent a single insertion of the pcDNA5/FRT vector - containing the receptor gene - at the recombinase target site (usually at least 3 out of 6 clones). Cells with twice as much binding activity were presumed to have an additional insertion of the vector (rare), clones with less binding activity were assumed to be inhomogenous and were not further propagated or reselected with hygromycin B.

### C.2.3 [<sup>3</sup>H]Bradykinin binding studies

For the determination of the receptor affinity  $K_d$ , confluent monolayers on 24-well/48-well trays were rinsed three times with PBS at 4°C and incubated with 0.3/0.2 ml of ice-cold incubation buffer containing increasing concentrations of [<sup>3</sup>H]BK (10 concentrations ranging from ~0.01 to 30 nM) for at least 90 min on ice. The incubation was stopped by rinsing the cells four times with ice-cold PBS. The cell monolayer was then lysed in 0.2 ml of 0.3 M NaOH and transferred to a scintillation vial. To calculate specific binding, the nonspecific binding (usually less than 5% of total binding) was determined in the presence of 5 μM of unlabelled BK and subtracted from total binding being determined with [<sup>3</sup>H]BK alone.

To determine the  $B_{max}$  and  $K_d$ , our data were fitted to the “One Site Binding Equation” using nonlinear regression. It describes the binding of a ligand to a receptor that follows the law of mass action:

$$Y = B_{max} \times X / (K_d + X),$$

where  $B_{max}$  is the maximal binding and  $K_d$  is the concentration of ligand required to reach half-maximal binding. All data analysis was performed using GraphPad Prizm, version 3.03. This equation describes a rectangular hyperbola or a binding isotherm (Figure 10).

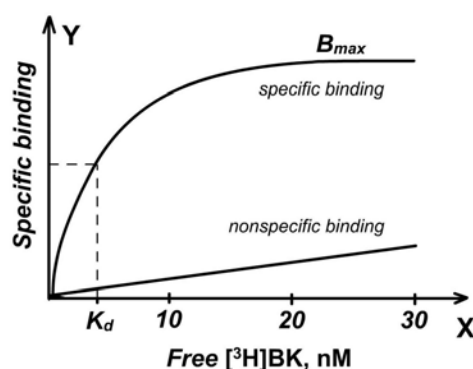


**Figure 10. Ligand concentration-receptor bound curve.**

A schematic representation of total and nonspecific radioactive ligand binding is shown. The concentration of free radioligand was plotted on the X-axis. Y-values reflect the total number of receptors expressed in cpm, sites/cell or fmol/mg protein. Nonspecific binding is usually linear with the concentration of radioligand.

Maximal binding capacities of the stable clones ( $B_{max}$ ) were either calculated from the equilibrium binding curves or estimated by incubation of the cells on ice with a saturating concentration of [<sup>3</sup>H]BK (10 nM).

## C.2.4 Receptor sequestration and ligand internalization assays

### C.2.4.1 Internalization of [<sup>3</sup>H]bradykinin

Monolayers on 12-well/24-well plates were rinsed three times with PBS and incubated with 0.3/0.15 ml of [<sup>3</sup>H]BK in incubation buffer for 90 min on ice to reach equilibrium binding. [<sup>3</sup>H]BK internalization was started by placing the plates in a waterbath at 37°C. The internalization process was stopped at the indicated times by putting the plates on ice and washing the cells four times with ice-cold PBS. Thereafter, the cell monolayers were treated with 0.2 ml of an ice-cold dissociation solution for 10 min on ice to induce dissociation of surface bound [<sup>3</sup>H]BK. The supernatant with formerly surface-bound [<sup>3</sup>H]BK was quantitatively transferred to a scintillation vial by rinsing the cells with another 0.2 ml of PBS. The remaining monolayer, containing the internalized [<sup>3</sup>H]BK, was lysed using 0.2 ml of 0.3 M NaOH and transferred with another 0.2 ml of water to a scintillation vial. The radioactivity of both samples was determined in a  $\beta$ -counter after addition of scintillation fluid. Non-receptor-mediated [<sup>3</sup>H]BK internalization and surface binding was determined in the presence of 5  $\mu$ M unlabelled BK and subtracted from total binding. Internalization was expressed as intracellular [<sup>3</sup>H]BK in percentage of the combined amounts of internalized and surface-bound [<sup>3</sup>H]BK.

### C.2.4.2 Receptor sequestration assay

Monolayers of cells on 12-well plates were rinsed three times with PBS and incubated on ice with 5  $\mu$ M unlabelled BK in 0.3 ml incubation buffer. After 60 min, the cells were placed in a waterbath at 37°C to start receptor sequestration. At the indicated times, the trays were placed on ice, washed two times with ice-cold wash buffer, and treated with a solution of 0.05 M glycine, pH 3.0 (Lamb *et al.*, 2001) for 10 min on ice to remove all unlabelled extracellular ligand. The cells were again washed twice with ice-cold wash buffer, and remaining specific surface binding was determined with 1–2 nM [<sup>3</sup>H]BK at 0°C.

### C.2.4.3 Measurement of changes in surface receptor number by ELISA

An ELISA assay was developed to measure the receptor sequestration by all HA-tagged receptor systems (including  $\beta_2$ -adrenergic receptors). This assay helped us to avoid buying of the expensive radio-labelled agonists for each used type of the receptor.

Particularly, this assay was used for the semi-quantitative measurement of surface-expressed HA-tagged  $\beta_2$ -adrenergic receptors and quantification of the receptor sequestration. Cells were plated out on 96-well plates 24 h before the experiments. They were rinsed twice with PBS and

exposed to 1  $\mu$ M ISO (isoproterenol) dissolved in DMEM for various times. Following the stimulation with ISO the cells were washed with PBS (three times) and fixed for 15 min at RT with fresh 2% (v/v) formaldehyde in PBS containing 0.1% (v/v) of glutaraldehyde. Cells were then again washed three times with PBS, blocked for 2 h at 37°C with DMEM supplemented with 10% (v/v) FCS and 1% (w/v) BSA, and incubated for 1 h at the same temperature with a 1:1000 dilution of rhodamine-labelled-anti-HA antibody in the same buffer. After final washes in PBS (four times), the reaction was developed using 100  $\mu$ l TMB peroxidase EIA substrate. The enzymatic reaction was stopped after ca.15 min at RT with 50  $\mu$ l of 1M H<sub>2</sub>SO<sub>4</sub>, and the optical density was determined at 405 nm using a DigiScan 400 microplate spectrophotometer. All experiments were performed in quadruplets. Nonspecific binding was measured using non-transfected *HEK293* and subtracted from total binding.

### C.2.5 Measurement of total inositol phosphate (IP) release

The HEK cells labelled with myo-[<sup>3</sup>H]-inositol were stimulated in the presence of lithium ions which inhibit enzymatic dephosphorylation of inositol phosphates. The accumulation of [<sup>3</sup>H]inositol phosphates has been stopped by the addition of formic acid. After separation from the neutral inositol by ion-exchange column chromatography the results were quantified by liquid scintillation counting.

80% confluent cell-monolayers in 12-well dishes were labelled overnight with 1  $\mu$ Ci of myo-[<sup>3</sup>H]-inositol in 0.5 ml DMEM containing fresh FCS and penicillin/streptomycin. The next day, the monolayers were then placed on ice, rinsed three times with ice-cold PBS (pH 7.2) and incubated with the indicated concentrations of BK in incubation buffer with 50 mM LiCl for at least 90 min. The stimulation was started by placing the tray in a waterbath at 37°C for 30 min and terminated by exchanging the buffer with 0.75 ml of ice-cold 20 mM formic acid and putting the tray on ice for additional 30 min. Subsequently, the supernatant was combined with another 0.75 ml of 20 mM formic acid and, after alkalization with 0.2 ml of 3% ammonium hydroxide solution, was applied to an AG 1-X8 anion exchange column. The column was washed with 1 ml 1.8% ammonium hydroxide solution, followed by 9 ml 5 mM tetraborate buffer containing 60 mM sodium formiate. Total inositol phosphates were eluted in 3 ml of 4 M ammonium formiate containing 0.2 M formic acid. The radioactivity was determined in a beta-counter after addition of scintillation fluid.

The [<sup>3</sup>H]BK binding was checked in parallel by incubation of the cells on ice with a saturating concentration of [<sup>3</sup>H]BK (10 nM).

## C.2.6 Protein biochemical methods

### C.2.6.1 Analysis of the total expression level of the B<sub>2</sub>R

Cell monolayer on a 100-mm dish was rinsed three times with PBS at 4°C and lysed in RIPA buffer (section C.1.7.2) including 0.5 mM Pefabloc SC and 10 μM each of 1.10-phenanthroline, aprotinin, leupeptin, and pepstatin A for 45 min at 4°C with gentle rocking. The lysate was centrifuged at 6.240×g for 20 min at 4°C. The supernatant (0.5 ml with ~1.5 mg of total protein) was incubated with 35 μl of protein G-agarose and 2.5 μl of antiserum AS346 for 3 h at 4 °C. The pellet obtained after centrifugation of the immunoprecipitation mixture was then washed twice with RIPA buffer and once with distilled water and subjected to SDS-PAGE electrophoresis (section C.2.6.3).

### C.2.6.2 Crude membrane preparation

- Cell monolayers were washed three times with ice-cold PBS (usually it was used 6×100-mm dishes were used pro construct).
- The cells expressing B<sub>2</sub>R and its mutants were stimulated with 1 μM BK in incubation buffer; the cells expressing β<sub>2</sub>-ADR receptor were stimulated with 1 μM ISO in DMEM.
- The cells were washed twice with PBS and scraped into 10 ml of ice-cold homogenization buffer.
- Then they were homogenized using a Dounce-homogenizer (10 strokes at 1400 rpm).
- The cell lysate was centrifuged for 15 min at 20.000×g.
- The resulting pellet was resuspended in the 5 ml of homogenization buffer (5 strokes at 1400 rpm).
- The homogenization and centrifugation were performed once more as described before.
- The final crude membrane preparation was resuspended in homogenization buffer at a concentration of 1 mg of protein pro ml.

### C.2.6.3 Co-immunoprecipitation assay

If not indicated otherwise, 1 mg of fresh crude membrane preparations was solubilized by adding 20 mM CHAPS dissolved in 20 mM PIPES, pH 6.8, to give a final concentration of 4 mM CHAPS. After incubation for 1 hour at 4°C the insoluble particles were removed by centrifugation at 10.000×g for 5 min. The supernatant was incubated overnight with 20 μl of anti-HA matrix at 4°C. The pellet obtained by centrifugation was washed twice with 4 mM CHAPS and once with distilled water and subjected to SDS-PAGE electrophoresis.

#### C.2.6.4 Electrophoresis of proteins on SDS-PAGE (*Laemmli method*)

The “discontinuous electrophoresis” was used for proteins separation according to Laemmli (1970):

The pellet obtained after immunoprecipitation was mixed with 30  $\mu$ l of sample buffer (section C.1.7) containing 25 mM DTT and heated for 6 min at 95°C in the thermomixer. Using a 50- $\mu$ l Hamilton syringe, the whole volume of the sample was gently loaded on 10% SDS-polyacrylamide gel avoiding the intake of the matrix.

The electrophoresis was performed in the vertical gel-chamber with running buffer using constant voltage 150 V for ca. 2 h.

#### C.2.6.5 Transfer of proteins from gel to nitrocellulose membrane

For detection of the proteins of interest, they were transferred after electrophoretic separation onto a nitrocellulose membrane.

Filter papers and 0.45  $\mu$ m nitrocellulose membrane were cut according to the size of the gel to be blotted and, together with blotting pads, soaked in  $\frac{1}{2}$  Towbin buffer (section C.1.7). Two soaked blotting pads were placed into the cathode (-) core of the blot module. The gel/membrane assembly was carefully collected and placed on the pad in the sequence shown in Figure 11 and two other pads were put on the top. Thereafter, the stack was covered with the anode (+) core and the electric field was applied for 2 h. After the transfer the nitrocellulose membrane was used for immunoprinting (section C.2.6.6) or autoradiography (section C.2.7.1).

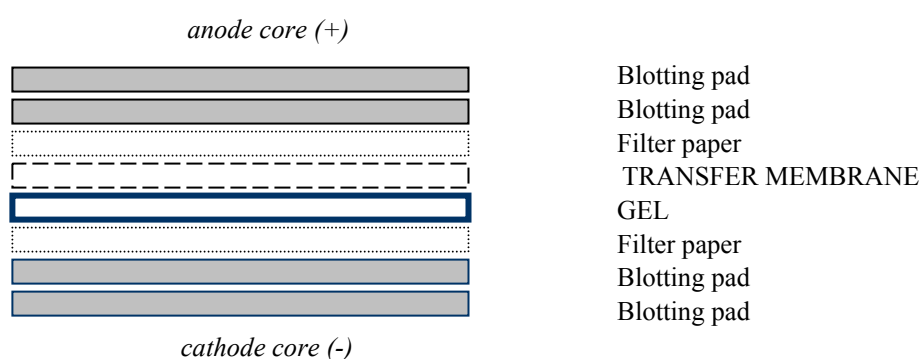


**Figure 11. Gel/membrane sandwich.**



### C.2.6.6 Immunoprinting of blotted proteins

Nitrocellulose membranes were incubated overnight in blocking buffer (C.1.7.2) at RT to block nonspecific binding sites on the membrane. The appropriate primary antibody (Table 7) was added for 2 h at RT in fresh blocking buffer. The unbound antibodies were washed off (2 x 10 min) with TBST (Tris-buffered saline buffer with 0.1% Tween 20) before adding the corresponding secondary horse-radish peroxidase-labelled (HRP) antibody (Table 8) for 1 h at RT. After washing in TBST three times each for 15 min the membranes were incubated in the *Western Blot Chemiluminescence Reagent Plus* for 5 min, afterwards intensively dried and exposed to the film.

**Table 7. Primary antibodies used in Western blotting.**

Antibody	Origin	Protein	Antibody dilutions
Anti-HA*, monoclonal	rat	HA-tagged protein	1:2000
AS346, polyclonal	rabbit	B <sub>2</sub> R and its mutants	-
MBR1, monoclonal	mouse	B <sub>2</sub> R and its mutants	1:1000
ST, monoclonal	mouse	B <sub>2</sub> R and its mutants	1:5000
Anti-G <sub>q/11</sub> protein, polyclonal	rabbit	G <sub>q/11</sub> protein	1:1000
Anti-C <sub>s</sub> protein, monoclonal	rabbit	C <sub>s</sub> protein	1:1000
Anti-GRK**2/3, monoclonal	mouse	GRK 2/3	1:5000

\* HA – hemagglutinin

\*\* GRK – G protein-coupled receptor kinase

**Table 8. Secondary antibodies used in Western blotting.**

Antibody	Origin	Antibody dilutions
Anti-mouse-HRP*	horse	1:5000
Anti-rabbit-HRP	sheep	1:2000
Anti-rat-HRP	rabbit	1:2000

\* HRP – horse-radish peroxidase

## C.2.7 Receptor phosphorylation and phosphopeptide mapping

### C.2.7.1 Phosphorylation assay

The receptor phosphorylation was checked according to the following procedure:

- Confluent cells expressing B<sub>2</sub>R or its mutants on 6-well plates were washed twice with phosphate-free DMEM and incubated in the same medium for 3 h at 37°C under standard condition (section C.2.2.1).
- [<sup>32</sup>P]Orthophosphate was diluted in phosphate-free DMEM to give a final concentration 0.2 mCi/ml.
- The cells were labelled with 1 ml of freshly prepared [<sup>32</sup>P]orthophosphate solution for ca. 12 h under standard condition.
- The radioactive solution was carefully removed and the cells were washed twice with TBS buffer.
- The cells were incubated with or without 1 μM BK diluted in incubation buffer in a waterbath at 37°C for 5 min.
- The cells were washed once with TBS.
- Then the cells were scraped into 500 μl of RIPA buffer including 0.5 mM Pefabloc SC and 10 μM each of 1.10-phenanthroline, aprotinin, leupeptin, pepstatin A, and phosphatase inhibitors (25 mM NaF, 1 mM sodium orthovanadate, 0.3 μM okadaic acid) and incubated for 60 min at 4°C with gentle rocking.
- The lysate was centrifuged at 6.240×g for 20 min at 4°C.
- The supernatant was incubated with 35 μl of protein G-agarose and 2.5 μl of antiserum AS346 for 3 h at 4°C.
- The mixture was centrifuged at 6.240×g for 5 min at 4°C.
- The pellet was then washed twice with RIPA buffer and once with distilled water, resuspended in 30 μl of Laemmli buffer, and incubated for 6 min at 95°C.
- The immunoprecipitated proteins were separated by electrophoresis on 10% SDS-polyacrylamide gels and then electroblotted onto 0.45-μm nitrocellulose.
- The membrane was put in a plastic pouch and exposed on a film for 4-12 h.

The agonist-induced phosphorylation of the β<sub>2</sub>-adrenergic receptor was performed as described before with minor modification. The cells were treated with 1 μM ISO dissolved in DMEM. For immunoprecipitation an anti-HA antibody was used in an amount of 20 μg pro sample.

### C.2.7.2 Two-dimensional phosphopeptide mapping

Two-dimensional mapping of the phosphorylation sites was performed as described (Blaukat *et al.*, 2001; Boyle *et al.*, 1991) with minor modifications:

- The band of interest was cut out from the nitrocellulose membrane and put into the 1.5 ml tubes.
- These pieces of membrane were soaked in 0.5% polyvinylpyrrolidone-40 in 0.6% acetic acid at 37°C for 30 min to block nonspecific absorption of trypsin.
- The membrane was washed three times with distilled water.
- The phosphopeptides were cleaved *in situ* in 200 µl of freshly made 50 mM (NH<sub>4</sub>)HCO<sub>3</sub> containing 1 µg of modified sequencing grade trypsin for ca. 12 h at 37°C.
- The supernatant was aspirated and transferred to a new tube. The membrane was washed with 200 µl of 50 mM (NH<sub>4</sub>)HCO<sub>3</sub> for 15 min at 37°C strong shaking. The resulting solution was combined with the former supernatant and vacuum-dried. In the meantime, the performic acid was prepared by adding 900 µl of formic acid (ca. 98%) and 100 µl of hydrogen peroxide (30%) to a 1.5 ml tube and incubating at RT for 60 min.
- The pellet obtained after lyophilization was oxidized in 50 µl of ice-cold performic acid for 1 h on ice.
- The oxidation was stopped by dilution the performic acid in 500 µl of distilled water.
- The obtained solution was vacuum-dried, resuspended in 100 µl of distilled water and vacuum-dried again. This step was repeated once or twice until all salts have been removed.
- The resulted pellet was dissolved in 50 µl of 50 mM (NH<sub>4</sub>)HCO<sub>3</sub> and sonificated in a waterbath for 5 min.
- 1 µg of modified sequencing grade trypsin was added to each tube.
- The second digestion lasted for 8-12 h at 37°C.
- Digestion was stopped by adding of 140 µl of electrophoresis buffer pH 1.9; the probes were vortexed and spun for 5 min.
- 180 µl of the supernatant was transferred to a new tube, carefully avoiding to take up insoluble material, and vacuum-dried.
- The obtained pellet was dissolved in 5 µl of electrophoresis buffer and intensively vortexed.
- The probe was applied in very small portions onto a cellulose thin layer chromatography plate; for drying a fan with no or very moderate heating was used.

- The first dimension separation was performed on cellulose thin layer plates in electrophoresis buffer at 2000 V for 30 min using the specially constructed *Hunter Thin-Layer Electrophoresis* equipment (HTLE 7002; CBS Scientific, Ins., Del Mar, CA).
- After electrophoresis the plates were air-dried for 3-4 h and subjected to ascending chromatography in the chromatography buffer until the solvent front reached the top of the plate.
- Plates were then extensively dried in a fume hood, wrapped in a plastic and exposed to Fuji X-ray film for 7–10 days at  $-80^{\circ}\text{C}$ .

### C.2.8 Confocal microscopy

Confocal microscopy is a specialized form of fluorescent microscopy. A confocal microscopy can take optical horizontal sections of the sample by focusing on one section of the sample at a time and blocking away any fluorescence that may be from adjacent sections of the sample. Cells were plated on glass coverslips pretreated with 0.01% poly-D-lysine in PBS. For confocal microscopy, cells were washed with and incubated for 2 h in serum-free medium with 20 mM HEPES, pH 7.3. Thereafter, rhodamine-labelled anti-HA antibody was added in the presence or absence BK. Images were taken halfway through most of the cells with a confocal microscope (Zeiss LSM 410) using a 63 $\times$ /1.4 oil immersion objective with no zoom.

### C.2.9 [ $^{35}\text{S}$ ]GTP $\gamma$ S binding assay

Aliquots of crude membrane preparations containing 20  $\mu\text{g}$  of total protein each were incubated for 15 min on ice in 500  $\mu\text{l}$  of assay buffer (section C.1.7.3), containing 2 mM bacitracin, 0.8 mM 1.10-phenanthroline, 100  $\mu\text{M}$  captopril including  $10^5$  cpm [ $^{35}\text{S}$ ]GTP $\gamma$ S in the absence or presence of 1  $\mu\text{M}$  BK. Incubation was continued for 30 min in a waterbath at  $30^{\circ}\text{C}$ . Free and protein-bound [ $^{35}\text{S}$ ]GTP $\gamma$ S were separated by rapid filtration of the preparation through glass fiber filters (Whatman GF/C) and thorough washing of the filters with 15 ml ice-cold 10 mM sodium phosphate buffer, pH 7.4. The radioactivity retained by the filters was determined in a  $\beta$ -counter using liquid scintillation mixture. Nonspecific binding was measured in the presence of 1 mM GTP and subtracted from all values to give specific binding.

### C.2.10 Determination of the protein concentration

Total protein was quantified with the “Micro BSA Protein Assay” reagent from Pierce (Rockford, IL) using BSA as the standard.

## D RESULTS

### D.1 Development of methods

#### D.1.1 Ligand internalization and receptor sequestration assays

Receptor endocytosis (internalization, sequestration) is the process by which cell surface receptors are translocated into intracellular compartments after exposure to ligand. According to Koenig (1997) there is no principal difference between the terms “internalization” and “sequestration”. But there are at least two different ways to measure receptor endocytotic capacity. We designated them as “ligand internalization” and “receptor sequestration” assays (Figure 12).

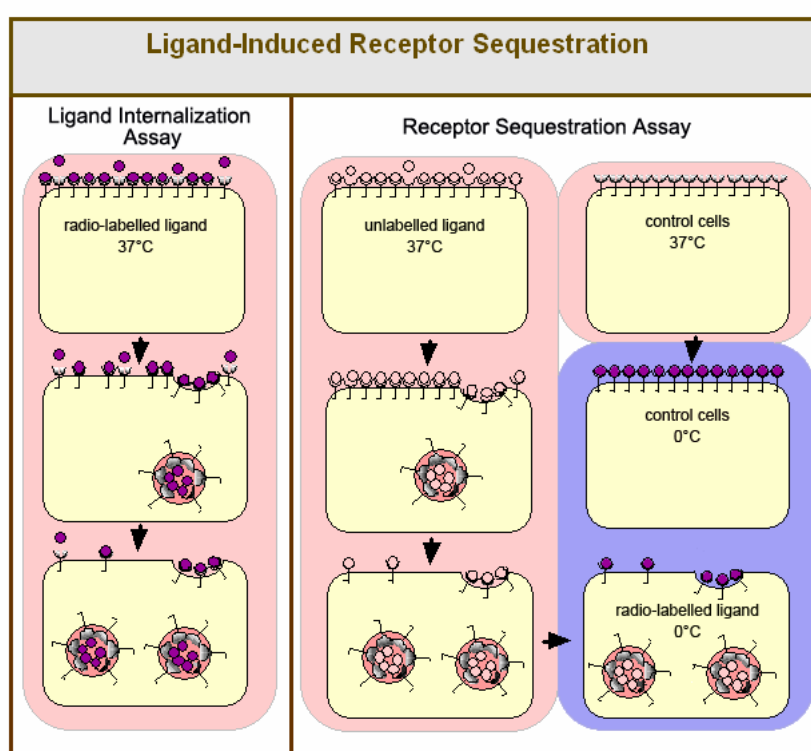


**Figure 12. Schematic presentation of the ligand internalization (left) and receptor sequestration (right) assays.**

Radio-labelled ligand is shown as filled circles, unlabelled ligand as open circles. See detailed explanation in the text.

##### D.1.1.1 Ligand internalization assay: optimization

The *ligand internalization assay* is based on the assumption that the receptor-bound ligand is endocytosed with its receptor before the ligand-receptor complex dissociates, it means that receptor and ligand share, at least for a certain initial time frame, the same fate, i.e. the same cellular localization. After reaching equilibrium binding with radiolabeled ligand at 4°C the cells were incubated at 37°C (Figure 12, *left*). At various times the amounts of surface bound and of internalized ligand were determined separately using a low pH dissociation technique. In this

approach, internalization was expressed as amount of internalized ligand in percentage of the total bound ligand (i.e. the sum of internalized and surface bound ligand).

This approach has been used successfully with the B<sub>2</sub> bradykinin receptor. However, the various publications reported rather large differences in the internalization rates for wild-type B<sub>2</sub>R ranging from <30% ligand internalization after 10 min in COS-7 cells (Pizard *et al.*, 1999) to over 80% in Chinese hamster ovary (CHO) cells (Faussner *et al.*, 1998). This was considered to be at least partially due to the use of different cell lines.

Using the *Flp-In* system (Invitrogen), we obtained several clones of *HEK293* cells expressing high amounts (10.4 pmol/mg protein) of B<sub>2</sub>R (B<sub>2</sub>R<sub>high</sub>). We could show that internalization of [<sup>3</sup>H]BK in these overexpressing cells is strongly dependent on the concentration of the applied ligand. Fast internalization occurred with low amounts of ligand (<1 nM), which slowed down drastically with higher concentrations of [<sup>3</sup>H]BK, from more than 80% internalization at 0.4 nM [<sup>3</sup>H]BK after 5 min to as low as 10% at 10 nM [<sup>3</sup>H]BK (Figure 13).

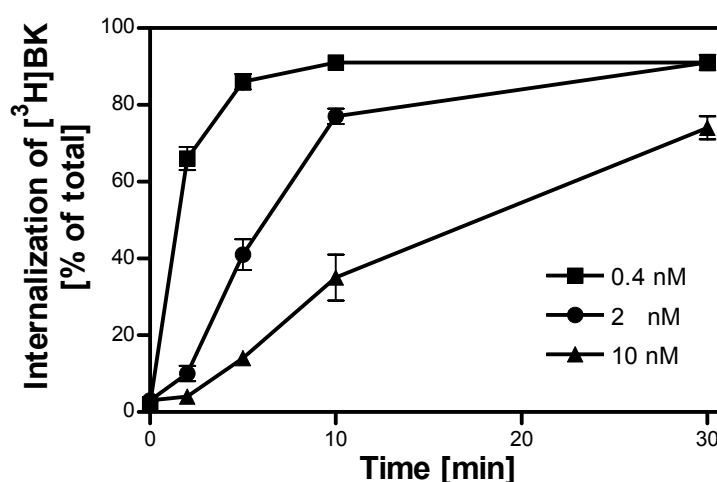


**Figure 13. Internalization of [<sup>3</sup>H]BK in high-expressing cells.**

*HEK293* cells, expressing B<sub>2</sub>R<sub>high</sub>, were pre-incubated with the indicated concentrations of [<sup>3</sup>H]BK for 90 min on ice. The internalization was started by placing the plates in a waterbath at 37°C. At the indicated times, the internalization process was stopped, and surface-bound and internalized ligand were determined as described in section C.2.4.1. The results are given as means ± S.D. of triplicate determination (from Publication C). In these cells, internalization is strongly dependent on the concentration of [<sup>3</sup>H]BK.

To test the hypothesis that overexpression of the kinin receptors is responsible for the concentration dependence of ligand internalization, we tried to generate clones with lower receptor expression. For this purpose, we exchanged the strong CMV-promoter regulating the expression of the gene of interest in the pcDNA5/FRT vector of the *Flp-In* system for the minimal CMV promoter. With this promoter, the *Flp-In* system enabled the production of

identical clones ( $B_2R_{low}$ ) with lower expression (4.2 pmol/mg protein). In these new *HEK293* clones internalization of [ $^3H$ ]BK was totally independent of the ligand concentration (Figure 14).

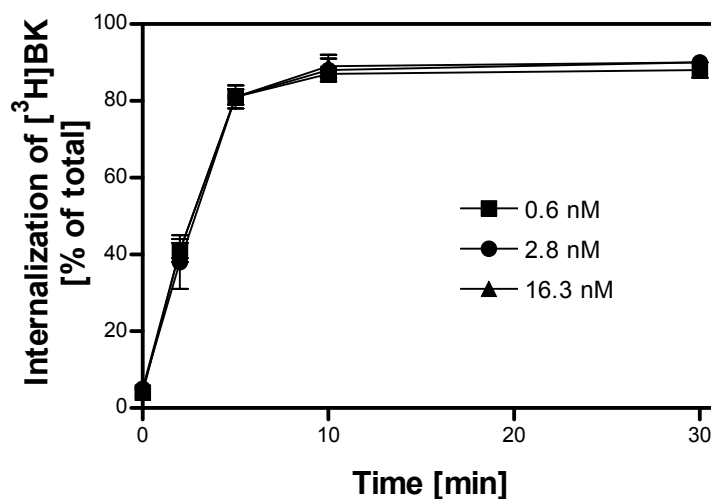


**Figure 14. Internalization of [ $^3H$ ]BK in low-expressing cells.**

*HEK293* cells expressing  $B_2R_{low}$  (4.2 pmol/mg protein) were treated as described in Figure 12. All time points represent the means  $\pm$  S.D. of triplicate determinations. For the representative experiments shown, two other experiments giving similar results were performed (from Publication C). The internalization rate was totally independent of the bradykinin concentration.

Thus, in all following ligand internalization assays a concentration of ca. 1 nM [ $^3H$ ]BK was used as the uptake rate by high and low-expressing cells showed no significant difference with this amount of [ $^3H$ ]BK.

#### D.1.1.2 Receptor sequestration assay: optimization

In contrast, in the *receptor sequestration assay* cells were stimulated at 37°C for various times with a saturating concentration of unlabeled agonist, and then a binding assay was performed at 4°C with a radiolabeled, non-membrane-permeable agonist or antagonist to assess remaining surface receptor expression (Figure 12, *right*). Comparison of the amount of remaining receptors on the cell surface of treated cells with that on untreated control cells gave the extent of receptor sequestration.

The  $B_2R_{high}$  responded to stimulation with 1  $\mu$ M BK with only very poor sequestration. Yet, the  $B_2R_{low}$ -expressing *HEK293* cells responded to stimulation with 1  $\mu$ M BK with rapid reduction of the receptor number on the cell surface, reaching a plateau of remaining surface binding of under 30% within 10 min (Figure 15).

Thus, the usage of the sequestration assay for cells that highly overexpress B<sub>2</sub>R may grossly underestimate “true” receptor sequestration, presumably because of an overload of the internalization machinery.

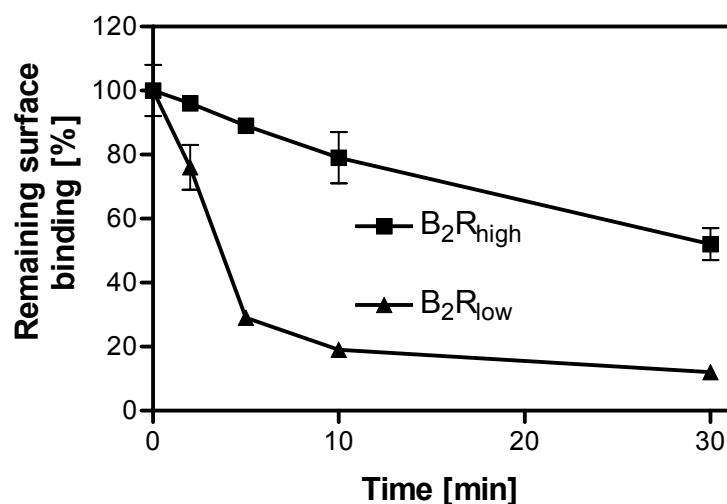


**Figure 15. B<sub>2</sub>R sequestration in high- and low-expressing cells.**

*HEK293* cells, stably expressing B<sub>2</sub>R<sub>high</sub> or B<sub>2</sub>R<sub>low</sub>, were preincubated with 1 μM BK for the indicated times at 37°C. Remaining surface binding was then determined at 0°C with ~2 nM [<sup>3</sup>H]BK as described in section C.2.4.1. The results are given as means ± S.D. of triplicate determinations indicating that in B<sub>2</sub>R<sub>high</sub> cells “true” receptor sequestration is highly underestimated (from Publication C).

The ligand internalization assay, in contrast, can be applied even under these conditions, if the appropriate low concentrations of radiolabeled agonist are used to avoid saturation of the internalization machinery.

#### D.1.2 Elaboration of the B<sub>2</sub>R immunoprecipitation and immunoprinting assay

GPCRs such as the kinin receptors are present in most natural cells, but even after over-expression their amount is still not enough to detect them in cell lysates using Western blotting. To overcome these problems, we applied radiolabelling and/or immunoprecipitation procedures. For receptor solubilization, we used RIPA (Radio-Immunoprecipitation Assay) buffer as described previously (Blaukat *et al.*, 1996). This buffer enabled efficient cell lysis and protein solubilization while avoiding protein degradation and interference with the protein immunoreactivity. Application of RIPA buffer also resulted in a low background of immunoprecipitation.



### D.1.2.1 Selection of the appropriate antibodies for receptor immunoprecipitation

Immunoprecipitation is a technique in which an antigen is isolated by binding to a specific antibody attached to a sedimentable matrix.

The attempts to detect B<sub>2</sub>R in the cell lysate by Western blotting without immunoprecipitation were vain, since the absolute amount of B<sub>2</sub>R applied per lane was well below the detection limit even with using our highly expressing constructs (10.4 pmol/mg protein). Thus, the main step in sufficient receptor immunoprecipitation and visualization is the choice of the appropriate antibody. To this end we tested the following four antibodies (Table 9):

- *AS346, polyclonal*. Immunization of rabbits was carried out in the laboratory of Prof. Dr. Müller-Esterl (School of Medicine, Johann Wolfgang Goethe University, Frankfurt) with the synthetic peptide CRS36 (CRSEPIQMENSMGTLATSISVERQIHKLQDWAGSRQ), derived from the carboxyl-terminal domain of the human B<sub>2</sub> receptor (Blaukat *et al.*, 1996).
- *MBR-1, subtype IgG<sub>2Bκ</sub> (monoclonal)* was also generated in the above mentioned laboratory. Immunization of B cells was carried out with the synthetic peptide CRS36 (see above) derived from the carboxyl-terminal domain of the human B<sub>2</sub> receptor (Publication D).
- *ST, mouse IgG<sub>2B</sub>* from BD Signal Transduction Laboratories was generated against the last 15 amino-acid residues of the B<sub>2</sub>R. No additional information is available.
- *Anti-HA high affinity antibody* (clone 3F10) from Roche was obtained by immunizing rats with a synthetic peptide (residues 76-111 of X47 hemagglutinin 1). Spleen cells were isolated and fused with P3-X63-Ag8.653 myeloma cells. Hybridomas secreting monoclonal antibodies specific for the HA-epitope were isolated and cloned.

**Table 9. Characteristics of the antibodies used in the immunoprecipitation assay.**

Antibody	Origin	Stock concentration	Working volume
AS346, polyclonal	Rabbit	ND	2.5 µl
MBR1, monoclonal	Mouse	0.2 mg/ml	4.5 µg
ST, monoclonal	Mouse	10 mg/ml	4.5 µg
Anti-HA, monoclonal	Rat	0.25 mg/ml	4.5 µg

To test the usefulness of antibodies for immunoprecipitation of B<sub>2</sub>R, we applied the above listed antibodies (Table 8) to lysates from non-transfected (control) or overexpressing B<sub>2</sub>R<sub>high</sub> HEK293 cells. Afterwards, the receptors were visualized by Western blotting using 0.1 µg/ml of anti-HA antibody.

The commercially available monoclonal *ST* antibody failed to produce specific bands (Figure 16). Under the same conditions, the polyclonal antibody AS346 gave a major band of 70 kDa,

indicating that it efficiently precipitated human B<sub>2</sub>R. This finding was confirmed by the application of a specific anti-HA antibody, which also precipitated the HA-tagged B<sub>2</sub>R. Moreover, the monoclonal antibody MBR1 also precipitated the HA-tagged B<sub>2</sub>R, though less efficiently than the polyclonal antibody AS346 or the monoclonal anti-HA antibody.

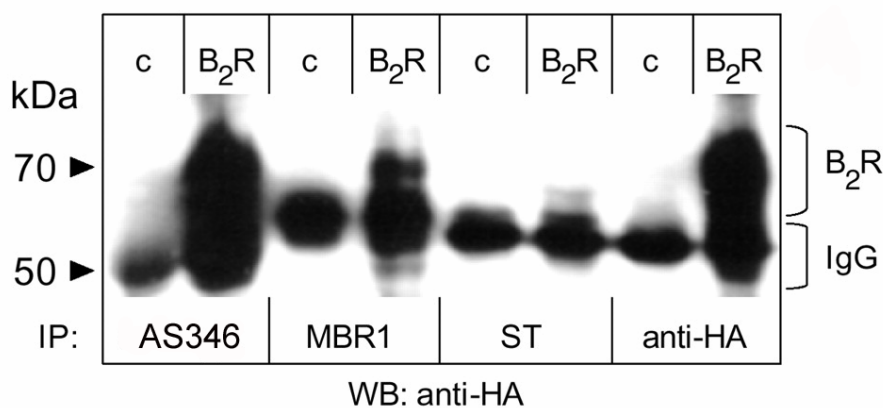


**Figure 16. Analysis of immunoprecipitation capacity of anti-B<sub>2</sub>R antibody.**

*HEK293* cells expressing HA-tagged B<sub>2</sub>R were lysed and HA-B<sub>2</sub>R was precipitated from 1.5 mg protein using antibodies shown in Table 8. Precipitates were separated by reducing 10% SDS-PAGE, transferred onto nitrocellulose membranes, and probed with 0.1 µg/ml anti-HA using the *Chemiluminescence Reagent Plus* method (from Publication D).

#### D.1.2.2 Selection of the appropriate antibodies for receptor immunoprinting

Then we focused on the development of a sensitive technique for B<sub>2</sub>R receptor visualization.

Using AS346 (2.5 µl pro sample) for immunoprecipitation and MBR1 (0.2 µg/ml) for Western blotting, we succeeded in detecting B<sub>2</sub>R overexpressed in *HEK293* cells (Figure 17, *left*). Applying HA-tagged B<sub>2</sub>R, we observed a similar pattern for anti-HA antibody (0.1 µg/ml), confirming the specificity of our detection system (Figure 17, *right*).

Under otherwise identical conditions, the *ST* antibody failed to produce specific bands, even at significantly higher antibody concentrations (2 µg/ml). However, usage of AS346 antibody in the Western blotting results in extremely high background due to so far unknown reasons. Thus, precipitating antibody AS346 in combination with reporter antibody MBR1 allowed detection of the B<sub>2</sub>R endogenously expressed by native cells, i.e., human foreskin fibroblasts. This detection system was also used in the investigation of the down-regulation of B<sub>2</sub>R in human fibroblasts during prolonged agonist exposure (Publication D).

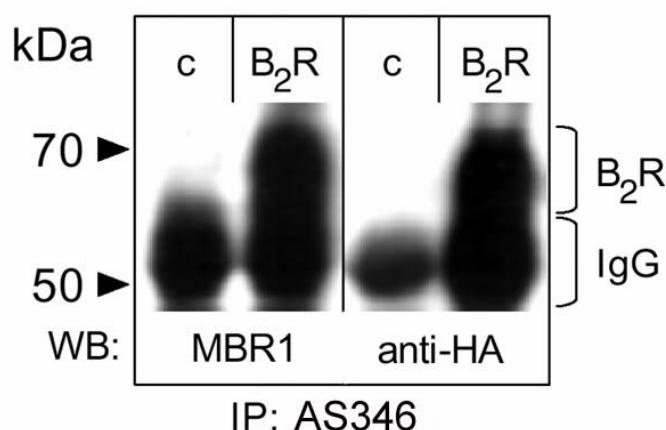


**Figure 17. Analysis of immunoprinting capacity of anti-B<sub>2</sub>R antibody.**

*HEK293* cells expressing HA-tagged B<sub>2</sub>R were lysed and HA-B<sub>2</sub>R was precipitated from 1.5 mg protein using 2.5  $\mu$ l of AS346 antibody. Precipitates were separated by reducing 10% SDS-PAGE, transferred onto nitrocellulose membranes, and probed with 0.2  $\mu$ g/ml MBR1 (left) or 0.1  $\mu$ g/ml anti-HA (right) using the *Chemiluminescence Reagent Plus* method (from Publication D).

Furthermore, we used AS346 or anti-HA antibodies for the investigation of the total expression level of the B<sub>2</sub>R and its mutants in Western blotting and for determination of an agonist-induced phosphorylation.

### D.1.3 Solubilization of the receptor in its active conformation

To investigate receptor coupling with the cognate G protein we needed mild detergents which are able to solubilize the receptor from the plasma membrane in an active form. Therefore, we took in mind the previous report (Faussner *et al.*, 1991) that the B<sub>2</sub> bradykinin receptor from cultured human foreskin fibroblast is successfully solubilized in an active and stable form using 4 mM of the non-denaturing hybrid-ionic detergent 3-[(3-cholamidopropyl)dimethylammonio]-1-propanesulfonic acid (CHAPS). CHAPS is a sulphonic acid derivative of cholic acid that is readily soluble in water. Additional experiments revealed that other detergents showed only minor (digitonin) or no (Triton X-100, n-octyl-glucopyranosid) efficacy at all. Moreover, concentrations of CHAPS below 3 mM were rather ineffective in terms of solubilization yield, whereas concentration of CHAPS above 4 mM resulted in a rapid loss in binding activity (Faussner *et al.*, 1991).

Summarizing, we used the described solubilization procedure with minor modifications (prolonged incubation of the cells with detergent by 4°C instead of RT) to solubilize the B<sub>2</sub>R from *HEK293* cells with high efficiency.

#### D.1.4 Elaboration of a co-immunoprecipitation assay

For a convenient co-immunoprecipitation of the solubilized receptor/G protein complex we ought to use anti-N-terminus antibody to overcome the steric competition between G protein or and antibody. So, actually, we could have used the anti-HA antibody which had a good account of itself as it was mentioned before, but in this case we faced the next problem. When immunoprecipitation assay is combined with Western blotting, a cross-reactivity between the chains of the antibody used in the immunoprecipitation and the secondary antibody used in the Western blotting is usually observed. In our experiments this cross-reactivity produced 20 kDa and 50 kDa bands that corresponded to the light and heavy chains of anti-HA antibody (Figure 18, *left*). As some of our adaptor proteins (e.g. GRK2/3 – see section D.2.4) are expected to be visualized at ca. 50 kDa, the potential use of a regular co-immunoprecipitation assay is strongly limited.

To overcome this problem, we applied for the immunoprecipitation an anti-HA antibody covalently linked to agarose beads. Consequently, after denaturation at 95°C the heavy chain of anti-HA antibody used for the immunoprecipitation remained bound to the anti-HA antibody covalently linked to agarose beads and was not submitted to the electrophoresis (Figure 18, *right*).

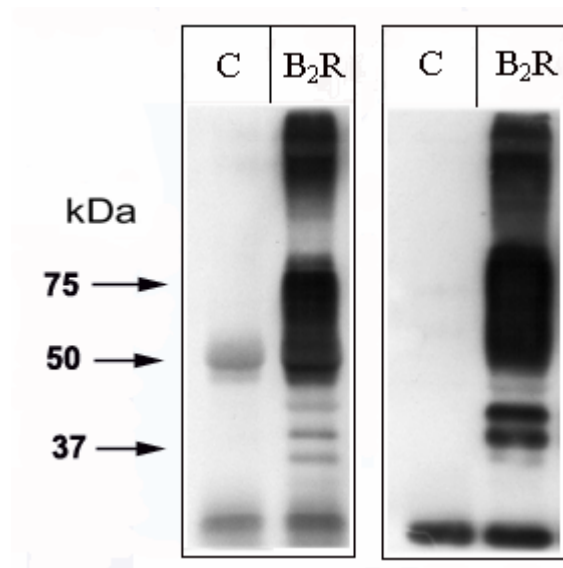


**Figure 18. Advantage of the use of an anti-HA antibody covalently linked to agarose beads in the co-immunoprecipitation.**

HA-B<sub>2</sub>R was immunoprecipitated from 1.5 mg protein using either 4.5 µg anti-HA antibody with 35 µg of protein-G-agarose (left) or 15 µl of the agarose beads covalently linked to an anti-HA antibody (right). Precipitates were separated by reducing 10% SDS-PAGE, transferred onto nitrocellulose membranes, and probed with 0.1 µg/ml anti-HA antibody using the *Chemiluminescence Reagent Plus* method. Relative molecular masses are indicated on the left. (C = control cells not expressing B<sub>2</sub>R)

### D.1.5 Co-immunoprecipitation of $G_{q/11}$ protein

The  $G_{q/11}$  subunits associated with immunoprecipitated receptors in our experiments were visualized by Western blotting with a well characterized and specific antibody from Santa Cruz raised against a peptide representing a domain common to  $G\alpha_q$  or  $G\alpha_{11}$  of mouse origin.

First we examined the ligand-induced association of  $B_2R$  wt with  $G_{q/11}$  protein. As shown in Figure 19, a low basal (i.e. in the absence of agonist) association between  $G_{q/11}$  protein and  $B_2R$  wt was observed in BK-untreated cells. In contrast, when cells were treated with 1  $\mu$ M BK for 5 min,  $G_{q/11}$  proteins were co-immunoprecipitated with  $B_2R$  and identified with the anti- $G_{q/11}$  antibodies as a band migrating at 42 kDa. The effect of BK on  $G_{q/11}$ - $B_2R$  complex formation was  $3.04 \pm 0.77$  of the basal level (mean  $\pm$ S.D. of 3 experiments). As a control, cell membrane preparations from non-transfected cells were solubilized and incubated with an anti-HA antibody covalently linked to agarose beads. Under these conditions, only a small amount of protein corresponding to the  $G_{q/11}$  subunits was detected that made up ca. 80% intensity compared to non-stimulated wt. These results revealed that the wild type receptor coupled specifically to  $G_{q/11}$  when stimulated by BK.

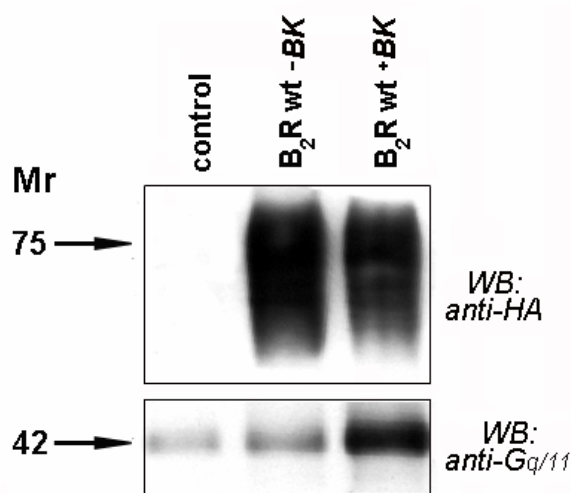


**Figure 19. Analysis of ligand-induced  $B_2R$  wt /  $G_{q/11}$  protein interaction.**

Cell monolayers expressing  $B_2R_{high}$  were incubated with or without 1  $\mu$ M BK for 5 min, scraped and used for crude membrane preparation. HA-tagged receptors present in 1 mg of the crude membrane preparations of *HEK293* cells were solubilized with 4 mM CHAPS and immunoprecipitated with an anti-HA antibody covalently linked to agarose beads. The immunoprecipitates were subjected to SDS-PAGE and Western blotting using anti-HA (*upper panel*) or anti- $G_{q/11}$  protein antibodies (*lower panel*). As a negative control, non-expressing cells were taken and subjected to the same procedure. The experiment shown was repeated seven times with identical results.

## D.2 Investigation of the role of highly conserved Y<sup>7.53</sup>

### D.2.1 Generation of high- and low-expressing B<sub>2</sub>R wt, Y7.53F and Y7.53A mutants

The *NPxxY* motif is a strongly conserved sequence in almost all class A GPCRs. To determine the structural and functional significance of the tyrosine from this motif in the human B<sub>2</sub>R, Y<sup>7.53</sup> was replaced by alanine giving rise to the mutant termed Y7.53A. In addition, a more conservative mutant was constructed replacing Y<sup>7.53</sup> by phenylalanine and termed Y7.53F.

Using the *Flp-In<sup>TM</sup>* system, we obtained clones of *Flp-In<sup>TM</sup> T-REx<sup>TM</sup>-293* cell line that stably expressed the human wild-type B<sub>2</sub>R, Y7.53F, Y7.53A in a homologous environment, i.e. a human receptor was expressed in a human cell line.

For comparison, we have also constructed two different wild-type receptors – low- (B<sub>2</sub>R<sub>low</sub>) and high-expressing (B<sub>2</sub>R<sub>high</sub>) systems – as mentioned already in section D.1. Expression levels of the wild type receptor in *HEK293* cells were varied by using a vector with either the original CMV promoter for higher (B<sub>2</sub>R<sub>high</sub>) expression, or the minimal CMV promoter for lower (B<sub>2</sub>R<sub>low</sub>) expression levels.

Yet, it should be mentioned that even cells with a low expression profile produced copy numbers of B<sub>2</sub>R that were consistently higher than those observed in native cells, e.g. human embryonic fibroblasts IMR-90 (70,000 receptors/cell) (Menke *et al.*, 1994).

All receptor coding sequences were preceded at the N-terminus by a single hemagglutinin (HA)-tag (MGYPYDVPDYAGS).

### D.2.2 Investigation of the receptor binding properties

[<sup>3</sup>H]BK binding was measured in intact *HEK* cells to determine the expression level and the integrity of the recombinant receptors at the plasma membrane as well as the receptor affinity.

The ligand affinities of B<sub>2</sub>R and all mutant receptors measured at 4°C did not differ markedly (Table 10), indicating that the mutations do not directly affect the ligand binding site and overall structure of the receptor.

However the surface expression of the constructs varied considerably, despite using the identical promoter. The mutant receptor Y7.53A exhibited considerably less surface binding (2.1 pmol/mg of protein) than either B<sub>2</sub>R wt (10.4 pmol/mg of protein) or mutant Y7.53F (12.5 pmol/mg of protein).

**Table 10. Binding properties of wild-type and mutated B<sub>2</sub>R.**

Construct	K <sub>d</sub> [nM]	B <sub>max</sub> [pmol/mg protein]
B <sub>2</sub> R <sub>high</sub>	4.71±0.99 (3)*	10.4 (3)
B <sub>2</sub> R <sub>low</sub>	1.87±0.36 (3)	4.4 (3)
Y7.53A	2.82±0.58 (5)	2.1 (4)
Y7.53F	4.68±0.58 (4)	12.5 (4)

\* The number of experiments is indicated in brackets.

### D.2.3 [<sup>3</sup>H]Bradykinin internalization

In the ligand internalization assays we used a concentration of ca. 1 nM [<sup>3</sup>H]BK since the uptake rate by high- and low-expressing cells showed no significant difference with these amount of ligand (section D.1.1.1, Publication C).

As can be seen in Figure 20, incubation of [<sup>3</sup>H]BK at 37°C with cells expressing B<sub>2</sub>R wt resulted in pronounced and rapid ligand internalization (~80% after 10 min) and reached a plateau after approximately 10 min.

Replacements of Y<sup>7.53</sup> with alanine or phenylalanine did not reduce the uptake of the [<sup>3</sup>H]BK (Figure 20) indicating that these residues apparently do not play a role in the regulation of the internalization process in the B<sub>2</sub>R.

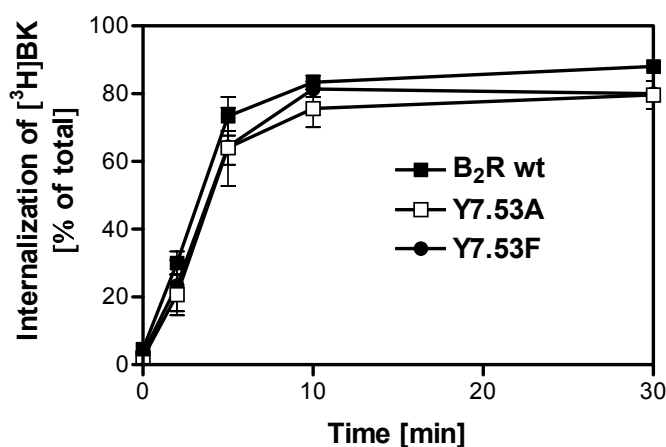


**Figure 20. Internalization of [<sup>3</sup>H]BK by B<sub>2</sub>R wt and mutants Y7.53F and Y7.53A.** Monolayers of stably transfected *HEK293* cells were incubated with 1 nM [<sup>3</sup>H]BK for 90 min on ice. The internalization was started by placing the plates in a waterbath at 37°C. At the indicated times, the internalization process was stopped and surface binding and internalized ligand were determined as described in section C.2.4.1. All values are the mean ±S.D. from at least three experiments performed in triplicates.

#### D.2.4 Investigation of Y7.53A mutant sequestration

As shown in section D.1.1.2, cells strongly overexpressing B<sub>2</sub>R respond to a saturating concentration of BK (1 μM) only with poor sequestration of the receptor from the cell surface, probably because of an overload of the internalization machinery. For the sequestration assay, therefore, we used the B<sub>2</sub>R<sub>low</sub>, which had an expression level closer to that of Y7.53A (section D.2.2).

This low-expressing B<sub>2</sub>R clone responded with a strong decrease in surface binding (more than 75 % within 10 min) when activated by 1 μM BK. By contrast, in the Y7.53A mutant, which was expressed at even lower levels (Table 9), receptor sequestration dropped only to a plateau at 50 % after 5 min (Figure 21).

As the mutant Y7.53F exhibited considerably high surface binding (12.5 pmol/mg of protein), its sequestration was not determined.

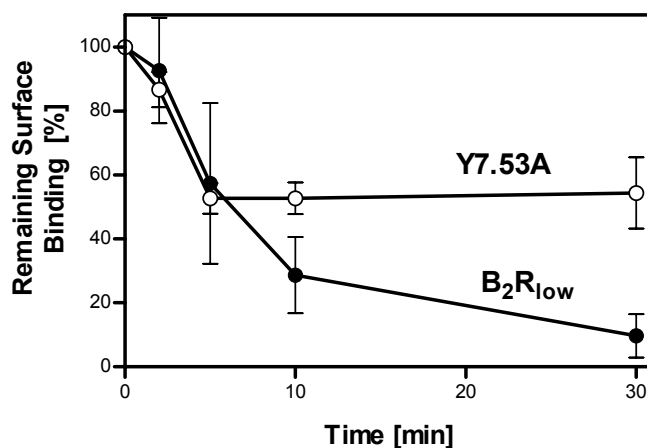


**Figure 21. Sequestration of B<sub>2</sub>R<sub>low</sub> wt and Y7.53A mutant.**

Cells were pre-incubated with 1 μM BK on ice for 90 min. Receptor sequestration was started by warming the cells to 37°C in a waterbath. At the indicated times, cells were set back on ice and treated with an acidic acid solution to remove unlabeled BK. Remaining surface binding was determined with 2 nM [<sup>3</sup>H]BK at 4°C. All values are the mean ±S.D. from at least three experiments each performed in triplicates (from Publication B).

#### D.2.5 Measurement of the PLC activation

We determined the accumulation of total inositol phosphates (IP) without (basal activity) and after stimulation with 1 μM bradykinin (stimulated activity) for 30 min in the presence of 50 mM LiCl and expressed it as x-fold increase over IP levels at the beginning of the assay.

Both wild type and mutant receptors showed the same level of agonist-independent signalling, indicating that the mutations do not produce constitutively active receptors (Table 11).

After incubation with BK the wild type receptor could be stimulated several fold above basal level. But we did not observe a linear correlation between expression rate of the B<sub>2</sub>R wild type



and IP response, i.e. despite highly different expression levels (10.4 pmol by B<sub>2</sub>R<sub>high</sub> *versus* 4.4 pmol of receptor/mg of protein by B<sub>2</sub>R<sub>low</sub>) we failed to find a significant difference in the corresponding ligand induced IP accumulation (12.68±1.37-fold *versus* 9.31±1.69- fold).

Despite the fact that the Y7.53A mutant exposed a much lower fraction of surface receptors than B<sub>2</sub>R<sub>high</sub> (2.1 pmol/mg of protein *versus* 10.4 pmol/mg of protein) or even B<sub>2</sub>R<sub>low</sub> (4.4 pmol/mg) it revealed a higher IP response (16.78±2.00-fold *versus* 12.86±1.37 and 9.31±1.69-fold, respectively), indicating that Y7.53A may be more efficiently coupled to G<sub>q/11</sub> than the wild-type receptor.

When we determined the EC<sub>50</sub> (the concentration of agonist at which the IP response is half-maximal) the wild type and mutated receptors of B<sub>2</sub>R exhibited similar values (Table 11).

**Table 11\*. Functional properties of wild-type and mutated B<sub>2</sub>R.**

Construct	IP accumulation (30 min/50 mM LiCl/37°C)		
	Basal	Stimulated	EC <sub>50</sub> , nM
B <sub>2</sub> R <sub>high</sub>	1.93±0.17 (7)**	12.86±1.37 (7)	0.79±0.34 (4)
B <sub>2</sub> R <sub>low</sub>	1.82±0.19 (3)	9.31±1.69 (3)	0.67±0.22 (3)
Y7.53A	1.88±0.16 (5)	16.78±2.00 (5)	1.16±0.67 (3)
Y7.53F	1.55±0.06 (4)	11.11±1.11 (4)	0.55±0.15 (4)

\* Data are taken from Publication B.

\*\* The number of experiments is indicated in brackets.

### D.2.6 Western blotting analysis of the expression level

Immunoprecipitation of the epitope-tagged receptors followed by Western blotting analysis revealed a similar major diffuse band in the region of 50–80 kDa for all constructs (Figure 22). In addition, low molecular mass bands at 37 and 40 kDa and a high molecular mass band at 100–150 kDa were detected (data not shown).

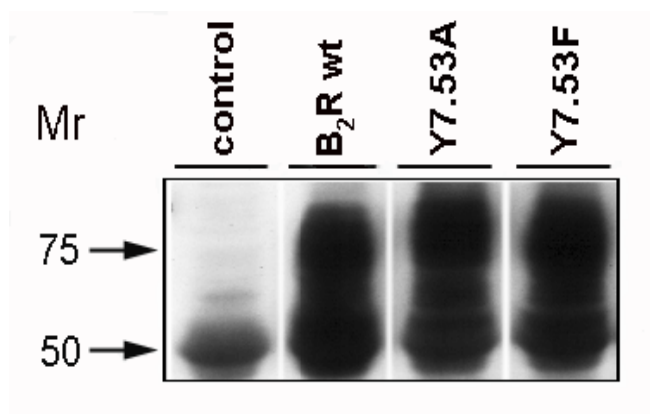


**Figure 22. Immunoprecipitation of wild-type and mutated B<sub>2</sub>R.**

B<sub>2</sub>R wt and receptor mutants containing an N-terminal HA-tag were immunoprecipitated from the lysates of a confluent 100-mm cell culture dish, using AS346 antibody. The precipitated proteins were separated by reducing 10% SDS-PAGE, transferred onto nitrocellulose, and immunoblotted with anti-HA. Relative molecular masses determined with standard proteins are indicated on the *left*. The blot is representative of three experiments with similar results (from Publication B).

### D.2.7 Receptor localization studies using eYFP-constructs

Despite the divergent levels of ligand surface binding in intact cells (Table 9), the total expression levels of B<sub>2</sub>R wt and Y7.53A were comparable (section D.2.5). These observed results suggested that the receptor mutants might be not completely accessible for the ligand because of an intracellular localization. To determine cellular localization of wt and mutated receptors, chimeric constructs were generated with eYFP joined to the C-terminus of B<sub>2</sub>R wt (B<sub>2</sub>ReYFP) or receptor mutants (Y7.53AeYFP and Y7.53FeYFP).

All eYFP constructs exhibited internalization rates of [<sup>3</sup>H]BK that were similar to their non-fused homologues (Figure 23).

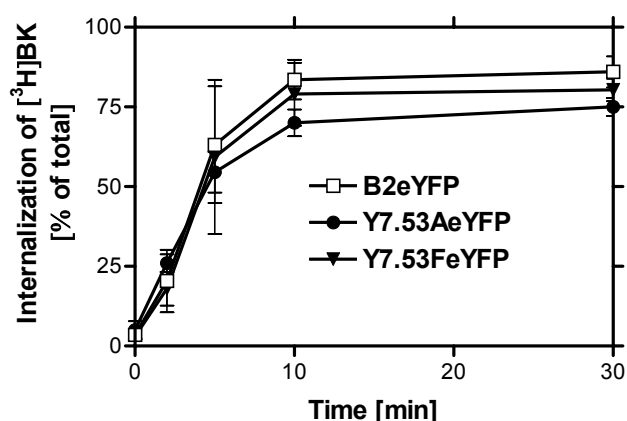


**Figure 23. Internalization of [<sup>3</sup>H]BK by eYFP chimera of the B<sub>2</sub>R wt and mutants.**

Monolayers of stably transfected *HEK293* cells were incubated with 1 nM [<sup>3</sup>H]BK for 90 min on ice. The internalization was started by placing the plates in a waterbath at 37°C. At the indicated times, the internalization process was stopped, and surface binding and internalized ligand were determined as described in section C.2.4.1. All values are the mean ±S.D. from at least three experiments performed in triplicates.

As shown by confocal laser scanning microscopy, B<sub>2</sub>ReYFP was located almost exclusively at the membrane and – in agreement with previous reports (Sabourin *et al.*, 2002) – was found in intracellular vesicles of various sizes only after stimulation with BK (Figure 24).

By contrast, the Y7.53AeYFP mutant was found predominantly inside the cell even in the absence of BK. Stimulation with BK induced minor changes in the intracellular distribution with appearance of Y7.53AeYFP in larger vesicles (Figure 24).

The mutant Y7.53FeYFP also displayed some intracellular localization in the absence of BK but, in contrast to Y7.53AeYFP, was mainly located at the plasma membrane and responded to BK exposure similarly to B<sub>2</sub>R wt, i.e. with a translocation from the plasma membrane to intracellular vesicles (Figure 24).

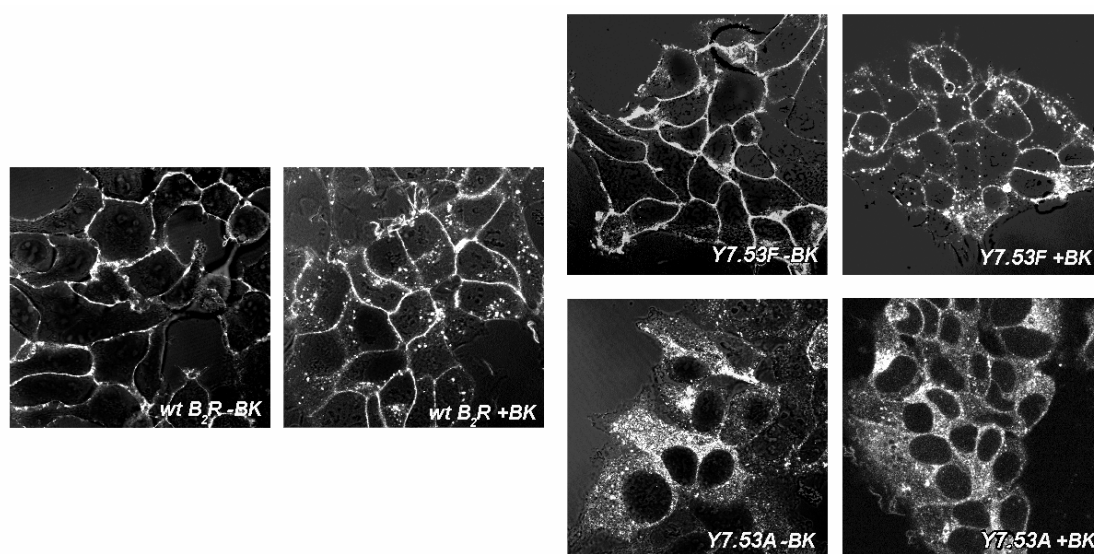


**Figure 24. Cellular distribution of wild type and mutated B<sub>2</sub>R fused to eYFP.**

*HEK293* cells stably expressing constructs of eYFP fused to the C-terminus of B<sub>2</sub>R wt, Y7.53F or Y7.53A were incubated in the absence (-BK) or presence (+BK) of 5  $\mu$ M BK for 30 min at 37°C and examined by confocal laser scanning microscopy. The experiments were repeated three times (from Publication B).

Two plausible explanations for these observations can be suggested: Either following *de novo* synthesis, most of the Y7.53A receptor proteins fail to reach the surface because of misguided trafficking, or the mutation causes the constitutive internalization of Y7.53A despite the fact that this mutant does not show constitutive accumulation of inositol phosphate (section D.2.5). As the internalization strongly depends on receptor phosphorylation, we decided to check the ligand-induced phosphorylation of the “tyrosine mutants”.

## D.2.8 Receptor phosphorylation

### D.2.8.1 Agonist-induced receptor phosphorylation assay

*In vivo* phosphoprotein labeling implicates the incubation of intact organisms, cells or tissues with [<sup>32</sup>P]orthophosphate. The next step involves the purification of the phosphorylated proteins without their further modification by cellular proteases and phosphatases.

The B<sub>2</sub>R displayed distinct phosphorylation even in the absence of a stimulus (Figure 25), as has been reported before in human fibroblasts and *HEK293* cells (Blaukat *et al.*, 2001). When stimulated for 5 min with a saturating concentration of BK at 37°C, however, the B<sub>2</sub>R wt responded with a marked increase (2.5±0.5-fold over basal) in phosphorylation (Figure 25).

The Y7.53F mutant had a slightly increased level of basal phosphorylation (probably due to higher surface expression – see Table 9) and displayed agonist-induced phosphorylation (1.8±0.1-fold above wt basal).

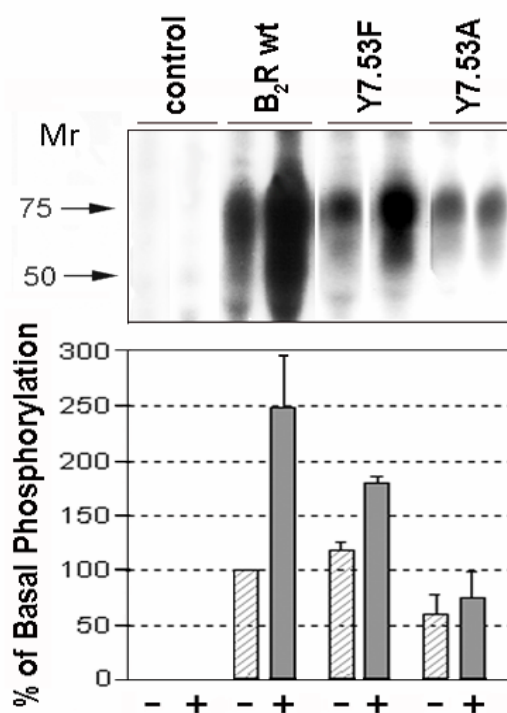


#### Figure 25. Agonist-induced phosphorylation of wild type and mutated B<sub>2</sub>R.

*Upper panel:* *HEK293* cells expressing B<sub>2</sub>R<sub>high</sub> and receptor mutants were labeled for 10–12 h with [<sup>32</sup>P]orthophosphate before stimulation with 1 μM BK for 5 min. Cells were lysed, and proteins were solubilized, precipitated, and visualized by autoradiography. Molecular size markers are indicated to the left.

*Lower panel:* protein phosphorylation, given as optical densities of the bands in the area between 50 and 85 kDa, are presented as means ±S.D. from five independent experiments; unstimulated wild type receptor was set as 100%.

The Y7.53A mutant also exhibited basal phosphorylation but, in contrast to B<sub>2</sub>R, responded with much less (in some experiments with no) additional phosphorylation when challenged with BK. At first sight, this result suggested that the Y7.53A mutant is resistant to agonist-induced

phosphorylation as has been reported for the analogous construct Y7.53A of the  $\beta_2$ -adrenergic receptor (Barak *et al.*, 1994). However, a phosphorylation resistant receptor usually does not show fast internalization as has been observed for Y7.53A mutant of the  $\beta_2$ -adrenergic receptors.

#### D.2.8.2 Two-dimensional phosphopeptide mapping

The method and results showing above are used for detecting overall receptor phosphorylation but do not give information about the specific location of the phosphate on the protein. Since detailed understanding of the mechanism by which phosphorylation regulates the activity of GPCRs requires the identification of specific residues within a given receptor, two-dimensional phosphopeptide mapping was performed.

There are two advantages for using this method: it is an extremely sensitive technique that requires only a few disintegrations per minute (dpm) of metabolically labeled product and (as cellulose is an inert substance) the peptide material can be recovered for secondary analysis, such as determination amino acid composition and sequence, or determining the presence and position of phosphoamino acid residues.

The [ $^{32}\text{P}$ ]-labeled B<sub>2</sub>R wt was digested *in situ* with trypsin and resulting peptides were separated on TLC plates by high voltage electrophoresis and ascending chromatography (Figure 26A). One major phosphopeptide was revealed in untreated cells mentioned here as a peptide 1 (Figure 26A, *left*). As it was previously shown (Blaukat *et al.*, 2001), it corresponds to the integration of the [ $^{32}\text{P}$ ] at the position S<sup>348</sup> (Figure 26B). The same peptide 1 was present in bradykinin-stimulated cells as well as three additional phosphopeptides, namely, peptides 2, 3 and 4 (Figure 26A, *right*). Peptide 2 indicated phosphorylation of pS<sup>339</sup>, peptide 3 that of pS<sup>348</sup> and pS<sup>346</sup> and peptide 4 that of pS<sup>339</sup> and pT<sup>342</sup> (Figure 26B).

Relative intensities and distribution of the observed spots were in full agreement with the results reported for human fibroblasts (Blaukat *et al.*, 2001).

Surprisingly, however, even without stimulation, the Y7.53A mutant exhibited a phosphorylation pattern similar to that observed in the B<sub>2</sub>R wt only after ligand stimulation (Figure 27). This clearly indicated that the Y7.53A mutant was, at least in part, constitutively phosphorylated on serine/threonine residues others than S<sup>348</sup>.

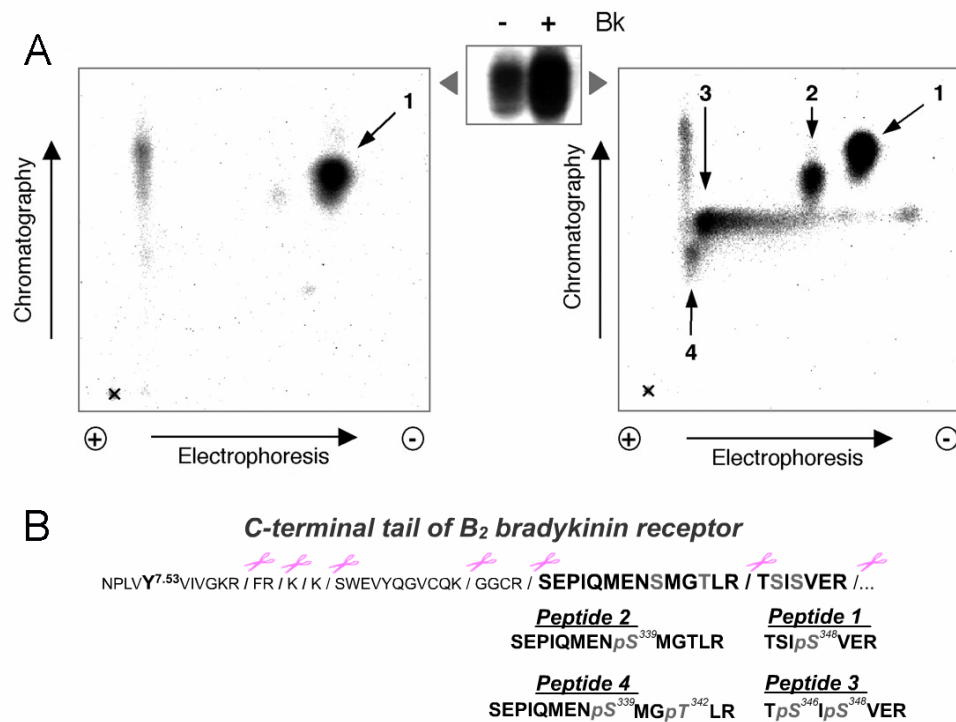


**Figure 26. Two-dimensional phosphopeptide maps of B<sub>2</sub>R wt.**

A) Cells expressing B<sub>2</sub>R<sub>high</sub> wt were cultured in the presence of [<sup>32</sup>P]orthophosphate and incubated for 5 min in the absence (*left*) or presence (*right*) of 1 μM BK. Receptors were immunoprecipitated from the cell lysates by the antibody AS346, the <sup>32</sup>P-labeled proteins were *in situ* digested with trypsin, and the resulting peptides were separated on thin layer chromatography plates as indicated. The sample application site is marked by x, and the polarity of the electrophoresis is indicated (+ and -). The phosphopeptide maps shown are representative for the results of six experiments.

B) Schematic representation of the amino acid sequence (single letter code) of the B<sub>2</sub>R C-terminus starting from NPxxY motif with indicated (scissors) trypsin cleavage positions. Identified phosphopeptides as well as Y<sup>7.53</sup> are highlighted. In addition, the numbered phosphopeptides are given with indicated phosphorylation sites.

Similar to our findings for total phosphorylation, the Y7.53F mutant showed a phosphopeptide map that was intermediate between B<sub>2</sub>R wt and Y7.53A. As it can be seen from Figure 27, without stimulation the pattern of Y7.53F showed an additional spot corresponding to peptide 2 (pS<sup>339</sup>) which is, however, not characteristic for the non-stimulated wild type. This suggests that the phenyl group of phenylalanine can at least partially mimic the effects of the 4-hydroxyphenyl group of Y<sup>7.53</sup>, whereas the aliphatic side chain of alanine can not react in a similar way.

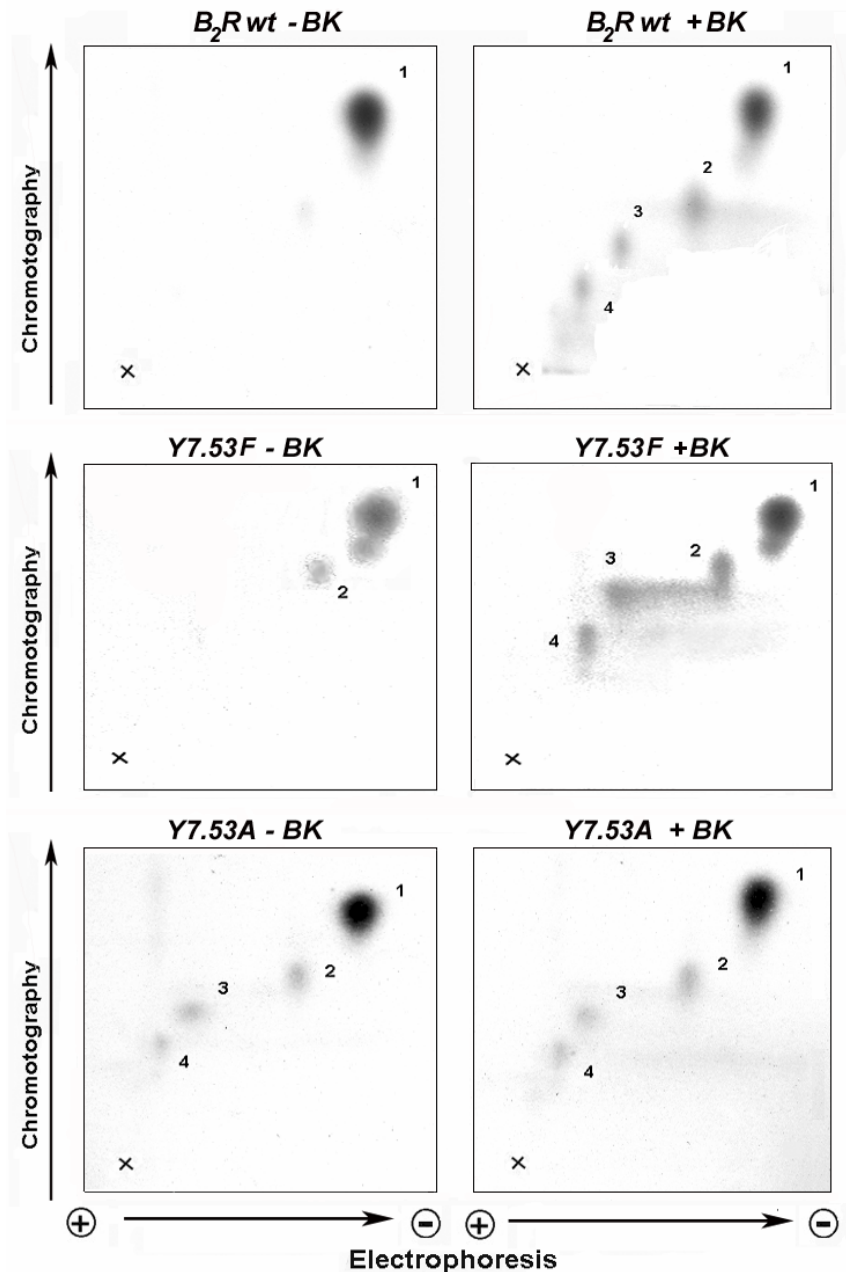


**Figure 27. Two-dimensional phosphopeptide maps of  $B_2R$  wt, Y7.53F and Y7.53A.** Cells cultured in the presence of [ $^{32}$ P]orthophosphate were incubated for 5 min in the absence or presence of 1  $\mu$ M BK. Receptors were immunoprecipitated from the cell lysates by the antibody AS346, the [ $^{32}$ P]-labeled proteins were *in situ* digested with trypsin, and the resulting peptides were separated on thin layer chromatography plates as indicated. The sample application site is marked by  $\times$ , and the polarity of the electrophoresis is indicated (+ and -). The phosphopeptide maps shown are representative for the results of at least three experiments (partially from Publication B).

### D.2.9 Uptake of rhodamine-labelled antibodies

The observed constitutive phosphorylation of mutant Y7.53A led us to hypothesize that the predominant intracellular localization may be a consequence of ongoing agonist-independent internalization. Immunofluorescence (confocal laser scanning) microscopy as one of the most

commonly used applications of epitope tagging in the cell biology of GPCRs was used to test this idea. For that we incubated *HEK293* cells stably expressing wild type or tyrosine mutants of B<sub>2</sub>R with a rhodamine-labeled antibody directed to their N-terminal HA-tag for 1 h at 37°C. In cells expressing B<sub>2</sub>R wt or Y7.53F mutant, the rhodamine staining was seen almost exclusively at the cell surface (Figure 28). In contrast, the Y7.53A mutant showed almost no staining of the plasma membrane but rather a significant translocation of the labeled antibody probe into intracellular compartments within 1 h (Figure 28), suggesting that this mutant internalized spontaneously from the cell surface. Co-incubation of Y7.53A with labeled antibody and antagonist JE049 (formerly also known as HOE140/Icatibant) resulted in distinctly weaker overall staining, with the majority of staining being associated with the plasma membrane. Thus, JE049 acts like an inverse agonist reducing the spontaneous receptor internalization of Y7.53A.

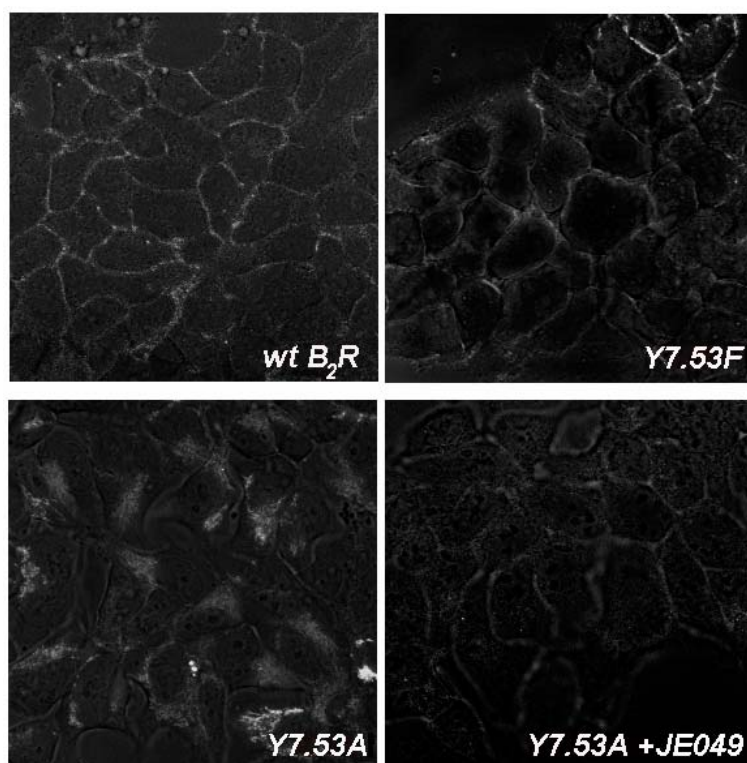


**Figure 28. Internalization of rhodamine-labeled antibodies of B<sub>2</sub>R wt and mutants.** Cells expressing HA-tagged B<sub>2</sub>R wt, Y7.53F and Y7.53A were incubated with rhodamine-labeled anti-HA antibody in the absence (*upper panels; lower panel, left*) or presence of antagonist JE049/HOE140 (*lower panel, right*) at 37°C for 1 h. Receptor distribution was monitored by confocal laser scanning microscopy. The experiment shown is representative of three independent experiments with identical results (from Publication B).



### D.2.10 Co-immunoprecipitation of $G\alpha_{q/11}$ protein

Given that our data thus far suggested that the mutant Y7.53A receptors at the plasma membrane became constitutively phosphorylated and internalized, the issue arose as to why significant amounts of Y7.53A are still detected on the cell surface?

Since Y7.53A does not display increased basal IP accumulation, we speculated that the mutant receptor may couple to  $G_q$  protein without promoting guanine nucleotide exchange. To test the notion whether that Y7.53A mutant interacts with  $G_{q/11}$  in non-stimulated cells, we elaborated a co-immunoprecipitation assay (see section D.1.5).

Immunoprecipitation of  $B_2R$  from unstimulated, highly expressing cells brought down small quantities of  $G_{q/11}$  similar to those observed in control cells (Figure 29). In contrast, when the same co-immunoprecipitation procedure was performed with cells expressing Y7.53A, a strong signal for  $G\alpha_{q/11}$  was observed even in the absence of bradykinin (Figure 29). This finding was obtained despite the fact that considerably less mutant receptor was applied to the gel, most likely because we used crude membrane preparations for the extract that express much less mutant than the ones expressing the  $B_2R$  wt.

Immunoprecipitation of Y7.53A from cells stimulated with BK pulled down different quantities of  $G_{q/11}$ : sometimes  $G\alpha_{q/11}$  protein dissociated after stimulation, giving a weaker band in comparison to non-stimulated cells, at other times it remained at the same level (data not shown as they were inconclusive).

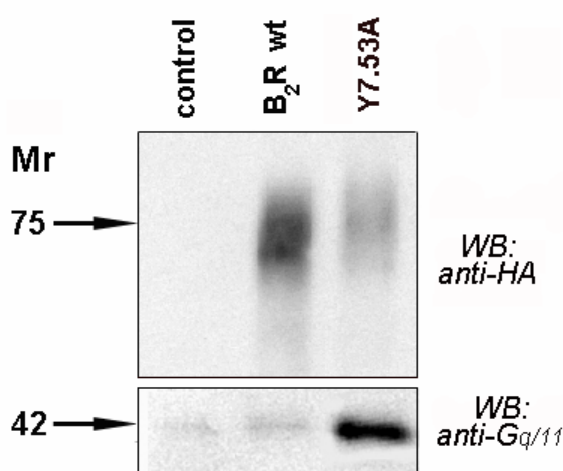


**Figure 29. Analysis of receptor/G-protein interaction.**

Receptors present in 1 mg of the crude membrane preparations of *HEK293* cells expressing indicated receptors were solubilized with 4 mM CHAPS and precipitated with anti-HA antibody covalently linked to agarose beads. The immunoprecipitates were subjected to SDS-PAGE and Western blotting using anti-HA (*upper panel*) or anti-G-protein antibodies (*lower panel*). The experiment shown was repeated three times with identical results (from Publication B).

### D.2.11 [<sup>35</sup>S]GTP $\gamma$ S binding assay

Although Y7.53A mutant was pre-coupled to G<sub>q/11</sub>, it simultaneously showed a low level of agonist-independent signalling. Now, it was of interest to check whether this mutant can induce (and if so, to what extent) GTP/GDP exchange in the non-activated state.

To monitor guanine nucleotide exchange, we used a [<sup>35</sup>S]GTP $\gamma$ S binding assay. This is a simple and rapid assay which is however not strictly specific for a special G protein. Potentially, any protein possessing a binding site with high affinity and specificity for guanidine nucleotides could be detected. Moreover, G<sub>i</sub> proteins show substantially higher rates of basal guanine nucleotide exchange than the other G proteins (Milligan, 2003).

[<sup>35</sup>S]GTP $\gamma$ S binding assay gave almost identical values of basal binding at 30°C for B<sub>2</sub>R wt (regardless of the expression level) and for Y7.53A (Figure 30), suggesting that the receptor mutant (despite being tightly pre-coupled to G<sub>q/11</sub>) does not significantly enhance guanine nucleotide exchange in the absence of an agonist. This finding is in agreement with our data from the IP accumulation assays (Table 11). We also observed that 1  $\mu$ M BK induced a moderate increase in [<sup>35</sup>S]GTP $\gamma$ S binding (28–39%) both for high and low expressing B<sub>2</sub>R wt and for Y7.53A mutant, probably because G<sub>q/11</sub> represents only a minor fraction (20%) of total G proteins contributing to basal [<sup>35</sup>S]GTP $\gamma$ S binding (Milligan, 2003).

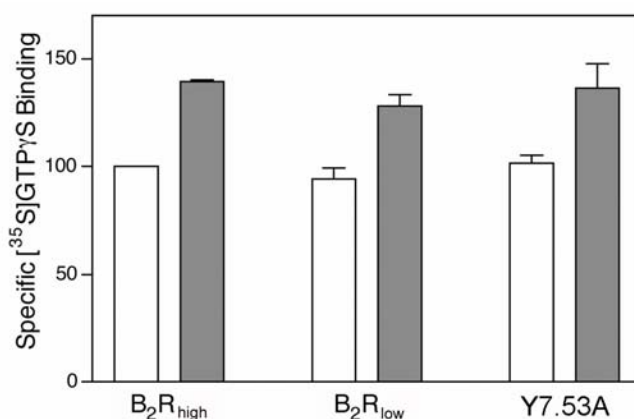


**Figure 30. [<sup>35</sup>S]GTP $\gamma$ S binding to crude membranes of B<sub>2</sub>R wt and Y7.53A mutant.** Aliquots of crude membrane preparations containing 20  $\mu$ g of total protein each of high- and low-expressing B<sub>2</sub>R wt (*left* and *center*, respectively) and of the Y7.53A mutant receptor (*right*) were incubated at 30°C with 500  $\mu$ l of assay buffer in the presence of 10<sup>5</sup> cpm [<sup>35</sup>S]GTP $\gamma$ S with (*gray bars*) or without (*open bars*) 1  $\mu$ M BK. After 30 min the binding was determined as described in section C.2.9. Data shown are the means  $\pm$ S.D. from three independent experiments each performed in triplicates and are presented as percentage of the basal binding obtained for high-expressing B<sub>2</sub>R wt (100%) (from Publication B).

### D.3 Role of Y<sup>7.53</sup> in the $\beta_2$ -adrenergic receptor

As it was mentioned in the introduction, the *NPxxY* motif is highly conserved among class A GPCRs, because 95% of all members of this family have a tyrosine at the position 7.53. Therefore, we were interested as to whether the model describing  $\beta_2$ R-Y7.53A mutant could be applicable for other “tyrosine mutants”. For this reason, we chose the  $\beta_2$ -adrenergic receptor ( $\beta_2$ -ADR) that can be considered as prototypical of class A-type GPCRs. Moreover, the Y7.53A mutant of  $\beta_2$ -ADR was one of the first generated and one of the best studied “tyrosine mutant” (Barak *et al.*, 1994; Ferguson *et al.*, 1995; Gabilondo *et al.*, 1996). This mutant is characterized by abolished signalling, loss of ligand-induced phosphorylation, and lack of sequestration. How this mutation of Y<sup>7.53</sup> results in such phenotype, is not clarified so far.

We received the  $\beta_2$ -ADR wt and  $\beta_2$ -ADR-Y7.53A genes from Prof. Dr. Lohse (Heidelberg, Germany) and inserted them in our expression vector pcDNA5/FRT. Thereafter, these receptors were stably expressed in the *HEK293* cells. All receptor coding sequences were preceded by a single HA-tag at the N-terminus.

#### D.3.1 Receptor sequestration

For the investigation of the receptor sequestration of HA-tagged  $\beta_2$ -ADR and its tyrosine mutant an ELISA assay was established. Agonist stimulation with isoproterenol resulted in the sequestration of ca. 70 % of expressed  $\beta_2$ -ADR. Mutation of the Y<sup>7.53</sup> to an alanine led to a  $\beta_2$ -ADR-Y7.53A mutant that is deficient in its agonist-promoted sequestration (Figure 31). This result was in full agreement with a number of published data about the sequestration behaviour of  $\beta_2$ -ADR wt and its tyrosine mutant (Barak *et al.*, 1994; Ferguson *et al.*, 1995).

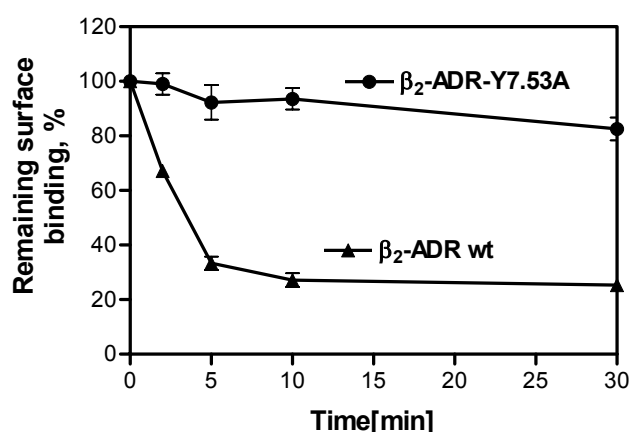


**Figure 31. Sequestration of  $\beta_2$ -ADR and  $\beta_2$ -ADR-Y7.53A.**

Cells were pre-incubated with 1  $\mu$ M isoproterenol (ISO) on ice for 90 min. Receptor sequestration was started by warming the cells to 37°C in a waterbath. At the indicated times, cells were set back on ice and an ELISA was performed as described in section C.2.4.3. All values are the mean  $\pm$ S.D. from at least three experiments each performed in quadruplets.

### D.3.2 Ligand-induced phosphorylation

Figure 32 shows the isoproterenol (ISO)-stimulated phosphorylation of the human  $\beta_2$ -ADR.  $\beta_2$ -ADR wt displayed no basal phosphorylation, but when stimulated with ISO at 37°C responded with a marked increase in phosphorylation. In contrast, the slowly internalizing  $\beta_2$ -ADR-Y7.53A exhibited no significant phosphorylation even when challenged with ISO (Figure 32). The result of this experiment was in agreement with data published earlier (Barak *et al.*, 1994).

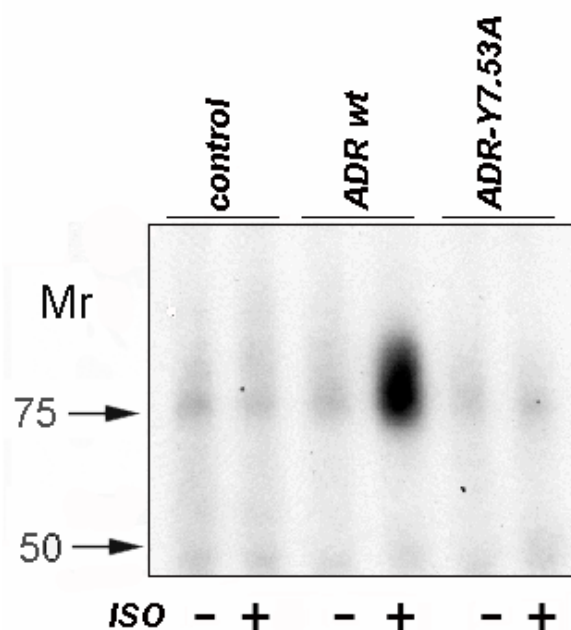


**Figure 32. Isoproterenol-induced phosphorylation of  $\beta_2$ -ADR and  $\beta_2$ -ADR-Y7.53A.** *HEK293* cells expressing  $\beta_2$ -ADR wt and mutant receptor were labelled for 10-12 h with [ $^{32}$ P]orthophosphate before stimulation with 1  $\mu$ M isoproterenol (ISO) for 5 min. Cells were lysed, and proteins were solubilized, precipitated, and visualized by autoradiography. Molecular size markers are indicated at the *left*.

Possibly, the  $\beta_2$ -ADR-Y7.53A mutant has a conformation similar to  $\beta_2$ R-Y7.53A. In this conformation it should also interact with its cognate G protein ( $G_s$ ) in a ligand-independent manner. This could explain a lack of phosphorylation and sequestration after stimulation as the bound G protein would block the access of the G protein-coupled receptor kinases (GRKs) to the receptor. To check this hypothesis, we performed a co-immunoprecipitation with the  $G_s$  protein.

### D.3.3 Interaction of $\beta_2$ -ADR-Y7.53A with $G_s$ proteins

$\beta_2$ -ADR wt and receptor mutant were immunoprecipitated with anti-HA antibody covalently linked to the agarose beads as it was previously described in section D.1.4. Afterwards, the

receptors were visualized with an anti-HA antibody and the  $G_s$  subunits were detected with an antibody from Calbiochem raised against a C-terminal sequence of  $G\alpha_s$ .

A low basal association between  $G_s$  subunits and wild type of  $\beta_2$ -ADR was observed in ISO-untreated cells similar to control preparation (Figure 33). The effect of ISO on the receptor /  $G_s$  protein complex formation was 3.1-fold in the case of the  $G_s$ -large and 2.5-fold by the  $G_s$ -small protein compared to the basal level.

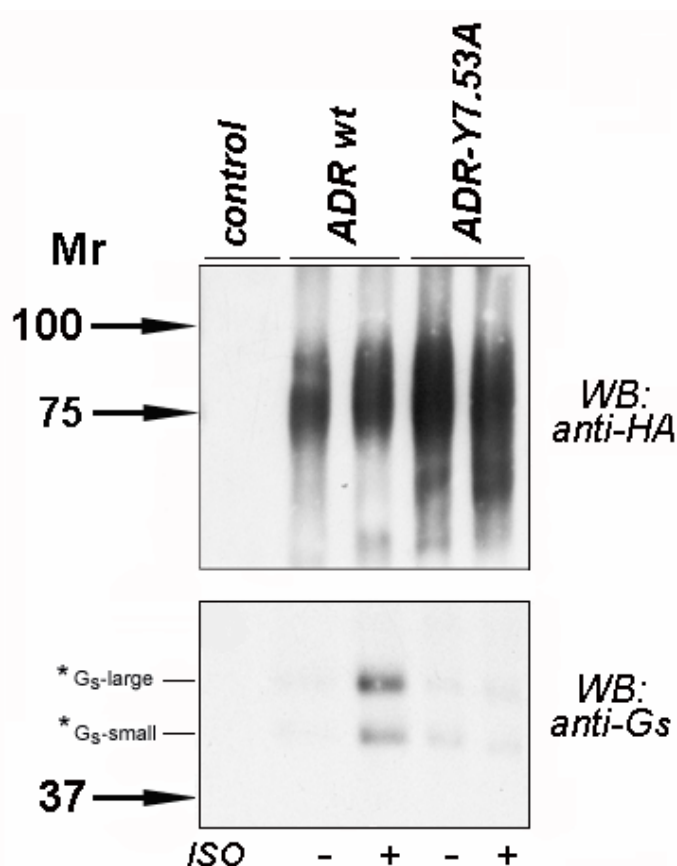


**Figure 33. Analysis of ligand-induced  $\beta_2$ -ADR /  $G_s$  protein interaction.**

Cell monolayers expressing  $\beta_2$ -ADR or  $\beta_2$ -ADR-Y7.53A were incubated with or without isoproterenol (ISO) for 5 min, scraped and used for crude membrane preparation. Receptors present in 1 mg of the crude membrane preparations of *HEK293* cells were solubilized with 4 mM CHAPS and precipitated with anti-HA antibody covalently linked to the agarose beads. The immunoprecipitates were subjected to SDS-PAGE and Western blotting using anti-HA (*upper panel*) or anti- $G_s$  protein antibodies (*lower panel*). As a negative control, non-expressing cells were taken and subjected to the same procedure. The experiment shown was repeated three times with identical results.

\* Cloning of the human  $G\alpha_s$  gene indicated that two major forms of  $G\alpha_s$  exist (Bray *et al.*, 1986; Mattera *et al.*, 1986). They were termed  $G\alpha_s$ -large and  $G\alpha_s$ -small and are present in many tissues as proteins with apparent molecular masses of 52 and 45 kDa, respectively. Both of these isoforms are products of alternatively spliced transcripts from the same gene.  $G\alpha_s$ -small cDNA is distinguished from  $G\alpha_s$ -large cDNA by the exclusion of 45 bases of exon 3 encoding 15 amino acids (Bray *et al.*, 1986; Mattera *et al.*, 1986).

In contrast, even after stimulation the cells highly expressing  $\beta_2$ -ADR-Y7.53A brought down very little of  $G_s$  protein in amounts similar to those observed in control cells. These results suggest that this mutant did not form a stable complex with  $G_s$  proteins neither in the inactive state nor when activated with ISO.

As it was shown in section D.2, the tyrosine mutant of  $B_2R$  was not only pre-coupled to  $G_{q/11}$ , but, due to its constitutive phosphorylation, it may also react with GRKs in an ligand-independent manner.

A second possibility to explain the phenotype of  $\beta_2$ -ADR-Y7.53A was that this mutant irreversibly interacts with GRK without getting phosphorylated. In order to test this hypothesis, a co-immunoprecipitation assay with GRK2/3 was performed.

#### **D.3.4 Interaction of $\beta_2$ -ADR-Y7.53A with GRKs**

The G protein-coupled receptor kinases (GRKs) were detected with mouse monoclonal anti-GRK2/3 antibody from Sigma. This antibody was produced using a partial GST fusion protein corresponding to the carboxyl terminus of GRK3 (residue 467-688) as an immunogen. This immunogen shares homology with GRK2, which therefore can also be detected. The minimal epitope recognized by the antibody comprises the amino acids 435-485.

To obtain a good signal for GRKs, we used for the solubilization 1.5 mg of the crude membrane preparation that is one and a half as much as applied for the G protein co-immunoprecipitation assay. Therefore, the samples look overloaded in Figure 34 (*upper panel*).

A low basal association between GRK2/3 and wild type of  $\beta_2$ -ADR was observed in ISO-untreated cells. After stimulation, a significant increase of the GRK2/3 signal was observed in comparison with ISO-untreated cells. In contrast, immunoprecipitates of  $\beta_2$ -ADR-Y7.53A revealed a strong signal for GRK2/3 even without stimulation.

These results suggest that this mutant is able to form a stable complex with GRK2/3 even in a non-active state despite of the fact that it exhibited no significant phosphorylation after activation (Figure 34).

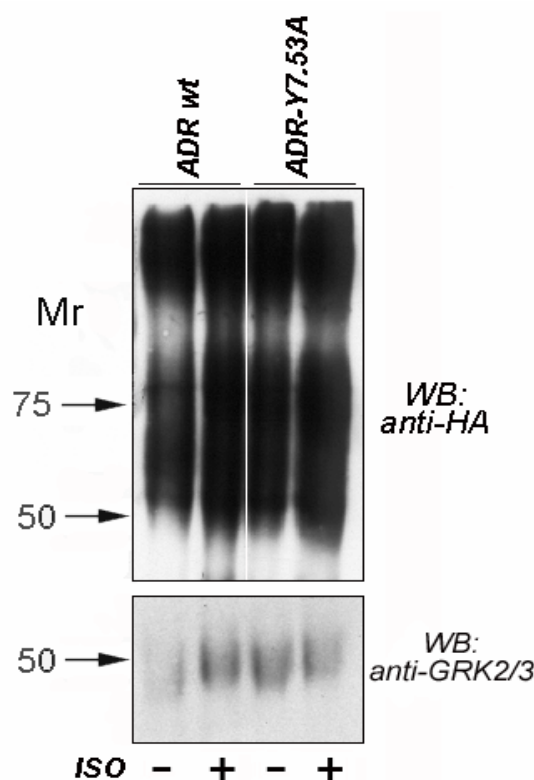


**Figure 34. Analysis of  $\beta_2$ -ADR / GRK interaction.**

Cell monolayers expressing  $\beta_2$ -ADR or  $\beta_2$ -ADR-Y7.53A were incubated with or without isoproterenol (ISO) for 5 min, scraped, and crude membrane preparation was made. Receptors present in 1.5 mg of the crude membrane preparations of *HEK293* cells were solubilized with 4 mM CHAPS and precipitated with anti-HA antibody covalently linked to the agarose beads. The immunoprecipitates were subjected to SDS-PAGE and Western blotting using anti-HA (*upper panel*) or anti-GRK2/3 antibodies (*lower panel*). The experiment reflects a pilot experiment.

#### D.4 Role of the interaction between Y<sup>7.53</sup> and F<sup>7.60</sup> in the human B<sub>2</sub>R

##### D.4.1 Generation of F7.60A, Y7.53F/Y7.60A and Y7.53A/F7.60A mutants

The resolution of the crystal structure of rhodopsin suggests that Y<sup>7.53</sup> in the *NPxxY* motif might interact with F<sup>7.60</sup> in helix VIII (Figure 3). F<sup>7.60</sup> is not as strongly conserved as Y<sup>7.53</sup>, since only 65% of all class A GPCRs have this residue at the indicated position (Oliveira *et al.*, 1999).

We decided now to investigate the function of this amino acid residue in human B<sub>2</sub> bradykinin receptor. The main strategy was to examine whether the exchange of F<sup>7.60</sup> to alanine leads to the same phenotype as Y7.53A or not. Therefore, we mutated F<sup>7.60</sup> to Ala termed mutant F7.60A.

The exchange of the Y<sup>7.53</sup> to phenylalanine by the human serotonin 5HT<sub>2C</sub> receptor leads to the abolished signalling, whereas mutation at the position Y<sup>7.60</sup> had no effect on the receptor functions. However, when the Y7.53F receptor was mutated at position 7.60 to either alanine, phenylalanine, leucine, or tryptophan (5HT<sub>2C</sub>-Y7.53F/Y7.60A(F,L,W)), the wild-type phenotype

was restored (Prioleau *et al.*, 2002). The authors also suggested that Y<sup>7.53</sup> and Y<sup>7.60</sup> contribute to a common functional microdomain connecting helices VII and VIII that influences the switching of the 5HT<sub>2C</sub> receptor among multiple active and inactive conformations.

To check whether the simultaneous mutations of the Y<sup>7.53</sup> and F<sup>7.60</sup> would restore the wild type phenotype of the B<sub>2</sub>R-Y7.53A mutant or not, we mutated at once Y<sup>7.53</sup> to alanine and F<sup>7.60</sup> to phenylalanine termed mutant Y7.53F/F7.60A and, even less conservatively, both residues were mutated to alanine producing the Y7.53A/F7.60A mutant.

#### D.4.2 Investigation of the binding properties of the constructed mutants

The affinities for B<sub>2</sub>R wild type and its mutants and the levels of expression are shown in the Table 11. Although the affinity for [<sup>3</sup>H]BK was slightly reduced for all receptor mutants, in most cases the changes were modest. All mutated receptors were expressed at lower level compared to the wild-type receptor. The Y7.53A/F7.60A was expressed less than 40% of wild-type levels.

**Table 12. Binding properties of wild type and mutated B<sub>2</sub>R.**

Construct	K <sub>d</sub> [nM]	B <sub>max</sub> [pmol/mg protein]
B <sub>2</sub> R <sub>high</sub>	4.71±0.99 (3)*	10.4 (3)
F7.60A	1.95±0.52 (4)	7.3 (4)
Y7.53F/F7.60A	1.36±0.55 (3)	8.5 (3)
Y7.53A/F7.60A	1.32±0.49 (3)	3.6 (3)

\* The number of experiments is indicated in brackets.

#### D.4.3 [<sup>3</sup>H]Bradykinin internalization

Replacements of F<sup>7.60</sup> with alanine did not reduce the uptake of the radioactive-labelled bradykinin as compared to B<sub>2</sub>R wt (Figure 35).

However, the simultaneous exchange of the Y<sup>7.53</sup> to phenylalanine and F<sup>7.60</sup> to alanine led to the almost complete loss of the ligand internalization capacity. These data suggest that the proper internalization absolutely requires either the hydroxyl group of Y<sup>7.53</sup> or the presence of F<sup>7.60</sup> in helix VIII, but not necessarily both.

As expected, the synchronous mutation of the Y<sup>7.53</sup> and F<sup>7.60</sup> to alanine also markedly impaired ligand internalization (Figure 35).



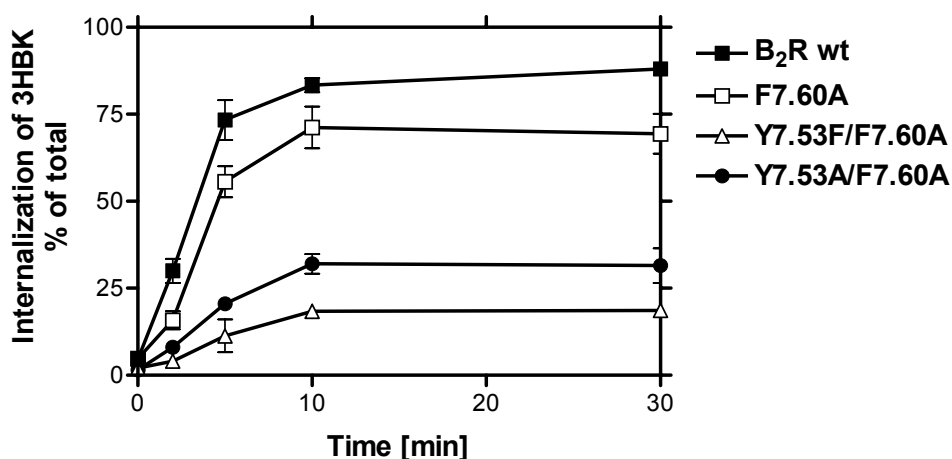


**Figure 35. Internalization of [<sup>3</sup>H]BK by wild-type and mutated B<sub>2</sub>Rs.**

Monolayers of stably transfected *HEK293* cells were incubated with 1 nM [<sup>3</sup>H]BK for 90 min on ice. The internalization was started by placing the plates in a waterbath at 37°C. At the indicated times, the internalization process was stopped, and surface binding and internalized ligand were determined as described in section C.2.4.1. All values are the mean ±S.D. from at least three experiments performed in triplicates.

#### D.4.4 Measurement of the activation of PLC

We determined the accumulation of total inositol phosphates (IP) without (basal activity) and after stimulation with 1 μM bradykinin (stimulated activity) for 30 min and expressed it as x-fold increase over IP levels at the beginning of the experiment.

Both wild type and mutated receptors showed a low level of agonist-independent signalling, indicating that the mutations do not produce constitutively active receptors (Table 13). F7.60A and Y7.53F/F7.60A mutants were able to stimulate a several-fold increase of IP above basal level.

Only Y7.53A/F7.60A showed a significantly reduced IP signal. Moreover, this mutant became less sensitive to BK as its EC<sub>50</sub> for the IP response was higher than that of B<sub>2</sub>R wt (Table 13).

Thus, our results suggest that the proper signalling absolutely requires either the aromatic ring of Y<sup>7.53</sup> or the presence of F<sup>7.60</sup> in helix VIII, but not necessarily both.

**Table 13. The functional properties of wild-type and mutated B<sub>2</sub>Rs.**

Construct	IP accumulation (30 min/50 mM LiCl/37°C)		
	Basal	Stimulated	EC <sub>50</sub> , nM
B <sub>2</sub> R <sub>high</sub>	1.93±0.17 (7)*	12.86±1.37 (7)	0.79±0.34 (4)
F7.60A	1.76±0.23 (4)	13.84±0.75 (4)	0.28±0.05 (5)
Y7.53F/F7.60A	1.91±0.12 (3)	13.82±1.55 (3)	1.30±0.16 (3)
Y7.53A/F7.60A	2.13±0.12 (3)	3.07±0.33 (3)	2.05±1.19 (3)

\* The number of experiments is indicated in brackets.

#### D.4.5 Ligand-induced phosphorylation and phosphopeptide mapping

The level of basal phosphorylation of mutant F7.60A was slightly decreased in comparison to B<sub>2</sub>R wt, possibly due to the lower expression level (Table 11), but the mutant still responded with additional phosphorylation when challenged with BK. Both double mutants also exhibited clear basal phosphorylation, but displayed no significant additional BK-inducible phosphorylation (Figure 36).

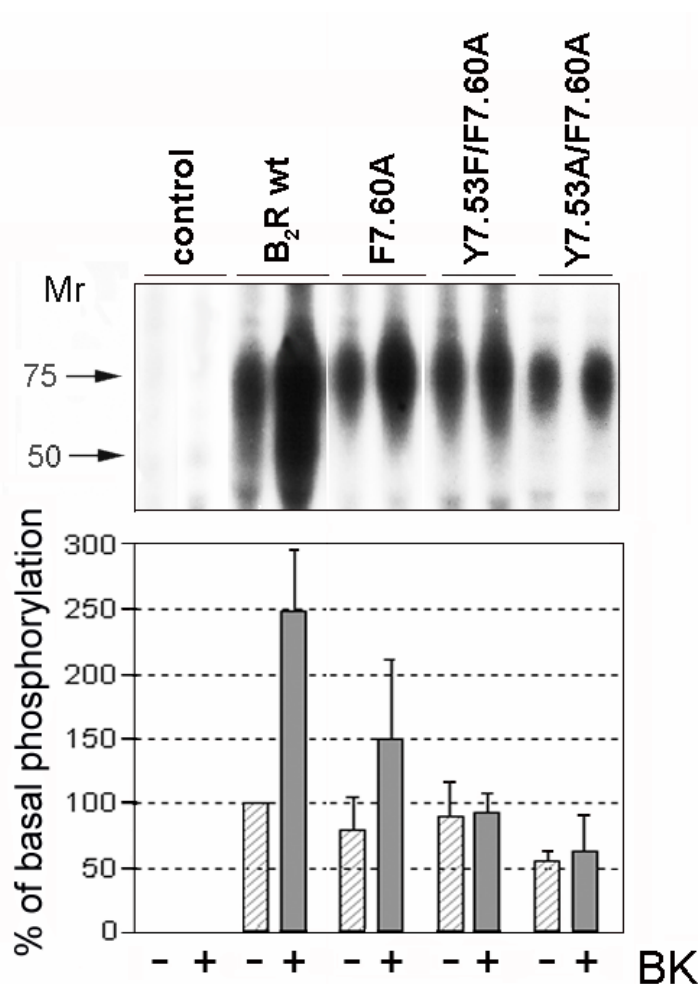


**Figure 36. Agonist-induced phosphorylation of wild type and mutated B<sub>2</sub>R.**

*Upper panel:* HEK293 cells expressing B<sub>2</sub>R wt and mutant receptors were labelled for 10-12 h with [<sup>32</sup>P]orthophosphate before stimulation with 1 μM BK for 5 min. Cells were lysed, and proteins were solubilized, precipitated, and visualized by autoradiography (section C.2.7.1). Molecular size markers are indicated at the *left*.

*Lower panel:* Protein phosphorylation, given as optical densities of the bands in the area between 50 and 85 kDa, are presented as means ± S.D. of five independent experiments; data of unstimulated wild type receptor was set as 100%.

To determine the contributions of the different phosphorylation sites, a two-dimensional phosphopeptide mapping of F7.60A, Y7.53F/F7.60A, and Y7.53A/F7.60A mutants was performed (Figure 37). Mutant F7.60A exhibited phosphorylation patterns similar to those

observed for the B<sub>2</sub>R wt (Figure 37B) with the exception that in the non-stimulated pattern an additional spot corresponding to peptide 2, and therefore to phosphoserine 339, did appear.

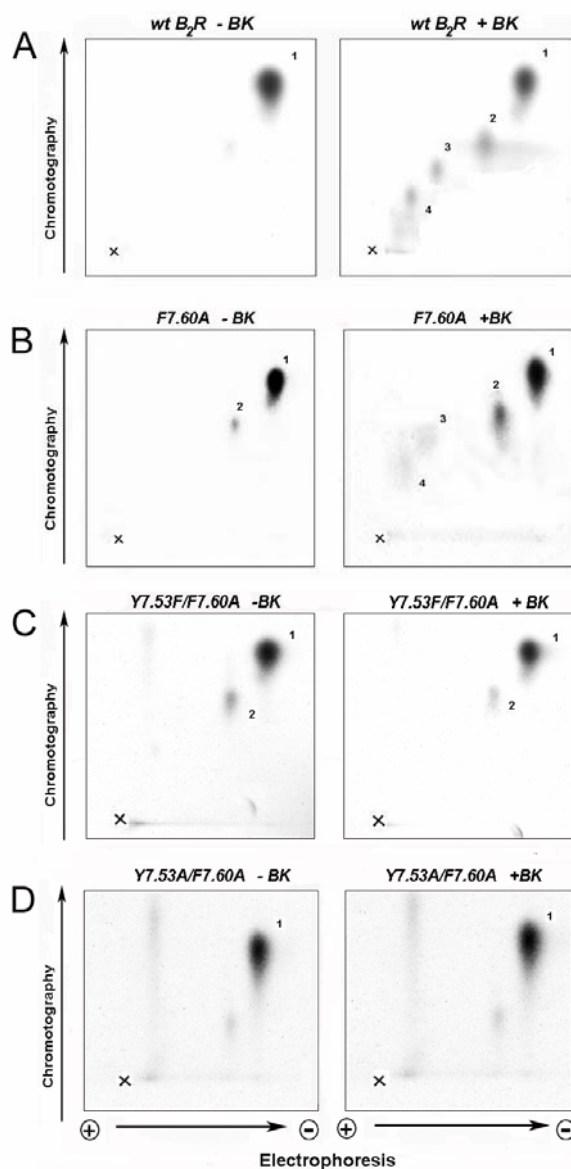


**Figure 37. Two-dimensional phosphopeptide mappings of B<sub>2</sub>R wt, F7.60A, Y7.53F/F7.60A and Y7.53A/F7.60A.**

Cells labelled with [<sup>32</sup>P]orthophosphate were incubated for 5 min in the absence or presence of 1 μM BK. The [<sup>32</sup>P]-labelled proteins were digested *in situ* with trypsin, and the resulting peptides were separated on thin layer chromatography plates as described in section C.2.7.2. The sample application site is marked by ×, and the polarity of the electrophoresis is indicated (+ and −). The maps shown are representative for the results of three experiments.

But both double mutants Y7.53F/F7.60A and Y7.53A/F7.60A, however, showed mainly the spot that can also be observed in the non-stimulated B<sub>2</sub>R wt and determined the basal phosphorylation (pS<sup>348</sup>). Moreover, a quite weaker spot corresponding to peptide 2 (pS<sup>346</sup>) was

observed. However, the peptides 3 and 4 did not appear either with or without stimulation (Figure 37C, D).

#### D.4.6 Interaction of Y7.53F/F7.60A mutant with the $G_{q/11}$ protein

To explain the phenotype of mutant Y7.53F/F7.60A, a co-immunoprecipitation assay was performed several times, but, although this mutant responded to ligand stimulation with IP-signal comparable with that of the wild type, we were not able to detect a significant increase for the  $G_{q/11}$  protein in the BK-stimulated cells (Figure 38, *left picture*). As a definitely lower amount of Y7.53F/F7.60A receptors (in comparison with that of the wild type) was applied to the gel, the observed signal for  $G_{q/11}$  could not be assumed as a basal one.

Therefore, we performed a co-immunoprecipitation assay with equal amounts of the receptors (Fig 38, *right picture*). Indeed, the amount of the  $G_{q/11}$  protein co-immunoprecipitated with Y7.53F/F7.60A was much higher than that arising from the non-stimulated  $B_2R$  wt, but was definitely lower than that exerted by the stimulated wild-type receptor.

Thus, similar to mutant Y7.53A,  $G_{q/11}$  was also pre-coupled to mutant Y7.53F/F7.60A, in spite of that fact that the tyrosine aromatic ring at 7.53 position was still present. With this assumption, we could explain the normal IP-signal, as pre-coupled G protein dissociated after stimulation, and due to high affinity of Y7.53F/F7.60A mutant to the cognate G protein, GRKs had no time to phosphorylate the receptor.

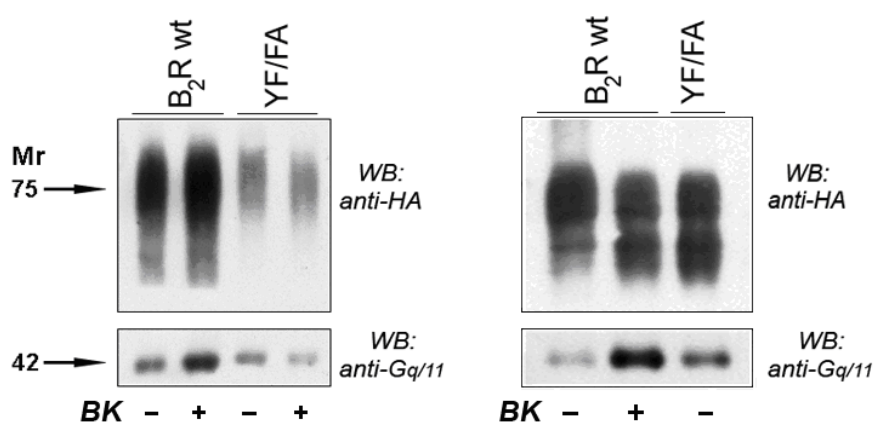


**Figure 38. Analysis of ligand-induced  $B_2R$ -Y7.53F/F7.60A /  $G_{q/11}$  protein interaction.** Cell monolayers expressing  $B_2R_{high}$  or Y7.53F/F7.60A were incubated with or without BK for 5 min, scraped and used for crude membrane preparation. Receptors present in 1 mg of the crude membrane preparations of *HEK293* cells were solubilized with 4 mM CHAPS and immunoprecipitated with anti-HA antibody covalently linked to the agarose beads (section C.2.6.2). The immunoprecipitates were subjected to SDS-PAGE and Western blotting using anti-HA (*upper panel*) or anti- $G_{q/11}$  protein antibodies (*lower panel*). Y7.53F/F7.60A mutant is depicted as YF/FA.

#### D.4.7 Interaction of Y7.53A/F7.60A mutant with the $G_{q/11}$ protein

Since the mutant Y7.53A/F7.60A was resistant to the phosphorylation and, as a result, did not undergo ligand-induced internalization and displayed a significantly reduced IP signal, it resembled in several ways the properties of  $\beta_2$ -ADR-Y7.53A described before. Therefore, we hypothesized that this double mutant could not interact with the cognate G protein similar to  $\beta_2$ -ADR-Y7.53A. To check this assumption, a co-immunoprecipitation assay was performed. As a positive control the high-expressing  $B_2R_{high}$  was used. As it was shown before, the wild-type receptor responded to the activation with a strongly increased signal for  $G_{q/11}$  (Figure 39). In contrast, Y7.53A/F7.60A did not show any increased signal for the cognate G protein after stimulation. A low precipitated amount of the  $G_{q/11}$  protein can be assumed as being nonspecific similar to the situation revealed by the non-stimulated wild-type receptor.

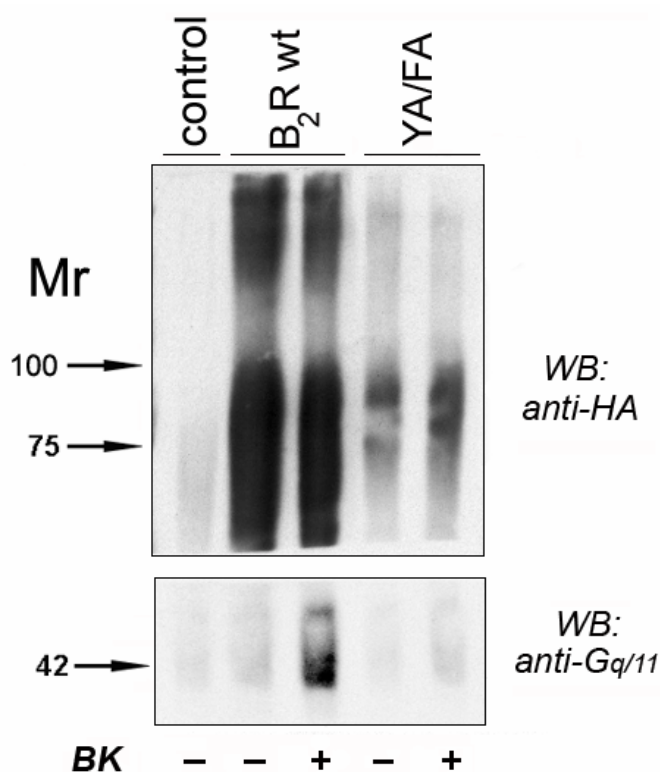


**Figure 39. Analysis of  $B_2R$ -Y7.53A/F7.60A /  $G_{q/11}$  protein interaction.**

Cell monolayers expressing  $B_2R_{high}$  or Y7.53A/F7.60A were incubated with or without BK for 5 min, scraped and used for crude membrane preparation. Receptors present in 1 mg of the crude membrane preparations of *HEK293* cells were solubilized with 4 mM CHAPS and immunoprecipitated with anti-HA antibody covalently linked to the agarose beads. The immunoprecipitates were subjected to SDS-PAGE and Western blotting using anti-HA (*upper panel*) or anti- $G_{q/11}$  protein antibodies (*lower panel*). Y7.53F/F7.60A mutant is given as YF/FA. A representative out of three experiments is shown.

#### D.4.8 Interaction of Y7.53A/F7.60A mutant with GRKs

The results of the co-immunoprecipitation of GRKs analysis illustrated in Figure 40 showed that we were not able to co-immunoprecipitate the activated B<sub>2</sub>R with GRKs, probably because they interact only for a very short time with each other. In contrast, immunoprecipitates of Y7.53A/F7.60A from unstimulated as well as from stimulated cells revealed a distinct signal for GRK2/3. This finding was obtained despite the fact that considerably less amounts of the mutated receptor was applied to the gel (Figure 40).

Thus, Y7.53A/F7.60A mutant of the B<sub>2</sub> bradykinin receptor seems to have a similar conformation as β<sub>2</sub>-ADR-Y7.53A allowing interaction with GRKs even in the non-activated state.

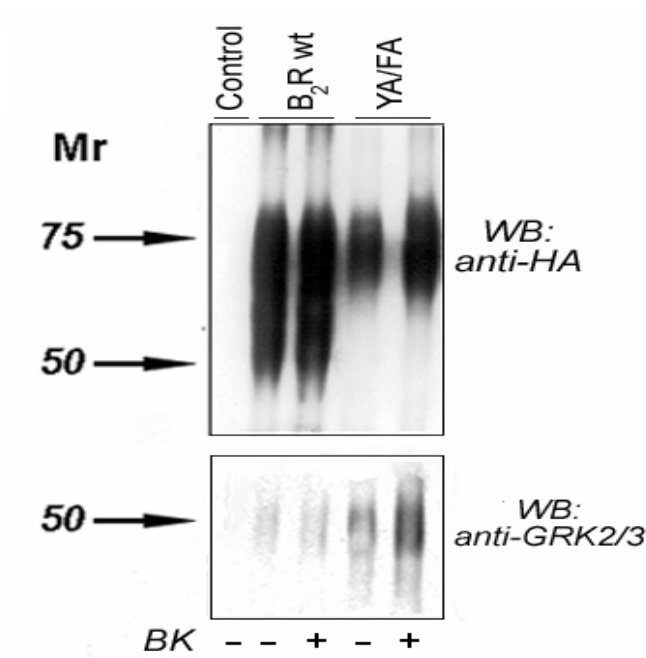


**Figure 40. Analysis of receptor / GRK interaction.**

Cell monolayers expressing B<sub>2</sub>R<sub>high</sub> or Y7.53A/F7.60A were incubated with or without BK for 5 min, scraped and used for crude membrane preparation. Receptors present in 1.5 mg of the crude membrane preparations of HEK293 cells were solubilized with 4 mM CHAPS and immunoprecipitated with anti-HA antibody covalently linked to the agarose beads. The immunoprecipitates were subjected to SDS-PAGE and Western blotting using anti-HA (*upper panel*) or anti-GRK2/3 antibodies (*lower panel*). Y7.53F/F7.60A mutant is depicted as Y7.53A/F7.60A.

*To summarize, these data demonstrate that the highly conserved Y<sup>7.53</sup> of the NPxxY motif and its potential partner F<sup>7.60</sup> play an important role in the interaction of the B<sub>2</sub>R and β<sub>2</sub>-ADR with GRKs and cognate G proteins.*

## E DISCUSSION

GPCRs contain highly conserved sequence motifs that identify them as members of the class A or rhodopsin/ $\beta$ -adrenergic-receptor-like family. Because these conserved side-chains are likely to have general roles pertinent to many members of this family, their function has been an area of active investigation in many laboratories. As a stimulus-dependent conformational rearrangement shared by all GPCRs, it is likely that many of the conserved side-chains mediate transition of these proteins to an activated state. The currently most developed activation model includes an agonist-induced separation of the cytosolic ends of the transmembrane domains (TMDs) III and VI and thus the opening of a space within the cytoplasmic side of the helix bundle. This is mainly achieved by a movement of the cytosolic part of TMD VI away from the receptor core and upwards towards the membrane bilayer, but also by a smaller movement of TMD III (Bissantz, 2003).

To determine the functional and structural role of the highly conserved tyrosine Y<sup>7.53</sup> of the *NPLVY* sequence and its potential interactive partners in the regulation of the human bradykinin receptor (B<sub>2</sub>R), we generated a series of site-mutated receptor constructs and established *HEK293* cell lines stably expressing these receptor mutants. Then we applied a complementary multi-assay approach measuring internalization of radiolabelled ligands as well as receptor sequestration and performed phosphorylation assay and phosphopeptide mapping. eYFP-receptor fusion proteins and fluorescent-labelled antibodies directed against an N-terminal receptor tag were used to check the localization of the receptor. Furthermore, we evaluated the sensitive technique for B<sub>2</sub>R receptor visualization in the Western blotting and highly informative co-immunoprecipitation assays.

### E.1 Mutation of tyrosine in the conserved *NPxxY* sequence leads to constitutive phosphorylation and internalization, but not signalling of the human B<sub>2</sub>R

Initially, Y<sup>7.53</sup> was mutated to alanine giving rise to a mutant termed Y7.53A. At first sight, mutant Y7.53A showed properties similar to those of B<sub>2</sub>R wt: it bound [<sup>3</sup>H]BK with the same affinity and exerted ligand internalization comparable to wild-type receptor; it exhibited a normal level of basal, i.e. agonist-independent signalling [accumulation of inositol phosphates (IPs)] and could be stimulated several fold above basal level.

Our initial studies of agonist-induced phosphorylation of Y7.53A suggested that this mutant is phosphorylation-resistant in the sense that its basal phosphorylation was not increased after agonist treatment, similar to previous reports on the corresponding  $\beta_2$ -adrenergic receptor mutant (Ferguson *et al.*, 1995). Phosphopeptide analysis, however, revealed that this apparent resistance might be due to the fact that the mutant receptors in the plasma membrane are already

fully phosphorylated at serine/threonine residues (like in the activated B<sub>2</sub>R wt) even in the absence of agonist (Figure 41, ① and ②). Moreover, the mutant Y7.53A (but not B<sub>2</sub>R wt) showed an ongoing translocation of rhodamine-labelled antibodies – directed against the HA-tagged receptor – into the cell, suggesting that this mutant is sequestering from the cell surface similar to an activated receptor (Figure 41, ③). This notion was further supported by the demonstration that a Y7.53AeYFP fusion protein was predominantly located inside the cell, even in the absence of a stimulus (Figure 41, ④).

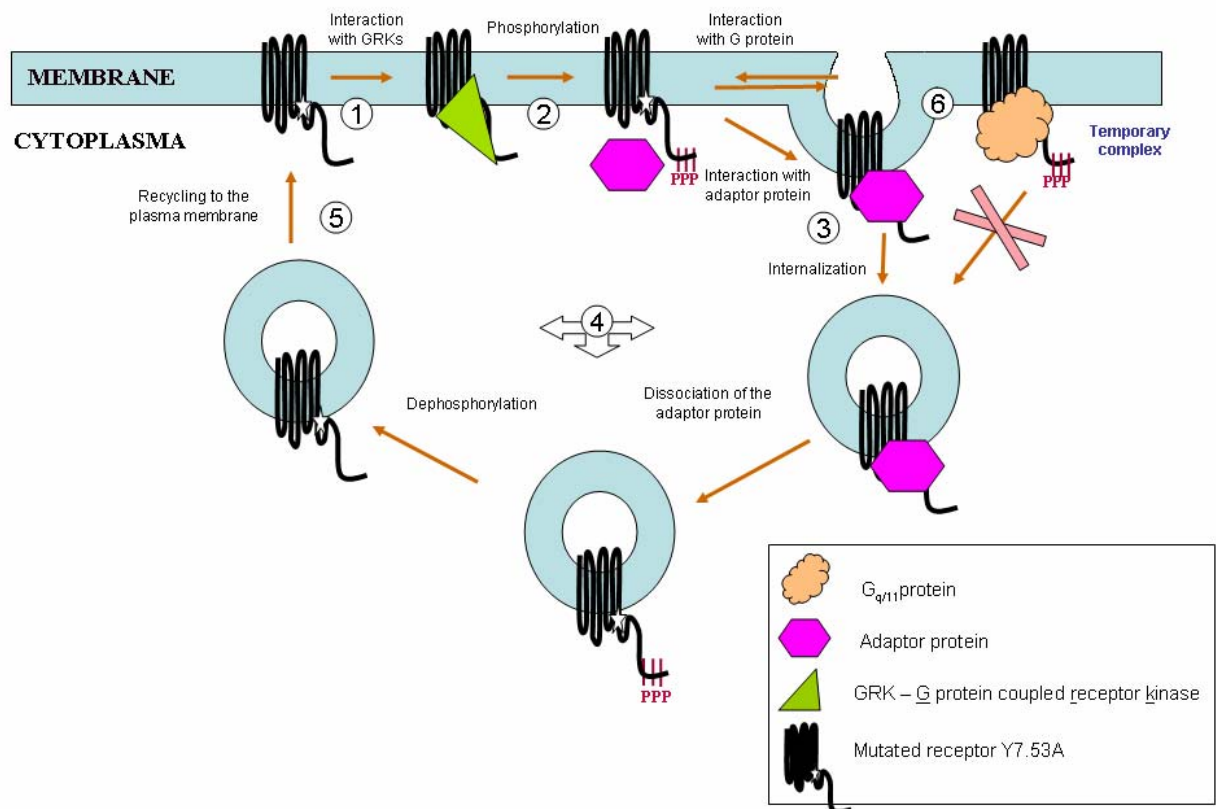


**Figure 41. An assumed model of the behaviour of mutant Y7.53A.**

The B<sub>2</sub>R wt in the non-active state interacts neither with the G<sub>q/11</sub> protein nor with the kinases. In contrast, the mutant Y7.53A is prone to binding of cognate G protein and GRKs even in the absence of BK ①. After ligand-independent phosphorylation ② the receptor is a target for the internalization machinery resulting in ligand-independent sequestration ③. Moreover, the receptor interacts with the cognate G protein but does not activate it ⑥. This interaction blocks the access of the internalization machinery to the phosphorylated receptor, therefore the receptor remains at the plasma membrane and can still be detected at the surface. However, after spontaneous dissociation of the G<sub>q/11</sub> protein from the receptor, the phosphorylated receptor can be targeted by the internalization machinery leading to the observed ligand-independent sequestration ③, which was revealed by the rhodamine-uptake assay. After receptor dephosphorylation, mutant Y7.53A returns to the cell membrane ⑤ and the process can be repeated again. As a result, one portion of the receptors is localized at the cell membrane, most of them phosphorylated and coupled to G<sub>q/11</sub> protein. The other receptor portion is inside the cells as demonstrated by confocal microscopy ④.



Despite its relatively low surface expression, Y7.53A showed markedly reduced sequestration. This dichotomous behavior, i.e. rapid ligand internalization and attenuated receptor sequestration, suggests that the mutant Y7.53A has the higher recycling rate (Figure 41, ⑤).

Although it became clear why the tyrosine mutant was preferably intracellularly localized, it still remained obscure why the receptors were still detectable at the cell surface despite the fact that the phosphorylated receptor is an excellent target for the internalization machinery. Using a convenient co-immunoprecipitation assay, we could show that the phosphorylated receptor interacts with the  $G_{q/11}$  protein, however, without activating it (Figure 41, ⑥). This interaction blocks the access of the internalization machinery to the receptor, therefore the receptor remains at the plasma membrane and can still be detected in considerable amounts at the surface. After spontaneous dissociation of the  $G_{q/11}$  protein from the receptor, the phosphorylated receptor can be targeted by the internalization machinery leading to the ligand-independent sequestration (Figure 41, ③).

The fact that Y7.53A gives a stronger ligand-induced IP response than  $B_2R$  wt may also be explained by our model. As mutant Y7.53A is already pre-coupled to  $G_{q/11}$  protein, receptor stimulation with agonist leads to the faster  $G_{q/11}$  protein activation, stimulation of the phospholipase C- $\beta$  and more effective accumulation of IPs than that by the  $B_2R$  wt. Additionally, a reduced desensitization rate and/or a higher recycling rate of Y7.53A may contribute to the observed increase in IP accumulation.

We further considered, whether our data could be explained in the context of the two-state model in which an equilibrium exists between the receptor in its inactive and its active state (Samama *et al.*, 1993). In the absence of agonist, one would expect this equilibrium to be in favor of the inactive state of  $B_2R$  wt, whereas it would be shifted markedly in favor of the active state in the mutant Y7.53A explaining the observed ligand-independent internalization. However, this model is inconsistent with the lack of increased basal IP accumulation and lack of constitutive guanine nucleotide exchange.

Therefore, we rather postulate that exchange of Y<sup>7.53</sup> to alanine in the human  $B_2R$  induces a semi-active receptor conformation that is prone to phosphorylation and consequently to internalization, and that is also able to couple to the  $G_{q/11}$  protein, however, without activating it (Figure 42) as otherwise all receptors would be immediately sequestered. Moreover, inverse agonists could exert the inhibition of the constitutive internalization either by converting Y7.53A back to a fully inactive conformation or, alternatively, through stabilization of the complex of Y7.53A with inactive  $G_{q/11}$ .

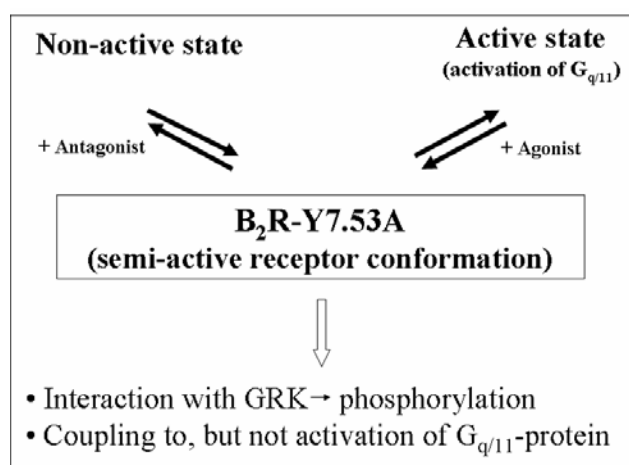


**Figure 42. Model of the semi-active mutant Y7.53A.**

This receptor mutant has a semi-active receptor conformation, which means an intermediate position between non-active and active state. In this conformation, it is prone to phosphorylation and, as a result, to internalization that, however, is slowed down as Y7.53A is also able to couple to the G<sub>q/11</sub> protein without activating it. Binding of an antagonist might promote the fully inactive state, attenuating spontaneous internalization. Interaction with an agonist leads to the fully active state and, consequently, to activation of the cognate G<sub>q/11</sub> protein, similar to B<sub>2</sub>R wt.

As it was previously published, the mutant Y7.53A of the gastrin-releasing peptide receptor internalized as fast as the wild-type, showed the same level of agonist-dependent signalling (accumulation of Ca<sup>2+</sup>) and bound the ligand with affinity similar to the unchanged receptor (Slice *et al.*, 1994). Therefore, it was concluded that exchange of Y<sup>7.53</sup> to alanine in this receptor does not have a role particularly in receptor/G protein interaction that is not readily apparent from the published data. As we demonstrated, B<sub>2</sub>R-Y7.53A exhibiting the wild-type phenotype according to the main receptor properties (ligand affinity, ligand internalization and signalling) has a semi-active conformation. It means that the “tyrosine mutant” of gastrin-releasing peptide receptor might be needed for a more detailed investigation, especially of ligand-induced phosphorylation and localization.

## E.2 Phenotypes of Y7.53F and F7.60A mutants resembled that of the wild-type

The question arising now was whether the aromatic ring or hydroxyl group of Y<sup>7.53</sup> or both are responsible for keeping the receptor in its inactive state. In order to address this, Y<sup>7.53</sup> was mutated to phenylalanine termed mutant Y7.53F.

Mutant Y7.53F had a slightly increased level of basal phosphorylation (probably due to higher surface expression) and displayed significant agonist-induced phosphorylation. Replacement of

Y<sup>7.53</sup> with phenylalanine did not reduce the uptake of the [<sup>3</sup>H]bradykinin. The mutated receptor showed a low degree of agonist-independent signalling and after incubation with the ligand it could be stimulated several fold above basal level. The eYFP fusion protein displayed only some intracellular localization in the absence of BK but, similar to B<sub>2</sub>R wt, responded to BK exposure with a strong translocation from the plasma membrane to intracellular vesicles. Thus, the mutant Y7.53F of the human B<sub>2</sub>R resembled the phenotype of the wild-type receptor.

The crystal structure of rhodopsin indicates a hydrophobic interaction between Y<sup>7.53</sup> and F<sup>7.60</sup> (Palczewski *et al.*, 2000). F<sup>7.60</sup> is also highly conserved among members of class-A GPCRs. Therefore, we studied whether the exchange of the aromatic rings of Y<sup>7.53</sup> and F<sup>7.60</sup> has the same effect on the receptor phenotype, in other words, whether the mutant F7.60A resembles the semi-active conformation phenotype of the mutant Y7.53A or not.

The level of basal phosphorylation of the mutant F7.60A was slightly decreased in comparison to B<sub>2</sub>R wt, but the mutant still responded with additional phosphorylation when challenged with BK. This mutation did not much affect the ligand internalization, as it was almost as rapid as the one observed in the wild type. Moreover, it showed an IP response similar to that seen for the wild type. So, the mutant F7.60A does not resemble the phenotype of the mutant Y7.53A, as it was assumed above. Moreover, its properties are quite similar to those of the wild-type receptor. Thus, we concluded that Y<sup>7.53</sup> is more important than F<sup>7.60</sup> for keeping the receptor in its inactive state. It indicates that either the aromatic rings of Y<sup>7.53</sup> and F<sup>7.60</sup> do not interact with each other in the human B<sub>2</sub>R or the hydroxyl group of tyrosine plays a significant role in the receptor conformation.

The crystal structure of the bovine rhodopsin indicates not only a hydrophobic interaction between Y<sup>7.53</sup> and F<sup>7.60</sup>, but also a hydrogen bond between the hydroxyl group of Y<sup>7.53</sup> and asparagine 2.40 from the second transmembrane helix (Figure 43). B<sub>2</sub>R at position 2.40 has a glutamate (Figure 44) that is also able to form a hydrogen bond with Y<sup>7.53</sup>.

Thus, on one side, in mutant F7.60A the potential hydrophobic interaction between Y<sup>7.53</sup>↔F<sup>7.60</sup> may be lost, but an interaction between Y<sup>7.53</sup>↔E<sup>2.40</sup> should still be possible; on the other side, in mutant Y7.53F the interaction between Y<sup>7.53</sup>↔E<sup>2.40</sup> would be missing, but the hydrophobic interaction between the aromatic rings would still be in place. As both mutants – Y7.53F and F7.60A – behave very similar to the B<sub>2</sub>R wt, this could indicate that one interaction could compensate for the absence of the other in maintaining a wild-type receptor conformation.

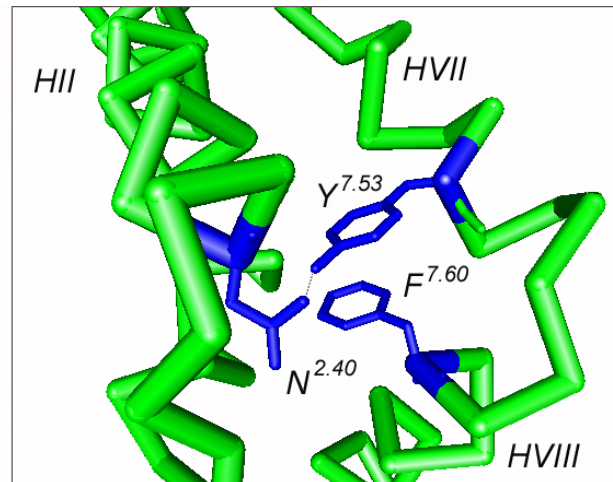


**Figure 43. Model of the bovine rhodopsin based on its crystal structure.**

This model shows the proximity of the Y<sup>7.53</sup>, F<sup>7.60</sup> and N<sup>2.40</sup> side chains. For clarity only helices II, VII and VIII are shown.

Rho_bovine	MNGTEGPNFYVPFSNKTGVVRSPEAPQYYLAEP-----WQFSML	40
E2R_human	MFSPWKISMFLSVREDSVPTTASFADMLNVTLQGP TLNGTFAQSKCPQVEWLGWLNTIQ	60
Rho_bovine	1.50 2.40 2.50	
Rho_bovine	AAVMFL IIMLGFPINFLTLVTVQHKKLRTPLEIYILLNLAVADLFHVFGGFTTTLTYSLH	100
E2R_human	PPFLWVLFVLATLENIFVLSVFLHKSSCTVAEIVLGNLAAADLILACGLPFWAITISNN	120
Rho_bovine	GYFVFGPTGCNLEGFATLGGELALWLSLVLAIERVVVCKPMSNFRFG-ENHAIMGVAF	159
E2R_human	FDWLFGETLCRVVNAIISMNLYSSICFLMLVSDRYLALVKTMMSGRMRGVRWAKLYSLV	180
Rho_bovine	4.50 5.50	
Rho_bovine	TWVMALACAAPPLVG--WSRYIPEGMQCS-CGIDYYTPHEETNNEFVIYMFVVFHIIPL	216
E2R_human	IWGCTLLSSPMLVFRMTKEYSDEGHNV TACVISYPSLIWEVFTN---MLLNVVGFLLPL	237
Rho_bovine	6.50	
Rho_bovine	IVIFFCYQQLVFTVKEAAAQQQESATTQKAEKEVTRNVIIMVIAFLICWLPYAGVAFYIF	276
E2R_human	SVITFCTMQIMQVLRNMEMQKFK---EIQTERRATLVLVVLLLFICWLPFPQISTFLDT	294
Rho_bovine	7.53 7.60	
Rho_bovine	TH-----QGSDFGPIFMTIPAFFAKTSAVYNPVIIMMNRQIRNCMVTTLCCGKNPL	321
E2R_human	LHRLGILSSCQDERIIDVITQIASFMAYSNSCLNPLVWVIVGKRIRRKKSWEVYQGVQCKG	354
Rho_bovine	GDDEASTTVSKTETSQV&PA-----	348
E2R_human	GCRSEPIQMENSMTLRSTSISVERQIHKLQDWAGSRQ	391

**Figure 44. Human B<sub>2</sub>R and bovine rhodopsin receptors alignments.**

The protein alignment was made on the base of the human B<sub>2</sub>R and bovine rhodopsin sequences using *ClustalW* on-line program from European Bioinformatics Institute. The alignment shows positions of the conserved amino acid residues: E/D<sup>2.40</sup>, Y<sup>7.53</sup> and F<sup>7.60</sup>.

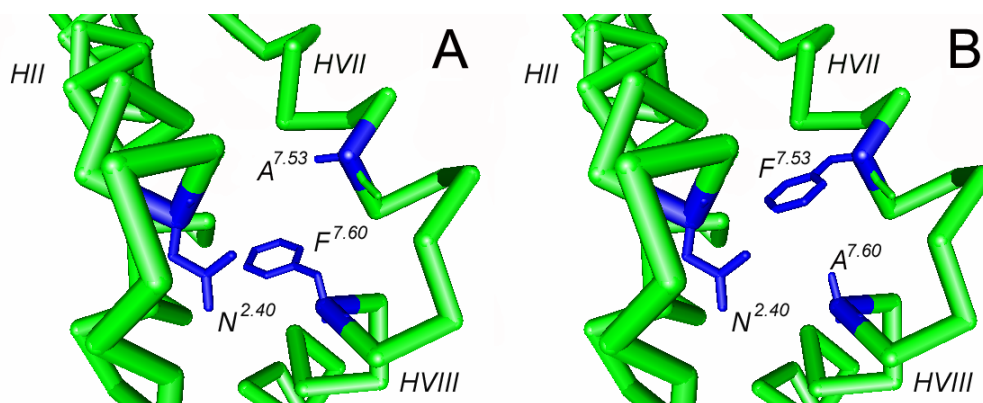


**Figure 45. Schematic representation of mutants Y7.53A (A) and Y7.53F/F7.60A (B).** The model is based on bovine rhodopsin crystal structure. For clarity only helices II, VII and VIII are shown.

However, after disruption of both interactions (as in mutant Y7.53A) a semi-active receptor conformation appears. If this is true, a simultaneous mutation of the hydroxyl group of Y<sup>7.53</sup> and the aromatic ring of F<sup>7.60</sup> should result in a mutant which is similar to Y7.53A (Figure 45). For this reason the double mutant Y7.53F/F7.60A was generated.

### E.3 Y7.53F/F7.60A construct did not resemble the phenotype of Y7.53A mutant

The simultaneous exchange of Y<sup>7.53</sup> to phenylalanine and F<sup>7.60</sup> to alanine strongly reduced the capacity to become phosphorylated and internalized. However, signalling was not altered as a normal IP signal after stimulation with bradykinin was observed. Moreover, similar to Y7.53A the mutant Y7.53F/F7.60A was pre-coupled to G<sub>q/11</sub> protein, but could activate it only after stimulation with the ligand. We assume that pre-coupled G<sub>q/11</sub> protein blocks interaction of the receptor with GRKs. Even after stimulation with the ligand and G<sub>q/11</sub> protein dissociation, new (non-stimulated) G protein and GRK compete for the interaction with receptor, but probably, as the affinity of Y7.53F/F7.60A for G<sub>q/11</sub> protein is higher than to GRK, the mutant binds again G protein being blocked from the interaction with GRK. Probably only a few amounts of mutated receptors become phosphorylated (that we could not detect with our phosphorylation assay) and internalized, as we observed 20% internalization rate in 10 min [in comparison to 80% in the wild-type receptor and 5% in the mutant where all phosphorylation sites were exchanged to alanine (our data; Pizard *et al.*, 1999)].

Thus, mutant Y7.53F/F7.60A did not resemble the phenotype of Y7.53A, as it has abolished ligand-induced phosphorylation and internalization, but the mechanism that described the observed properties seems to be similar. We suggested that Y7.53F/F7.60A has also a semi-active conformation (as it was pre-coupled to G<sub>q/11</sub> protein), but differed from those of the mutant Y7.53A. In addition, a simultaneous mutation of the hydroxyl group of Y<sup>7.53</sup> and the aromatic ring of F<sup>7.60</sup> does not result in a mutant similar to Y7.53A (Figure 45), as it was suggested before. These data provided us with the first hint that Y<sup>7.53</sup>↔F<sup>7.60</sup>↔E<sup>2.40</sup> loci of the human B<sub>2</sub>R have one more interaction partner. If it is true, the less conservative mutant Y7.53A/F7.60A (Figure 46), where both aromatic rings were exchanged to alanine (thereby disrupting all possible interactions in these loci), will have a phenotype less similar to the wild-type receptor than Y7.53F/F7.60A.

### E.4 Y7.53A/F7.60A exhibited a less conservative phenotype than Y7.53F/F7.60A

The less conservative double mutant Y7.53A/F7.60A (Figure 46B) was phosphorylation resistant and had lost the capacity to become internalized like Y7.53F/F7.60A. In addition, it

also showed a significantly reduced IP as well as no increased signal for the cognate G protein after stimulation with bradykinin. It probably means that this mutant could not interact with the cognate G protein due to "incorrect" receptor conformation or that G<sub>q/11</sub> protein does not have an access to the mutated receptor.

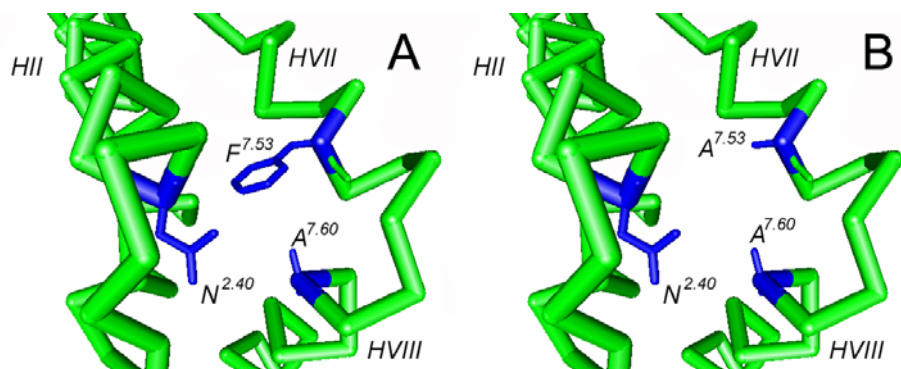


**Figure 46. Schematic representation of the mutants Y7.53F/F7.60A (A) and Y7.53A/F7.60A (B) based on the crystal structure of the bovine rhodopsin.**

In spite of the fact that already in mutant Y7.53F/F7.60A both potential interactions ( $Y^{7.53} \leftrightarrow E^{2.40}$  and  $Y^{7.53} \leftrightarrow F^{7.60}$ ) were disrupted, mutant Y7.53A/F7.60A has less conservative phenotype than Y7.53F/F7.60A. Therefore, we could assume an additional interaction partner for  $Y^{7.53}$  in the human B<sub>2</sub>R.

Additional investigations showed that the mutant Y7.53A/F7.60A inclined to interact with the GRKs in an agonist-independent manner. This protein complex was quite stable, since we were able to detect it after 5 min incubation with bradykinin. But, in contrast to the mutant Y7.53A, GRK phosphorylates the receptor neither prior nor after stimulation probably staying bound to the receptor. This may be an explanation for the abolished signalling, as the receptor would not have excess to the cognate G protein, as it is blocked by the bound GRK. In addition, as Y7.53A/F7.60A was pre-coupled to GRK, we could assume for this mutant also a semi-active conformation that was, however, different from those of mutants Y7.53A and Y7.53F/F7.60A.

Similar to a corresponding mutant Y7.53F/Y7.60A of the 5HT<sub>2C</sub> receptor (Prioleau *et al.*, 2002), double mutant Y7.53A/F7.60A of the B<sub>2</sub>R does not reflect the properties of the point mutants. Usually, if two mutations are independent in their contribution to a measured property, the effects of a double mutation should be additive (Ward *et al.*, 1990; Carter *et al.*, 1984). Point mutant F7.60A displayed a phosphorylation and internalization pattern similar to the B<sub>2</sub>R wt, whereas mutant Y7.53A was prone to phosphorylation and consequently to internalization in a ligand-independent manner. In contrast, mutant Y7.53A/F7.60A had lost the capacity to internalize, probably due to abolished ligand-inducible phosphorylation. So, the phenotypes produced by these mutations not only failed to be additive (in the case of additivity the mutant

Y7.53A/F7.60A should display the phenotype of the mutant Y7.53A, as F7.60A showed the properties of the wild-type receptor), but they strongly aggravated receptor dysfunction. Therefore, the results indirectly indicate that these two loci (Y<sup>7.53</sup> and F<sup>7.60</sup>) share a common micro-domain similar to the bovine rhodopsin and 5HT<sub>2C</sub> serotonin receptor (Palczewski *et al.*, 2000; Prioleau *et al.*, 2002).

Moreover, in spite of the fact that in mutant Y7.53F/F7.60A all known interactions were already disrupted (Figure 46A), the mutant Y7.53A/F7.60A (Figure 46B) showed an even less conservative phenotype. So, our suggestion about an additional interaction partner in Y<sup>7.53</sup> ↔ F<sup>7.60</sup> ↔ E<sup>2.40</sup> loci (more probably for Y<sup>7.53</sup>) seems to be plausible.

### E.5 Y<sup>7.53</sup> and its microenvironment are important for keeping B<sub>2</sub>R in its inactive state

Biophysical studies provided evidence for conformational changes during receptor activation. It was assumed that the inactivated state is stabilized by interactions that have to be broken during receptor activation. Evidence therefore was given by the observation of mutations that lead to mutant receptors with significant agonist-independent, constitutive activity (Cohen *et al.*, 1993; Rasmussen *et al.*, 1999; Alewijjnse *et al.*, 2000). Such constitutively active receptors are characterized by structural instability (measured in a binding assay after incubation of crude membrane preparations of cells expressing wild type and mutated receptors at 37°C for 2, 6, 12, 24 h), suggesting that these mutations indeed break interactions stabilizing the inactive state and thus promote the transition to an active conformation (Gether *et al.*, 1997).

The binding to/activation of the specific G proteins or recognition by specific kinases requires presentation of the intracellular docking sites that are normally hidden (closed) in the inactive state. In our mutation series of Y<sup>7.53</sup> and F<sup>7.60</sup> we identified receptor mutants that were pre-coupled to G protein or to GRK, indicating that these mutated receptors had semi-active conformations. This variety of semi-active phenotypes suggested that Y<sup>7.53</sup> and its interactive partner F<sup>7.60</sup> may be involved in the transitions among several conformers (Figure 47). Consequently, our results suggest that these mutations all interfered with mechanisms responsible for stabilizing the receptor in its fully inactive conformation.

GPCR activation is initiated by binding of an extracellular ligand to the receptor. This triggers first a conformational change of the receptor from its inactivated ground state to an activated state in which the cytosolic part of the GPCR can interact with a G protein (conformer trapped in mutant Y7.53F/F7.60A), activate it inducing a pharmacological effect [conformation represented by a constitutive active mutant that was not found among our constructs, but was described for mutants Y7.53A and Y7.53C of the 5HT<sub>2C</sub> serotonin receptor (Rosendorff *et al.*,

2000)], afterwards interacts with GRKs (conformer trapped in mutant Y7.53A/F7.60A) and, at last, be phosphorylated and internalized as seen with Y7.53A mutant of the B<sub>2</sub>R (Figure 47).

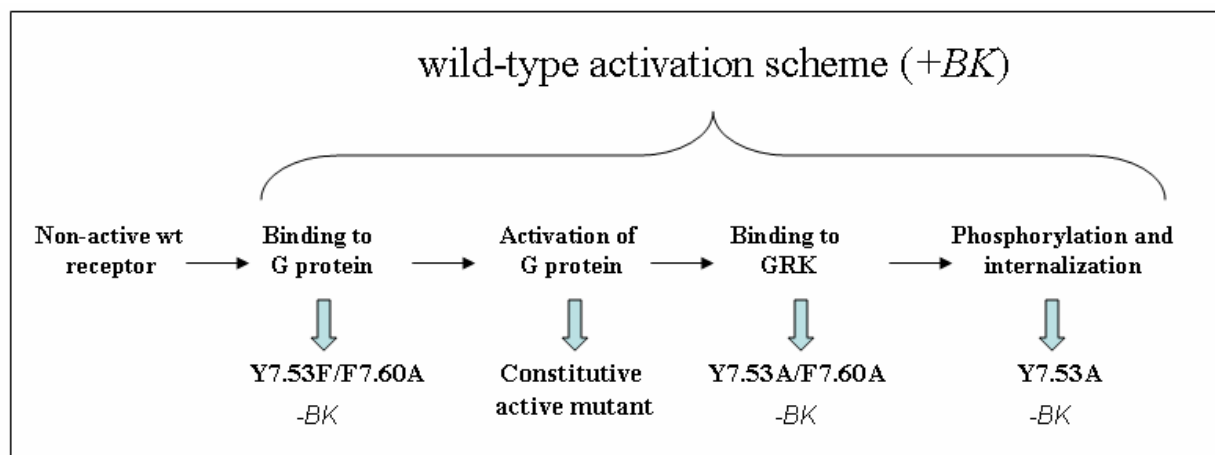


**Figure 47. Schematic representation of the series of the B<sub>2</sub>R mutants in compliance with appropriate protein conformations during activation of the wild-type receptor.**

After stimulation the wild-type receptor interacts with the G<sub>q/11</sub> protein with a conformation corresponding to the conformation of the mutant Y7.53F/F7.60A as this mutant is pre-coupled to G<sub>q/11</sub> in the absence of agonist. Then the receptor activates the cognate G protein. Conformation of a constitutive active mutant was not found among Y<sup>7.53</sup> derivations of the human B<sub>2</sub>R. After G protein dissociation the receptor binds to GRK. This conformational state is trapped in mutant Y7.53F/F7.60A as it pre-coupled to GRK even without stimulation with ligand. Finally, receptor becomes phosphorylated and internalized. The mutant Y7.53A reflects this receptor conformation.

*Summarizing, our observations suggested that Y<sup>7.53</sup> is a key residue for molecular rearrangements that occur when the receptor switches between different conformational states. Mutation of this locus may alter the distribution and accessibility of specific receptor conformations and, consequently, the phenotype of the resulting receptors.*

### **E.6 Mutation of Y<sup>7.53</sup> to alanine in the human β<sub>2</sub>-adrenergic receptor leads to irreversible interaction with GRKs**

Finally, we were interested in whether the model found for mutant Y7.53A of the human B<sub>2</sub>R could be applicable for the “tyrosine mutants” of other GPCRs. In order to address this question we took the β<sub>2</sub>-adrenergic receptor (β<sub>2</sub>-ADR) that can be considered as a prototypical A-class GPCR.

At first glance, β<sub>2</sub>-ADR-Y7.53A does not share any traits with the tyrosine mutant of the human B<sub>2</sub>R: it is resistant to ligand-induced phosphorylation and, as a consequence, to receptor sequestration after activation.



Our first attempt to explain all the effects observed in the mutant  $\beta_2$ -ADR-Y7.53A was done according to the model proposed for  $\beta_2$ R-Y7.53A. We suggested that  $\beta_2$ -ADR-Y7.53A has a high affinity for cognate  $G_s$  protein combined with the observed inability of this mutant to activate it. It would explain the lack of sequestration and resistance to phosphorylation, as well as the fact that this mutant is located preferentially in the plasma membrane (Gabilondo *et al.*, 1996). However, we found with a co-immunoprecipitation assay that the  $\beta_2$ -ADR-Y7.53A mutant is not able to interact with  $G_s$  either prior to or after stimulation in contrast to  $\beta_2$ -ADR wt.

Nevertheless, similar to  $\beta_2$ R-Y7.53A/F7.60A,  $\beta_2$ -ADR-Y7.53A interacts with GRK without stimulation, but does not get phosphorylated even after activation with the ligand. The bound 50-kDa GRK protein showed a complete blockage of the access of  $G_s$  protein and the internalization machinery to the cytosolic region of the receptor. As the wild-type receptor could interact with GRKs only after stimulation, we could assume that the mutant  $\beta_2$ -ADR-Y7.53A has a semi-active conformation.

Moreover, as shown by several authors the mutant  $\beta_2$ -ADR-Y7.53A could activate adenylyl cyclase similar to wild type (Barak *et al.*, 1994), to 60% of wild type level (Barak *et al.*, 1995) or only to 20% of wild type (Gabilondo *et al.*, 1996). As it was discussed in the latter publication, these differences may be largely attributed to different levels of receptor expression. When the receptor expression level was about 1 pmol/mg, this mutation did not affect the ability of the receptor to activate maximally adenylyl cyclase, whereas clones of mutant  $\beta_2$ -ADR-Y7.53A with an expression in the range of 200-300 fmol/mg showed only 20% of wild-type activity. With our hypothesis it was possible to explain this discrepancy. As the amount of the GRK molecules per cell is limited, with high  $\beta_2$ -ADR-Y7.53A expression not every mutated receptor was blocked by GRK, so the “free” receptors could interact and stimulate  $G_s$  protein after stimulation. Therefore the results with abolished signalling seemed to be plausible and should be taken into account.

### **E.7 The various phenotypes of “tyrosine mutants” could be explained on the basis of their different affinities for cognate G proteins and/or GRKs**

Because conservation of the sequence  $NPxxY$  in helix VII implies an important structural or functional role, this motif has been examined by mutagenesis studies in several GPCRs. Especially, the mutation of the tyrosine in the conserved  $NPxxY$  motif was found to affect agonist affinity, signal transduction and sequestration in different receptors, and even resulted in constitutive activity (Rosendorff *et al.*, 2000). However, the results concerning the mutation of

Y<sup>7.53</sup> that have been published so far are very contradictory and from the first point of view it is almost impossible to work out a general theory to put them together. In addition, almost all “tyrosine mutants” were investigated taking into account only three main pharmacological characteristics: receptor affinity, ligand-induced signalling, and internalization/sequestration. Almost no information was published about ligand-induced phosphorylation, intracellular trafficking or interaction with intracellular proteins. Thus, the B<sub>2</sub>R-Y7.53A mutant is so far the most completely characterized “tyrosine mutant”.

In Table 14 an attempt was made to systematize all results concerning “tyrosine mutants” published up to now. All “tyrosine” mutants “7.53” can be divided by the phenotype into five groups on the basis of the influence of this substitution on signalling and receptor sequestration. The classification of the observed effects on signalling and/or receptor sequestration/internalization was made in the following way: conservation of the function to 90-100% in comparison to the wild type was considered as “not changed”, to 70-90% as “slightly reduced”, to 40-70% as “reduced”, to 20-40% as “highly reduced”, and to 0-20% as “abolished”:

- A. group A comprises receptors where replacement of Y<sup>7.53</sup> to alanine leads to complete abolishment of the main receptor functions: agonist-induced signalling and internalization. The most prominent sample is the human β<sub>2</sub>-adrenergic receptor (Gabilondo *et al.*, 1996; Ferguson *et al.*, 1995). Moreover, the hamster α<sub>1b</sub>-adrenergic (Wang *et al.*, 1997) and the mouse gonadotropin-releasing hormone (Arora *et al.*, 1996) receptors belong to this group (Table 14, # 1-3).
- B. group B represents the exact antithesis to the first one: lack of the Y<sup>7.53</sup> did not affect receptor internalization and signalling at all (Table 14, # 4-6). This group includes the rat gastrin-releasing peptide receptor (Slice *et al.*, 1994), rat cholecystokinin type A receptor (Go *et al.*, 1998) and the B<sub>2</sub> bradykinin receptor (Publication C).
- C. group C includes three members: rat and human angiotensin II type 1 (Hunyady *et al.*, 1995; Laporte *et al.*, 1996), rat neurokinin type 1 (Böhm *et al.*, 1997), and human platelet-activating factor (Le Gouill *et al.*, 1997). This group is characterized by unchanged sequestration and reduced signalling (Table 14, # 7-10).
- D. in group D the tyrosine mutant of human N-formyl peptide receptor (He *et al.*, 2001) shown abolished ligand internalization but normal or only slightly changed signalling (Table 14, # 11).
- E. in group E the substitution of the Y<sup>7.53</sup> to alanine or cysteine in the serotonin receptor 5HT<sub>2C</sub> leads to ligand-independent activity (Table 14, # 12).

**Table 14. Summary of effects of substitutions of Y<sup>7.53</sup> to alanine.**

	#	Receptor, origin	Endocytosis (used method)	Signal transduction	Other remarks	References
A	1	$\beta_2$ -adrenergic, human	abolished (RS <sup>**</sup> )	abolished (AC <sup>*</sup> )	Ligand-induced phosphorylation is abolished	Ferguson <i>et al.</i> , 1995 Gabilondo <i>et al.</i> , 1996
	2	$\alpha_{1b}$ -adrenergic, hamster	abolished (RS)	abolished (IP <sup>*</sup> and Ca <sup>2+</sup> )	-	Wang <i>et al.</i> , 1997
	3	Gonadotropin-releasing hormone, mouse	reduced (LI <sup>**</sup> )	abolished (IP)	short C-terminus	Arora <i>et al.</i> , 1996
B	4	Gastrin-releasing peptide, rat	not changed (LI)	not changed (Ca <sup>2+</sup> )	-	Slice <i>et al.</i> , 1994
	5	Cholecystokinin type A, rat	not changed (RS)	not changed (IP)	-	Go <i>et al.</i> , 1998
	6	B <sub>2</sub> bradykinin, human	not changed (LI)	not changed (IP)	cytosolic localization	Publication B
C	7	Angiotensin II type 1a, rat	slightly reduced (LI)	reduced (IP)	-	Hunyady <i>et al.</i> , 1995
	8	Angiotensin II type 1, human	slightly reduced (LI)	abolished (IP)	-	Laporte <i>et al.</i> , 1996
	9	Neurokinin type 1, rat	not changed (LI)	highly reduced (Ca <sup>2+</sup> )	cytosolic localization	Böhm <i>et al.</i> , 1997
	10	Platelet-activating factor, human	not changed (LI)	reduced (IP)	-	Le Gouill <i>et al.</i> , 1997
D	11	N-formyl peptide, human	abolished (LI)	slightly reduced (IP) not changed (Ca <sup>2+</sup> )	-	He <i>et al.</i> , 2001
E	12	Serotonin 5HT <sub>2c</sub> , human	ND <sup>***</sup>	Slightly reduced (IP)	basal activity	Rosendorff <i>et al.</i> , 2000 Prioleau <i>et al.</i> , 2002

\* AC – adenylyl cyclase, IP – inositol phosphate stimulation.

\*\* Used method of the receptor endocytosis measurement: LI – ligand internalization, RS – receptor sequestration (the principal difference between “ligand internalization” and “receptor sequestration” methods is explained in section D.1.1)

\*\*\* ND – not determined.

We assume that the receptor phenotype of group A corresponds to our double mutant B<sub>2</sub>R-Y7.53A/F7.60A, the group D – to B<sub>2</sub>R-Y7.53F/F7.60A and group B – to whether B<sub>2</sub>R-Y7.53A or wild-type phenotype (Figure 48).

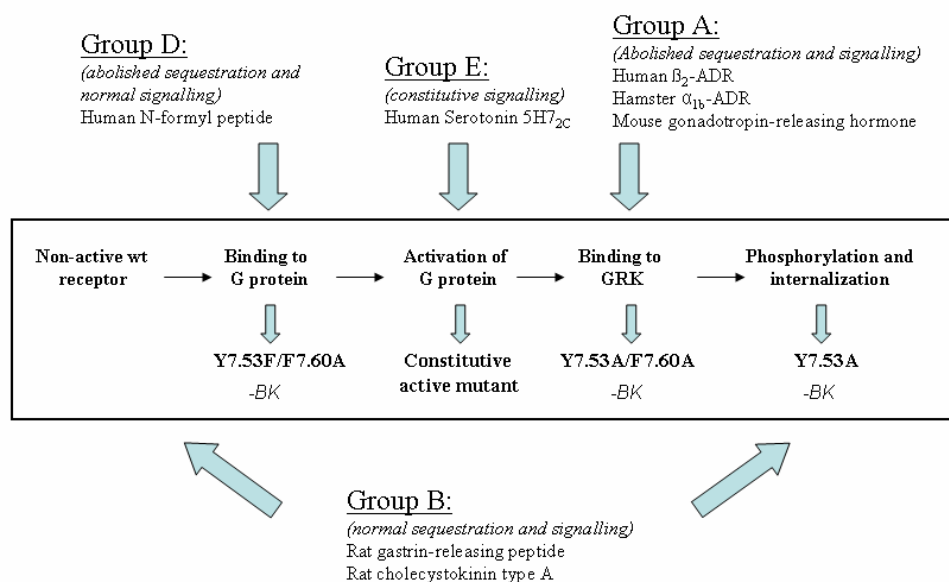


**Figure 48. The phenotypes of the different “tyrosine mutants”.**

The phenotypes of the receptor mutants cited in Table 14 could be explained on the base of “a semi-active receptor conformation model”. For example, the receptors belonging to group A, characterized by abolished sequestration and signalling, correspond to our mutant B<sub>2</sub>R-Y7.53A/F7.60A and possibly irreversibly bind the GRK. The receptors of group B with normal sequestration and signalling could either have a phenotype of the wild-type receptor as it was usually assumed in the appropriate publication or be characterized by constitutive phosphorylation and sequestration as our B<sub>2</sub>R-Y7.53A mutant. The remarks concerning group C see in the text.

The phenotype of group C (abolished signalling and normal sequestration) could be explained, for example, on the base of the assumption that cognate G protein does not have an access to the receptor due to high affinity of these mutants for GRKs.

*Thus, possibly depending on the microenvironmental surrounding of Y<sup>7.53</sup> in each GPCR subtype, substitution of the Y<sup>7.53</sup> leads to different effects that could be explained, according to our model, on the basis either of different affinities of these mutants for their cognate G proteins and/or for their GRKs. We suggest that these various phenotypes represent different states of the receptor activation.*

## F OUTLOOK

In the context of this work the following methods were elaborated: ligand internalization and receptor sequestration assay, effective procedure of the B<sub>2</sub>R visualization by Western blotting, phosphorylation assay and two-dimensional phosphopeptide mapping of the B<sub>2</sub>R and its mutants, as well as co-immunoprecipitation assay of receptor/G protein complex.

Our results suggest that the highly conserved Y<sup>7.53</sup> in the human B<sub>2</sub> bradykinin receptors plays an important role in keeping the receptor in an inactive uncoupled state, thereby preventing spontaneous phosphorylation and subsequent interaction with the internalization machinery.

Moreover, the presented set of mutants provides unique substrates for the computational and experimental investigation of the microenvironment of Y<sup>7.53</sup> in particular, and of mechanisms of the receptor activation in general. We expect that this information, together with the structures solved by X-ray crystallography, will contribute to a better understanding of the activation mechanism of the B<sub>2</sub> receptor. Thereby, these data will be very helpful in the creation of the new metabolically resistant B<sub>2</sub> receptor agonists and antagonists which has very high therapeutic potential for the treatment of diseases such as hereditary angioedema or refractory ascites in liver cirrhosis.

Nevertheless, the anticipated experiments should allow an even more detailed clarification of the B<sub>2</sub>R activation way:

- studies of the stability of the performed mutants as the semi-active mutants usually have a reduced protein stability.
- mutagenesis studies of the E<sup>2.40</sup> as a potential partner of the highly conserved Y<sup>7.53</sup>.
- investigation of the highly conserved P<sup>7.50</sup> and N<sup>7.51</sup> of NPxxY motif and their potential interaction partners.

**G REFERENCES**

- Abd-Alla S., Godovac-Zimmermann J., Braun A., Roscher A.A., Müller-Esterl W., & Quitterer U. (1996) Structure of the bradykinin B2 receptors' amino terminus. *Biochemistry* 35, 7514-7519.
- Abd-Alla S., Zaki E., Lothar H., & Quitterer U. (1999) Involvement of the amino terminus of the B-2 receptor in agonist-induced receptor dimerization. *J. Biol. Chem.* 274, 26079-26084.
- Abdulaev N.G. & Ridge K.D. (1998) Light-induced exposure of the cytoplasmic end of transmembrane helix seven in rhodopsin. *Proc. Natl. Acad. USA* 95, 12854-12859.
- Abelous J.E. & Bardier E. (1909) Les substances hypotensives de l'urine humaine normale. *S.R. Soc. Biol. (Paris)* 66, 511-512.
- Alewijnse A.E., Timmerman H., Jacobs E.H., Smit M.J., Roovers E., Cotecchia S., & Leurs R. (2000) The effect of mutations in the DRY motif on the constitutive activity and structural instability of the histamine H-2 receptor. *Mol. Pharm.* 57, 890-898.
- Altenbach C., Cai K.W., Khorana H.G., & Hubbell W.L. (1999) Structural features and light-dependent changes in the sequence 306-322 extending from helix VII to the palmitoylation sites in rhodopsin: a site-directed spin-labeling study. *Biochemistry* 38, 7931-7937.
- Andrade S.O. & Rocha e Silva M. (1956) Purification of bradykinin by ion-exchange chromatography. *Biochem. J.* 64, 701-705.
- Arora K.K., Cheng Z.Y., & Catt K.J. (1996) Dependence of agonist activation on an aromatic moiety in the DPLIY motif of the gonadotropin-releasing hormone receptor. *Mol. Endocrinol.* 10, 979-986.
- Austin C.E., Faussner A., Robinson H.E., Chakravarty S., Kyle D.J., Bathon J.N., & Proud D. (1997) Stable expression of the human kinin B1 receptor in CHO cells: characterization of ligand binding and effector pathway. *J. Biol. Chem.* 272, 11420-11425.
- Baldwin J.M. (1994) Structure and function of receptors coupled to G proteins. *Curr. Opin. Cell Biol.* 6, 180-190.
- Ballesteros J. & Weinstein H. (1995) Integrated methods for the construction of three dimensional models and computational probing of structure-function relations in G protein-coupled receptors. *Meth. Enzymol.* 25, 366-428.
- Barak L.S., Tiberi M., Freedman N.J., Kwatra M.M., Lefkowitz R.J., & Caron M.G. (1994) A highly conserved tyrosine residue in G protein-coupled receptors is required for agonist-mediated  $\beta$ 2-adrenergic receptor sequestration. *J. Biol. Chem.* 269, 2790-2795.
- Barak L.S., Menard L., Ferguson S.S.G., Colapietro A.M., & Caron M.G. (1995) The conserved 7-transmembrane sequence NP(X)<sub>(2,3)</sub>Y of the G protein-coupled receptor superfamily regulates multiple properties of the beta(2)-adrenergic receptor. *Biochemistry* 34, 15407-15414.
- Bhoola K.D., Figueroa C.D., & Worthy K. (1992) Bioregulation of kinins – kallikreins, kininogens, and kininases. *Pharmacol. Rev.* 44, 1-80.

- Birnboim H.C. & Doly J. (1979) Rapid alkaline extraction procedure for screening recombinant plasmid DNA. *Nucleic Acids Res.* 7, 1513-1523.
- Bissantz C. (2003) Conformational changes of G protein-coupled receptors during their activation by agonist binding. *J. Recept. Sig. Transd.* 23, 123-153.
- Blaukat A., Abdalla S., Lohse M.J., & Müller-Esterl W. (1996) Ligand-induced phosphorylation dephosphorylation of the endogenous bradykinin B2 receptor from human fibroblasts. *J. Biol. Chem.* 271, 32366-32374.
- Blaukat A. & Müller-Esterl W. (1997) Inhibition of B2 receptor internalization delays its dephosphorylation. *Immunopharm.* 36, 115-119.
- Blaukat A., Barac A., Cross M.J., Offermanns S., & Dikic I. (2000) G protein-coupled receptor-mediated mitogen-activated protein kinase activation through cooperation of G alpha(q), and G alpha(i) signals. *Mol. Cell. Biol.* 20, 6837-6848.
- Blaukat A., Pizard A., Breit A., Wernstedt C., Alhenc-Gelas F., Müller-Esterl W., & Dikic I. (2001) Determination of bradykinin B2 receptor in vivo phosphorylation sites and their role in receptor function. *J. Biol. Chem.* 276, 40431-40440.
- Böhm S.K., Khitin L.M., Smeekens S.P., Grady E.F., Payan D.G., & Bunnett N.W. (1997) Identification of potential tyrosine-containing endocytic motifs in the carboxyl-tail and seventh transmembrane domain of the neurokinin 1 receptor. *J. Biol. Chem.* 272, 2363-2372.
- Boissonnas R.A., Guttmann S., & Jaquenoud P.A. (1960) Synthèse de la L-Arginyl-L-Prolyl-L-Prolyl-Glycyl-L-Phenylalanyl-L-Seryl-L-Prolyl-L-Phenylalanyl-L-Arginine, Un Nonapeptide Presentant les Propriétés de la Bradykinine. *Helv. Chim. Acta* 43, 1349-1358.
- Bouley R., Sun T.X., Chenard M., McLaughlin M., Mckee M., Lin H.Y., Brown D., & Ausiello D.A. (2003) Functional role of the NPxxY motif in internalization of the type 2 vasopressin receptor in LLC-PK1 cells. *Am. J. Physiol. - Cell Ph.* 285, C750-C762.
- Boyle W.J., Vandergeer P., & Hunter T. (1991) Phosphopeptide mapping and phosphoamino acid analysis by two-dimensional separation on thin-layer cellulose plates. *Meth. Enzymol.* 201, 110-149.
- Bray P., Carter A., Simons C., Guo V., Puckett C., Kamholz J., Spiegel A., & Nirenberg M. (1986) Human cDNA clones for 4 species of G alpha s signal transduction protein. *Proc. Natl. Acad. USA* 83, 8893-8897.
- Brown M.S. & Goldstein J.L. (1976) Analysis of a mutant strain of human fibroblasts with a defect in internalization of receptor-bound low-density lipoprotein. *Cell* 9, 663-674.
- Burch R.M. & Axelrod J. (1987) Dissociation of bradykinin-induced prostaglandin formation from phosphatidylinositol turnover in swiss 3T3 fibroblasts - evidence for G protein regulation of phospholipase-A2. *Proc. Natl. Acad. USA* 84, 6374-6378.
- Campbell D.J., Kladis A., & Duncan A.M. (1993) Bradykinin peptides in kidney, blood, and other tissues of the rat. *Hypertension* 21, 155-165.
- Campbell D.J., Kladis A., Briscoe T.A., & Zhuo J.L. (1999) Type 2 bradykinin-receptor antagonism does not modify kinin or angiotensin peptide levels. *Hypertension* 33, 1233-1236.

- Carter P.J., Winter G., Wilkinson A.J., & Fersht A.R. (1984) The use of double mutants to detect structural changes in the active site of the tyrosyl-transfer RNA-synthetase (*Bacillus Stearotherophilus*). *Cell* 38, 835-840.
- Cayla C., Merino V.F., Cabrini D.A., Silva J.A. Jr., Pesquero J.B., & Bader M. (2002) Structure of the mammalian kinin receptor gene locus. *Int. Immunopharmacol.* 2, 1721-1727.
- Chini B. & Parenti M. (2004) G-protein coupled receptors in lipid rafts and caveolae: how, when and why do they go there? *J. Mol. Endocrinol.* 32, 325-338.
- Claing A., Laporte S.A., Caron M.G., & Lefkowitz R.J. (2002) Endocytosis of G protein-coupled receptors: roles of G protein-coupled receptor kinases and beta-arrestin proteins. *Prog. Neurobiol.* 66, 61-79.
- Cohen G.B., Yang T., Robinson P.R., & Oprian D.D. (1993) Constitutive activation of opsin - influence of charge at position-134 and size at position-296. *Biochemistry* 32, 6111-6115.
- de Weerd W.F.C. & Leeb-Lundberg L.M.F. (1997) Bradykinin sequesters B2 bradykinin receptors and the receptor-coupled G alpha subunits G alpha(q) and G alpha(1) in caveolae in DDT<sub>1</sub> MF-2 smooth muscle cells. *J. Biol. Chem.* 272, 17858-17866.
- Dixon R.A.F., Kobilka B.K., Strader D.J., Benovic J.L., Dohlman H.G., Frielle T., Bolanowski M.A., Bennett C.D., Rands E., Diehl R.E., Mumford R.A., Slater E.E., Sigal I.S., Caron M.G., Lefkowitz R.J., & Strader C.D. (1986) Cloning of the gene and cDNA for mammalian beta-adrenergic receptor and homology with rhodopsin. *Nature* 321, 75-79.
- Duncan A.M., Kladis A., Jennings G.L., Dart A.M., Esler M., & Campbell D.J. (2000) Kinins in humans. *Am. J. Physiol. – Reg. I.* 278, R897-R904.
- Ernst O.P., Meyer C.K., Marin E.P., Henklein P., Fu W.Y., Sakmar T.P., & Hofmann K.P. (2000) Mutation of the fourth cytoplasmic loop of rhodopsin affects binding of transducin and peptides derived from the carboxyl-terminal sequences of transducin alpha and gamma subunits. *J. Biol. Chem.* 275, 1937-1943.
- Faussner A., Heinzerian P., Klier C., & Roscher A.A. (1991) Solubilization and characterization of B2-bradykinin receptors from cultured human fibroblasts. *J. Biol. Chem.* 266, 9442-9446.
- Faussner A., Proud D., Towns M., & Bathon J.M. (1998) Influence of the cytosolic carboxyl termini of human B1 and B2 kinin receptors on receptor sequestration, ligand internalization, and signal transduction. *J. Biol. Chem.* 273, 2617-2623.
- Ferguson S.S.G., Menard L., Barak L.S., Koch W.J., Colapietro A.M., & Caron M.G. (1995) Role of phosphorylation in agonist-promoted beta(2)-adrenergic receptor sequestration - rescue of a sequestration-defective mutant receptor by beta-Ark1. *J. Biol. Chem.* 270, 24782-24789.
- Frey E.K. (1926) Zusammenhänge zwischen Herzarbeit und Nierentätigkeit. *Arch. Klin. Chir.* 142, 663-669.
- Frey E.K. & Kraut H. (1926) Über einen von der Niere ausgeschiedenen, die Herztaetigkeit anregenden Stoff. *Hoppe-Seyler's Z. Physiol. Chemie* 157, 32-61.



Fritze O., Filipek S., Kuksa V., Palczewski K., Hofmann K.P., & Ernst O.P. (2003) Role of the conserved NPxxY(x)(5,6)F motif in the rhodopsin ground state and during activation. *Proc. Natl. Acad. USA* 100, 2290-2295.

Gabilondo A.M., Krasel C., & Lohse M.J. (1996) Mutations of Tyr(326) in the beta(2)-adrenoceptor disrupt multiple receptor functions. *Eur. J. Pharmacol.* 307, 243-250.

Gether U., Ballesteros J.A., Seifert R., Sanders-Bush E., Weinstein H., & Kobilka B.K. (1997) Structural instability of a constitutively active G protein-coupled receptor - Agonist-independent activation due to conformational flexibility. *J. Biol. Chem.* 272, 2587-2590.

Gilman A.G. (1987) G Proteins – Transducers of Receptor-Generated Signals. *Annu. Rev. Biochem.* 56, 615-649.

Go W.Y., Holicky E.L., Hadac E.M., Rao R.V., & Miller L.J. (1998) Identification of a domain in the carboxy terminus of CCK receptor that affects its intracellular trafficking. *Am. J. Physiol. – Gastr. L.* 38, G56-G62.

Graness A., Adomeit A., Ludwig B., Muller W.D., Kaufmann R., & Liebmann C. (1997) Novel bradykinin signalling events in PC-12 cells: stimulation of the cAMP pathway leads to cAMP-mediated translocation of protein kinase C( $\epsilon$ ). *Biochem. J.* 327, 147-154.

Haasemann M., Cartaud J., Müller-Esterl W., & Dunia I. (1998) Agonist-induced redistribution of bradykinin B-2 receptor in caveolae. *J. Cell Sci.* 111, 917-928.

He R., Browning D.D., & Ye R.D. (2001) Differential roles of the NPxxY motif in formyl peptide receptor signaling. *J. Immunol.* 166, 4099-4105.

Hess J.F., Borkowski J.A., Young G.S., Strader C.D., & Ransom R.W. (1992) Cloning and pharmacological characterization of a human bradykinin (Bk-2) receptor. *Biochem. Bioph. Res. Co.* 184, 260-268.

Hess J.F., Hey P.J., Chen T.B., O'Brien J., Omalley S.S., Pettibone D.J., & Chang R.S.L. (2001) Molecular cloning and pharmacological characterization of the canine B1 and B2 bradykinin receptors. *Biol. Chem.* 382, 123-129.

Hibino T., Takemura T., & Sato K. (1994) Human eccrine sweat contains tissue kallikrein and kininase-II. *J. Invest. Dermatol.* 102, 214-220.

Hunyady L., Bor M., Baukal A.J., Balla T., & Catt K.J. (1995) A conserved NPLFY sequence contributes to agonist binding and signal-transduction but is not an internalization signal for the type-1 angiotensin-II receptor. *J. Biol. Chem.* 270, 16602-16609.

Ju H., Venema V.J., Liang H.Y., Harris M.B., Zou F., & Venema R.C. (2000) Bradykinin activates the Janus-activated kinase/signal transducers and activators of transcription (JAK/STAT) pathway in vascular endothelial cells: localization of JAK/STAT signalling proteins in plasmalemmal caveolae. *Biochem. J.* 351, 257-264.

Kammerer S., Braun A., Arnold N., & Roscher A.A. (1995) The human bradykinin B2 receptor gene - full-length cDNA, genomic organization and identification of the regulatory region. *Biochem. Bioph. Res. Co.* 211, 226-233.

- Kobilka B.K., Dixon R.A.F., Frielle T., Dohlman H.G., Bolanowski M.A., Sigal I.S., Yangfeng T.L., Francke U., Caron M.G., & Lefkowitz R.J. (1987) cDNA for the human beta2-adrenergic receptor – a protein with multiple membrane-spanning domains and encoded by a gene whose chromosomal location is shared with that of the receptor for platelet-derived growth-factor. *Proc. Natl. Acad. USA* 84, 46-50.
- Koenig J.A. & Edwardson J.M. (1997) Endocytosis and recycling of G protein-coupled receptors. *Trends Pharmacol. Sci.* 18, 276-287.
- Kraut H., Frey E.K., & Werle E. (1930) Der Nachweis eines Kreislaufhormons in der Pankreasdruse. *Hoppe-Seyler's Z. Physiol. Chemie* 187, 97-106.
- Laemmli U.K. (1970) Cleavage of structural proteins during assembly of head of bacteriophage-T4. *Nature* 227, 680-685.
- Lamb M.E., de Weerd W.F.C., & Leeb-Lundberg L.M.F. (2001) Agonist-promoted trafficking of human bradykinin receptors: arrestin- and dynamin-independent sequestration of the B2 receptor and bradykinin in HEK293 cells. *Biochem. J.* 355, 741-750.
- Lamb M.E., Zhang C., Shea T., Kyle D.J., & Leeb-Lundberg L.M.F. (2002) Human B<sub>1</sub> and B<sub>2</sub> bradykinin receptors and their agonists target caveolae-related lipid rafts to different degrees in HEK293 cells. *Biochemistry* 41, 14340-14347.
- Langen R., Cai K.W., Altenbach C., Khorana H.G., & Hubbell W.L. (1999) Structural features of the C-terminal domain of bovine rhodopsin: a site-directed spin-labeling study. *Biochemistry* 38, 7918-7924.
- Laporte S.A., Servant G., Richard D.E., Escher E., Guillemette G., & Leduc R. (1996) The tyrosine within the NPX<sub>(n)</sub>Y motif of the human angiotensin II type 1 receptor is involved in mediating signal transduction but is not essential for internalization. *Mol. Pharm.* 49, 89-95.
- Laporte S.A., Miller W.E., Kim K.M., & Caron M.G. (2002) beta-arrestin/AP-2 interaction in G protein-coupled receptor internalization - Identification of a beta-arrestin binding site in beta(2)-adaptn. *J. Biol. Chem.* 277, 9247-9254.
- Le Gouill C., Parent J.L., Rola-Pleszczynski M., & Stankova J. (1997) Structural and functional requirements for agonist-induced internalization of the human platelet-activating factor receptor. *J. Biol. Chem.* 272, 21289-21295.
- Liebmann C. (2001) Bradykinin signalling to MAP kinase: Cell-specific connections versus principle mitogenic pathways. *Biol. Chem.* 382, 49-55.
- Ma J.X., Wang D.Z., Ward D.C., Chen L.M., Dessai T., Chao J., & Chao L. (1994) structure and chromosomal localization of the gene (Bdkrb2) encoding human bradykinin B2 receptor. *Genomics* 23, 362-369.
- Madeddu P., Varoni M.V., Palomba D., Emanuelli C., Demontis M.P., Glorioso N., DessiFulgheri P., Sarzani R., & Anania V. (1997) Cardiovascular phenotype of a mouse strain with disruption of bradykinin B2-receptor gene. *Circulation* 96, 3570-3578.
- Madeddu P., Emanuelli C., Salis M.B., Milia A.F., Stacca T., Carta L., Pinna A., Deiana M., & Gaspa L. (2001) Role of calcitonin gene-related peptide and kinins in post-ischemic intestinal reperfusion. *Peptides* 22, 915-922.

Marceau F. & Regoli D. (2004) Bradykinin receptor ligands: therapeutic perspectives. *Nat. Rev. Drug Discov.* 3, 845-852.

Marcic B., Deddish P.A., Skidgel R.A., Erdos E.G., Minshall R.D., & Tan F.L. (2000) Replacement of the transmembrane anchor in angiotensin I-converting enzyme (ACE) with a glycosylphosphatidylinositol tail affects activation of the B2 bradykinin receptor by ACE inhibitors. *J. Biol. Chem.* 275, 16110-16118.

Marin E.P., Krishna K.G., Zvyaga T.A., Isele J., Siebert F., & Sakmar T.P. (2000) The amino terminus of the fourth cytoplasmic loop of rhodopsin modulates rhodopsin-transducin interaction. *J. Biol. Chem.* 275, 1930-1936.

Marrero M.B., Venema V.J., Ju H., He H., Liang H.Y., Caldwell R.B., & Venema R.C. (1999) Endothelial nitric oxide synthase interactions with G protein-coupled receptors. *Biochem. J.* 343, 335-340.

Mattera R., Codina J., Crozat A., Kidd V., Woo S.L.C., & Birnbaumer L. (1986) Identification by molecular cloning of two forms of the  $\alpha$ -subunit of the human liver stimulatory (Gs) regulatory component of adenylyl cyclase. *FEBS Lettes* 206, 36-42.

McEachern A.E., Shelton E.R., Bhakta S., Obernolte R., Bach C., Zuppan P., Fujisaki J., Aldrich R.W., & Jarnagin K. (1991) Expression cloning of a rat B2 bradykinin receptor. *Proc. Natl. Acad. USA* 88, 7724-7728.

Meneton P., Bloch-Faure M., Hagege A.A., Ruetten H., Huang W., Bergaya S., Ceiler D., Gehring D., Martins I., Salmon G., Boulanger C.M., Nussberger J., Crozatier B., Gasc J.M., Heudes D., Bruneval P., Doetschman T., Menard J., & Alhenc-Gelas F. (2001) Cardiovascular abnormalities with normal blood pressure in tissue kallikrein-deficient mice. *Proc. Natl. Acad. USA* 98, 2634-2639.

Menke J.G., Borkowski J.A., Bierilo K.K., Macneil T., Derrick A.W., Schneck K.A., Ransom R.W., Strader C.D., Linemeyer D.L., & Hess J.F. (1994) Expression cloning of a human B1 bradykinin receptor. *J. Biol. Chem.* 269, 21583-21586.

Milligan G. (2003) Principles: extending the utility of [<sup>35</sup>S]GTP gamma S binding assays. *Trends Pharmacol. Sci.* 24, 87-90.

Nishizuka Y. (1992) Intracellular signaling by hydrolysis of phospholipids and activation of protein kinase C. *Science* 258, 607-614.

Oliveira L., Paiva A.C.M., & Vriend G. (1999) A low resolution model for the interaction of G proteins with G protein-coupled receptors. *Protein Eng.* 12, 1087-1095.

Palczewski K., Kumasaka T., Hori T., Behnke C.A., Motoshima H., Fox B.A., Le Trong I., Teller D.C., Okada T., Stenkamp R.E., Yamamoto M., & Miyano M. (2000) Crystal structure of rhodopsin: a G protein-coupled receptor. *Science* 289, 739-745.

Patel S., Robb-Gaspers L.D., Stellato K.A., Shon M., & Thomas A.P. (1999) Coordination of calcium signalling by endothelial-derived nitric oxide in the intact liver. *Nat. Cell Biol.* 1, 467-471.

- Pizard A., Blaukat A., Müller-Esterl W., Alhenc-Gelas F., & Rajerison R.M. (1999) Bradykinin-induced internalization of the human B2 receptor requires phospho-rylation of three serine and two threonine residues at its carboxyl tail. *J. Biol. Chem.* 274, 12738-12747.
- Pizard A., Blaukat A., Michineau S., Dikic I., Müller-Esterl W., Alhenc-Gelas F., & Rajerison R.M. (2001) Palmitoylation of the human bradykinin B2 receptor influences ligand efficacy. *Biochemistry* 40, 15743-15751.
- Powell S.J., Slynn G., Thomas C., Hopkins B., Briggs I., & Graham A. (1993) Human bradykinin B2 receptor – nucleotide-sequence analysis and assignment to chromosome-14. *Genomics* 15, 435-438.
- Prioleau C., Visiers I., Ebersole B.J., Weinstein H., & Sealfon S.C. (2002) Conserved helix 7 tyrosine acts as a multistate conformational switch in the 5HT<sub>2C</sub> receptor - identification of a novel "locked-on" phenotype and double revertant mutations. *J. Biol. Chem.* 277, 36577-36584.
- Rasmussen S.G.F., Jensen A.D., Liapakis G., Ghanouni P., Javitch J.A., & Gether U. (1999) Mutation of a highly conserved aspartic acid in the beta(2)-adrenergic receptor: constitutive activation, structural instability, and conformational rearrangement of transmembrane segment 6. *Mol. Pharm.* 56, 175-184.
- Roberts R.A. & Gullick W.J. (1990) Bradykinin receptors undergo ligand-induced desensitization. *Biochemistry* 29, 1975-1979.
- Rocha e Silva M., Beraldo W.T., & Rosenfeld G. (1949) Bradykinin, a hypotensive and smooth muscle stimulating factor released from plasma globulin by snake venoms and by trypsin. *Am. J. Physiol.* 156, 261-273.
- Rosendorff A., Ebersole B.J., & Sealfon S.C. (2000) Conserved helix 7 tyrosine functions as an activation relay in the serotonin 5HT<sub>2C</sub> receptor. *Mol. Brain Res.* 84, 90-96.
- Sabourin T., Bastien L., Bachvarov D.R., & Marceau F. (2002) Agonist-induced translocation of the kinin B1 receptor to caveolae-related rafts. *Mol. Pharm.* 61, 546-553.
- Sakmar T.P., Menon S.T., Marin E.P., & Awad E.S. (2002) Rhodopsin: insights from recent structural studies. *Annu. Rev. Bioph. Biom.* 31, 443-484.
- Samama P., Cotecchia S., Costa T., & Lefkowitz R.J. (1993) A mutation-induced activated state of the beta(2)-adrenergic receptor - extending the ternary complex model. *J. Biol. Chem.* 268, 4625-4636.
- Sambrook J. & Gething M.J. (1989) Protein-structure – chaperones, paperones. *Nature* 342, 224-225.
- Schöneberg T., Schulz A., & Gudermann T. (2002) The structural basis of G protein-coupled receptor function and dysfunction in human diseases. *Rev. Physiol. Bioch. P.* 144, 143-227.
- Schremmer-Danninger E., Hermann A., Fink E., Fritz H., & Roscher A.A. (1999) Identification and occurrence of mRNAs for components of the kallikrein-kinin system in human skin and in skin diseases. *Immunopharm.* 43, 287-291.

- Slice L.W., Wong H.C., Sternini C., Grady E.F., Bunnett N.W., & Walsh J.H. (1994) The conserved NPX<sub>n</sub>Y motif present in the gastrin-releasing peptide receptor is not a general sequestration sequence. *J. Biol. Chem.* 269, 21755-21761.
- Teller D.C., Okada T., Behnke C.A., Palczewski K., & Stenkamp R.E. (2001) Advances in determination of a high-resolution three-dimensional structure of rhodopsin, a model of G-protein-coupled receptors (GPCRs). *Biochemistry* 40, 7761-7772.
- Tippmer S., Quitterer U., Kolm V., Faussner A., Roscher A., Mosthaf L., MullerEsterl W., & Haring H. (1994) Bradykinin induces translocation of the protein kinase C isoform-alpha, isoform-epsilon, and isoform-zeta. *Eur. J. Biochem.* 225, 297-304.
- Trowbridge I.S., Collawn J.F., & Hopkins C.R. (1993) Signal-dependent membrane-protein trafficking in the endocytic pathway. *Annu. Rev. Cell Biol.* 9, 129-161.
- van Rhee A.M. & Jacobson K.A. (1996) Molecular architecture of G protein-coupled receptors. *Drug Develop. Res.* 37, 1-38.
- Venema V.J., Ju H., Sun J.M., Eaton D.C., Marrero M.B., & Venema R.C. (1998) Bradykinin stimulates the tyrosine phosphorylation and bradykinin B2 receptor association of phospholipase C gamma 1 in vascular endothelial cells. *Biochem. Biophys. Res. Co.* 246, 70-75.
- von Zastrow M., Link R., Daunt D., Barsh G., & Kobilka B. (1993) Subtype-specific differences in the intracellular sorting of G protein-coupled receptors. *J. Biol. Chem.* 268, 763-766.
- Wang J.F., Zheng J.L., Anderson J.L., & Toews M.L. (1997) A mutation in the hamster alpha(1B)-adrenergic receptor that differentiates two steps in the pathway of receptor internalization. *Mol. Pharm.* 52, 306-313.
- Ward W.H.J., Timms D., & Fersht A.R. (1990) Protein Engineering and the Study of Structure-Function-Relationships in Receptors. *Trends Pharmacol.* 11, 280-284.
- Werle E., Gotz W., & Kepler A. (1937) Über die Wirkung des Kallikreins auf den isolieren Darm und über eine neue darmkontrahierende Substanz. *Biochem. Z.* 289, 217-233.
- Werle E. & Grund M. (1939) Zur Kenntnis der darmkontrahierende Uterus erregenden und blutdrucksenkenden Substanz DK. *Biochem. Z.* 301, 429-436.
- Wess J., Nanavati S., Vogel Z., & Maggio R. (1993) Functional-Role of Proline and Tryptophan Residues Highly Conserved Among G-Protein-Coupled Receptors Studied by Mutational Analysis of the M3-Muscarinic-Receptor. *EMBO Journal* 12, 331-338.
- Wess J. (1997) G-protein-coupled receptors: Molecular mechanisms involved in receptor activation and selectivity of G protein recognition. *FASEB Journal* 11, 346-354.
- Wess J. (1998) Molecular basis of receptor/G-protein coupling selectivity. *Pharmacol. Therapeut.* 80, 231-264.

**H CURRICULUM VITAE****1. Personal data**

NAME Irina Alexandrovna Kalatskaya  
DATE OF BIRTH 25. January 1979  
PLACE OF BIRTH Minsk, Belarus  
CITIZENSHIP Belarus

**2. Pre-university education**

1985-1994 Secondary school # 53, Minsk, Belarus  
1994-1996 Secondary school # 40 with profound study of chemistry, Minsk  
Awarded with the silver medal

**3. University studies and working experience**

1996-2001 International Sakharov Environmental University, Faculty of  
Radiobiology, Minsk, Belarus  
Diploma in Radiobiology and Radiation Medicine (equivalent to M.S.),  
*summa cum laude*

1997-1999 Experimental work as a student assistant in the Laboratory of Molecular  
Markers of Ecological Effects, Faculty of Radiobiology, International  
Sakharov Environmental University, Minsk, Belarus  
Research project:  
*Investigation of the products of lipid peroxidation in the membrane  
components of the blood of rats after acute gamma irradiation.*

1999-2001 Research work as a diploma student in the Department of Protein  
Chemistry, Institute of Bioorganic Chemistry, National Academy of  
Science of Belarus, Minsk, Belarus  
Title of Diploma:  
*“Recombinant  $V_H$  domain of the monoclonal immunoglobulin F11:  
expression, refolding, antigen-binding activity and spectral properties.”*

**4. Postgraduate studies and professional career**

2001-2005 Experimental work for a PhD thesis at the Department of Clinical  
Chemistry and Clinical Biochemistry of the Faculty of Medicine of the  
Ludwig-Maximilians University, Munich, Germany  
Title of Thesis:  
*“Role of the tyrosine in the highly conserved NPxxY sequence of the  
human  $B_2$  bradykinin receptor.”*